

Virus like particle displaying the major allergen Der p 1 as a vaccine candidate
against house dust mite allergy



A Thesis Submitted in Partial Fulfillment of the Requirements
for the Degree of Master of Science in Medical Sciences

Common Course

FACULTY OF MEDICINE

Chulalongkorn University

Academic Year 2020

Copyright of Chulalongkorn University

อนุภาคเสมือนไวรัสที่นำเสนอสารก่อภูมิแพ้หลักชนิด Der p 1 เพื่อเป็นวัคซีนต้นแบบ
ต่อโรคภูมิแพ้ฝุ่น



วิทยานิพนธ์นี้เป็นส่วนหนึ่งของการศึกษาตามหลักสูตรปริญญาวิทยาศาสตรมหาบัณฑิต
สาขาวิชาวิทยาศาสตร์การแพทย์ ไม่สังกัดภาควิชา/เทียบเท่า
คณะแพทยศาสตร์ จุฬาลงกรณ์มหาวิทยาลัย
ปีการศึกษา 2563
ลิขสิทธิ์ของจุฬาลงกรณ์มหาวิทยาลัย

Thesis Title Virus like particle displaying the major allergen Der p 1
 as a vaccine candidate against house dust mite allergy
By Miss Sirikarn Jitthamstaporn
Field of Study Medical Sciences
Thesis Advisor Associate Professor Alain Jacquet, Ph.D.

Accepted by the FACULTY OF MEDICINE, Chulalongkorn University in Partial
Fulfillment of the Requirement for the Master of Science

..... Dean of the FACULTY OF MEDICINE
(Professor SUTTIPONG WACHARASINDHU, M.D.)

THESIS COMMITTEE

..... Chairman
(Associate Professor WILAI ANOMASIRI, Ph.D.)

..... Thesis Advisor
(Associate Professor Alain Jacquet, Ph.D.)

..... Examiner
(Assistant Professor WACHAREE LIMPANASITHIKUL, Ph.D.)

..... External Examiner
(Associate Professor Surapon Piboonpocanun, Ph.D.)

สิริกาญจน์ จิตธรรมสถาพร : อนุภาคเสมือนไวรัสที่นำเสนอสารก่อภูมิแพ้หลักชนิด Der p 1 เพื่อเป็นวัคซีนต้นแบบ ต่อโรคมภูมิแพ้ไรฝุ่น . (Virus like particle displaying the major allergen Der p 1 as a vaccine candidate against house dust mite allergy) อ.ที่ปรึกษาหลัก : รศ. ดร.อลัน แจ็คเคว

ไรฝุ่นบ้านเป็นหนึ่งในแหล่งสารก่อภูมิแพ้ที่สำคัญที่สุดทั่วโลก สารก่อภูมิแพ้จากไรฝุ่นกระตุ้นให้เกิดอาการแพ้ในกลุ่มผู้ป่วยโรคภูมิแพ้ ผ่านทางการตอบสนองต่อภูมิแพ้ประเภทเซลล์ทีเฮลเปอร์ชนิดที่ 2 (Th2 cell) ซึ่งนำไปสู่การพัฒนาของโรคจมูกอักเสบโรคหอบหืดหรือโรคผิวหนังอักเสบจากภูมิแพ้ การตอบสนองต่อการแพ้ไรฝุ่นส่วนใหญ่เกิดจากเซลล์ทีเฮลเปอร์ชนิดที่ 2 ที่มีความจำเพาะต่อสารก่อภูมิแพ้นั้นเกิดการกระตุ้นและนำไปสู่การผลิตแอนติบอดีชนิด E (IgE) ซึ่งก่อให้เกิดอาการแพ้ Der p 1 จัดอยู่ในกลุ่มของเอนไซม์ย่อยกรดอะมิโนชนิดซิสเตอีน (cysteine protease) ซึ่งมีคุณสมบัติคล้ายกับเอนไซม์ปาเปนอิน (papain) ซึ่งเป็นสารก่อภูมิแพ้หลักที่พบในไรฝุ่นสายพันธุ์ *Dermatophagoides pteronyssinus* โดยสามารถก่อให้เกิดอาการแพ้ได้ประมาณ 80 เปอร์เซ็นต์ของกลุ่มประชากรผู้ป่วยโรคภูมิแพ้ไรฝุ่น การรักษาด้วยภูมิคุ้มกันบำบัดจำเพาะต่อสารก่อภูมิแพ้ (AIT) เป็นการรักษาที่มีความพิเศษวิธีหนึ่งซึ่งสามารถใช้สารก่อภูมิแพ้ที่ผู้ป่วยแพ้มากระตุ้นให้ร่างกายสร้างภูมิคุ้มกันเกิดและการตอบสนองต่อการแพ้ไรฝุ่นโดยฉีดสารสกัดจากไรฝุ่นเข้าไปซ้ำผ่านทางชั้นใต้ผิวหนังหรือให้ทางช่องปากโดยอมหรือหยดใต้ลิ้น อย่างไรก็ตามการรักษาด้วยวิธีภูมิคุ้มกันบำบัดแบบดั้งเดิม มักใช้เวลาในการรักษายาวนานอย่างต่ำประมาณ 2-3 ปี รวมถึงพบปัญหาด้านประสิทธิภาพและผลข้างเคียงที่มักจะเกิดขึ้นนำไปสู่การตอบสนองต่อการรักษาที่มีประสิทธิภาพต่ำในกลุ่มผู้ป่วย การรักษาด้วยวิธีภูมิคุ้มกันบำบัดที่ประสบความสำเร็จนั้นแสดงให้เห็นว่ามีความสัมพันธ์ของระดับแอนติบอดีชนิด G (IgG) ซึ่งมีความสามารถในการยับยั้งปฏิกิริยาการก่อให้เกิดอาการแพ้จาก IgE ดังนั้นการรักษาด้วยภูมิคุ้มกันบำบัดสมัยใหม่จึงมีวัตถุประสงค์เพื่อส่งเสริมการยับยั้งปฏิกิริยาการก่อให้เกิดอาการแพ้จาก IgE ซึ่งมีประสิทธิภาพมากขึ้นกว่าเมื่อเปรียบเทียบกับรักษาด้วยภูมิคุ้มกันบำบัดแบบดั้งเดิม อนุภาคเสมือนไวรัส (VLP) เป็นที่รู้จักกันอย่างแพร่หลายในการช่วยกระตุ้นการตอบสนองแอนติบอดีที่ประสิทธิภาพแบบหนึ่ง ดังนั้นการวิจัยในครั้งนี้จึงต้องการออกแบบ VLP ที่มีโปรตีนรีคอมบีแนนท์สารก่อภูมิแพ้ Der p 1 ในรูปของ ProDer p 1 (PD1) เพื่อทดสอบความสามารถในการก่อให้เกิดอาการแพ้และความสามารถในการกระตุ้นภูมิคุ้มกัน VLP ชนิด AP205 ถูกประดับไปด้วย PD1 โดยใช้เทคโนโลยี SpyTag/SpyCatcher การทดสอบ Competitive ELISA IgE assays แสดงให้เห็นว่า โปรตีนรูปผสมกับอนุภาคเสมือนไวรัสชนิด VLP-PD1 ก่อให้เกิดอาการแพ้น้อยกว่า Der p 1 ตามธรรมชาติ ที่น่าสนใจคือ VLP-PD1 มีความสามารถในการป้องกันการหลั่งสารที่สำคัญต่อกระบวนการอักเสบจากเม็ดเลือดขาวชนิดเบโซฟิล นอกจากนี้ยังสามารถกระตุ้นการตอบสนองในการสร้าง IgG ได้อย่างมากโดยไม่พบการตอบสนองต่อ IgE โดยปราศจากสารเสริมกระตุ้นภูมิคุ้มกัน (adjuvant) IgG ที่เกิดจาก VLP-PD1 สามารถยับยั้งการจับกันของของ IgE ของมนุษย์ต่อโปรตีน Der p 1 เช่นเดียวกับในการกระตุ้นเม็ดเลือดขาวชนิดเบโซฟิลที่จำเพาะต่อโปรตีน Der p 1 สำหรับการทดสอบ lymphoproliferative assays แสดงให้เห็นว่า VLP-PD1 สามารถกระตุ้นให้เกิดการพัฒนา Th1 ที่จำเพาะสารก่อภูมิแพ้และกระตุ้นการหลั่งของไซโตไคน์ชนิดอินเตอร์เฟอรอนแกมมา (IFN- γ) จึงสรุปได้ว่า VLP-PD1 นั้นไม่ก่อให้เกิดอาการแพ้และสามารถการตอบสนองในการสร้าง IgG ยับยั้งการเกิดอาการแพ้อย่างมีประสิทธิภาพ ทั้งนี้ VLP-PD1 จึงอาจใช้เป็นตัวแทนของวัคซีนต้นแบบสำหรับป้องกันโรคมภูมิแพ้โดยให้ภูมิคุ้มกันและการรักษาด้วยภูมิคุ้มกันบำบัดต่อไป

สาขาวิชา วิทยาศาสตร์การแพทย์
ปีการศึกษา 2563

ลายมือชื่อนิสิต
ลายมือชื่อ อ.ที่ปรึกษาหลัก

6074085230 : MAJOR MEDICAL SCIENCES

KEYWORD: House dust mite (HDM) / VLP-PD1 / Der p 1 / Virus-like particles (VLPs) / AIT

Sirikarn Jitthamstaporn : Virus like particle displaying the major allergen Der p 1 as a vaccine candidate against house dust mite allergy. Advisor: Assoc. Prof. Alain Jacquet, Ph.D.

House dust mite (HDM) represents one of the most important allergenic sources worldwide. HDM allergens trigger in atopic patients potent Th2-biased inflammatory responses leading to the development of allergic rhinitis/asthma and atopic dermatitis. The HDM allergic response is mediated mainly by the allergen-specific Th2 cells and IgE. Der p 1, a papain-like cysteine protease, is a major HDM allergen from the *Dermatophagoides pteronyssinus* species, inducing allergic sensitizations in around 80 percent of HDM allergic populations. Allergen-specific immunotherapy (AIT) represents a unique specific treatment capable to revert the house dust mite (HDM) allergic response into immune tolerance through repetitive subcutaneous or sublingual administrations of mite allergen extracts. However, the AIT duration (minimum 2-3 years), efficacy issues, and side-effect developments could explain the poor adherence of the HDM allergic patients to conventional AIT. As successful AIT was shown to be correlated with the levels of blocking IgG antibodies inhibiting allergen-IgE interactions, new generations of immunotherapies, aimed to boost such blocking of IgE responses, could be more effective than conventional allergen extract-based AIT. Virus-like particles (VLP) are well-known to elicit potent antibody responses, the goal of the present study was to design VLPs displaying a recombinant form of Der p 1 zymogen (ProDer p 1, PD1) and to test the allergenicity and immunogenicity of these chimeric particles. AP205 bacteriophage-based VLPs were decorated with PD1 using the split-protein (SpyTag/SpyCatcher) conjugation technology. To get successful conjugation of PD1 to SpyCatcher-VLP, we had to express SpyTagged-PD1C34A (mutation of the active site cysteine residue of Der p 1). Competitive ELISA IgE assays evidenced that VLP-PD1 has a much lower IgE reactivity in comparison with natural Der p 1 (nDer p 1). Remarkably, PD1 multimerization prevented basophil degranulation. Unadjuvanted VLP-PD1 elicited strong anti-nDer p 1 IgG responses but no specific IgE. Specific IgG induced by VLP-PD1 could inhibit the binding of human IgE to nDer p 1 as well as nDer p 1-specific basophil activation. Finally, lymphoproliferative assays showed that VLP-PD1 triggered allergen-specific Th1 cells as shown by the potent production of IFN- γ . In conclusion, VLP decorated with PD1 was hypoallergenic and induced potent blocking IgG antibody response. Such chimeric VLPs could represent a promising vaccine candidate for HDM-specific immunoprophylaxis and immunotherapy.

Field of Study: Medical Sciences

Student's Signature

Academic Year: 2020

Advisor's Signature

ACKNOWLEDGEMENTS

This thesis project was started in August 2018 to May 2021 at the faculty of Medicine, Chulalongkorn University. The effort is devoted to all persons suffering from HDM allergies all around the world. Hopefully, this study would be one of many contributing factors to the future development of HDM treatment. During my four years of master's study, it is an honor to work on this extraordinary project under the advisor of Assoc. Prof. Alain Jacquet.

I would like to express my special thanks of gratitude to Assoc. Prof. Alain Jacquet who gave me the great opportunity to do this challenging project. I would like to say for me he is the best professor I ever met. He always supports and gives much practical advice only in the way of study but also in my real life. With his patience, assistance, constructive suggestions, and unique recommendations encourage which bring me to the success of this project.

My completion of this project could not have been accomplished without the support of our collaboration with Prof. Adam Sander from the Department of Immunology and Microbiology, University of Copenhagen, Denmark), and Assoc. Prof. Dr. Theerayuth Kaewamatawong (D.V.M. Ph.D), from the Department of Veterinary Pathology for kindly training animal techniques. I also would like to thank Assist Prof. Dr. Narrissara Suratannon (M.D.) and her team for providing us HDM patient sera. I am truly appreciated and felt thankful for their commitment in HDM patient's sera collection.

I would like to sincerely show appreciation to Chulalongkorn University for providing me the 60/40 Study Scholarship in Academic Year 2018 and the 90th Anniversary of Chulalongkorn University Scholarship for financial assistance.

I also would like to acknowledge all Room #807 members, Ms. Termsri Peepim, Ms. Karntichar Mongkorntanyatip, and Mr. Tewarit Soongrung, and members of the Center of Excellence in Vaccine Research and Development (Chula VRC) for their kind support.

Last but not least, I would like to warmly thank my family and beloved friends for their support and encouragement when the times got rough are much appreciated and duly noted.

Sirikarn Jitthamstaporn

TABLE OF CONTENTS

	Page
.....	iii
ABSTRACT (THAI).....	iii
.....	iv
ABSTRACT (ENGLISH).....	iv
ACKNOWLEDGEMENTS.....	v
TABLE OF CONTENTS.....	vi
List of Tables.....	x
List of Figures.....	xi
LIST OF ABBREVIATIONS.....	1
CHAPTER I INTRODUCTION.....	1
CHAPTER II LITERATURE REVIEW.....	4
2.1 Allergy.....	4
2.2 Mechanism of the allergic response.....	6
2.3 Sensitization phase of the allergic response.....	6
2.4 Early-phase of the allergic response.....	8
2.5 Late phase of the allergic response.....	8
2.6 House dust mite (HDM).....	9
10	
2.7 House dust mite (HDM) allergens.....	11
2.8 Der p 1.....	16
2.9 Allergen-specific immunotherapy.....	20

2.10 Importance of allergen-specific blocking IgG responses for successful AIT	26
2.11 Virus-like particles	28
2.12 AIT based on VLP displaying allergens	33
CHAPTER III MATERIALS AND METHODS	35
3.1 Patients' sera.....	35
3.2 Cloning of PD1-ST derivatives.....	35
3.3 In gel DNA fragment isolation.....	37
3.4 DNA ligation	37
3.5 <i>E. coli</i> competent cell preparation and Transformation	38
3.6 Bacterial Colony PCR.....	39
3.7 Purification of recombinant plasmid for <i>P.pastoris</i> transformation.....	39
3.8 <i>P.pastoris</i> transformation.....	39
3.9 Cloning of SpyCatcher-AP205 VLP (SC-VLP).....	40
3.10 Protein Expression.....	41
3.10.1 Recombinant SpyTagged-ProDer p 1	41
3.10.2 Recombinant SpyCatcher-AP205 VLP (SC-AP205 VLP)	41
3.11 Protein Purification	42
3.11.1 Purification of recombinant SpyTagged-PD1	42
3.11.2 Purification of of SpyCatcher-VLP AP205	43
3.12 SDS-PAGE and Western blot analysis.....	43
3.13 Protein assay	44
3.14 Enzymatic activity	44
3.15 Conjugation of SpyTagged-PD1 to SC-VLP	44
3.16 Dynamic light scattering (DLS) analysis.....	45

3.17	Detection of RNA in VLP-PD1.....	45
3.18	IgE reactivity to VLP-PD1.....	45
3.19	RBL-SX38 IgE binding assay	46
3.20	Mouse immunization.....	47
3.21	IgG1, IgG2a and IgE antibodies detection	47
3.22	Lymphoproliferative assays.....	48
3.23	Cytokine detection	49
3.24	ELISA Inhibition assay	49
3.25	RBL-SX38 Inhibition assay.....	49
3.26	Statistic.....	50
CHAPTER IV RESULTS		51
4.1	Cloning, expression and purification of wild-type (WT) or N52Q SpyTagged-PD1 proteins.....	51
4.2	Expression and purification of SC-VLP	54
4.3	Conjugation and characterization of wild-type (WT) or N52Q SpyTagged-PD1 proteins to SC-VLP.....	56
4.4	Cloning, expression and purification of double mutant of SpyTagged-PD1 proteins.....	59
4.5	Conjugation of double mutant PD1-ST to SC-VLP	65
4.6	Dynamic light scattering (DLS) of VLP-PD1.....	67
4.7	RNA detection in VLP-PD1	68
4.8	Allergenicity of VLP-PD1.....	69
4.9	Immunogenicity of VLP-PD1.....	72
4.10	Blocking capacity of VLP-PD1	74
CHAPTER V DISCUSSION		76

CHAPTER VI CONCLUSION AND PERSPECTIVE	81
REFERENCES	85
VITA.....	96



List of Tables

	Page
Table. 1 HDM Allergome from WHO-IUIS Database (5), Last accessed 14 Jul 21	12
Table. 2 Vaccine candidate development based on Der p 1 allergen (modified from (66)).....	24
Table. 3 Description of synthetic genes designed for the production of the different SpyTagged-PD1 proteins.....	60



List of Figures

	Page
Figure 1.1 Der p 1-SpyTag conjugated with SpyCatcher-VLPs model (Modified from (18)).....	3
Figure 2.1 The prevalence rate of HDM sensitized patient in countries from South, South-East and Far East Asia (3)	5
Figure 2.2A and 2.2B mechanism of the allergic response (28).....	6
Figure 2.3 Taxonomy of HDM (35).....	9
Figure 2.4 Life cycle of HDM (33).....	10
Figure 2.5 (A) IgE response to individual HDM allergen and (B) Levels of IgE specific for HDM allergens (y-axis, log ₁₀ scale) in adult allergic cohorts from Canada, Europe, South Africa and the United States of America (USA) (N=685) (modified from (4))	15
Figure 2.6 Amino-acid sequence of PreProDer p 1 (50).....	16
Figure 2.7 3D-Crystal structure of ProDer p 1 red color represents α -Helices, orange color represents β -strands, and yellow color represents disulfide bridges (modified from (52)).....	17
Figure 2.8 Proven and hypothetical immunomodulations mediated by the proteolytic activity of Der p 1 in the airways (58).....	19
Figure 2.9 Mechanism of tolerance induction by Allergen-specific immunotherapy (63)	21
Figure 2.10 Overview of new allergen-specific immunotherapy approaches (modified from (15)).....	23
Figure 2.11 Mode of action of specific IgG blocking antibodies in successful AIT (14). (A) direct allergen neutralization, (B) prevention of the inhibitory Fc receptor (Fc γ RIIb) to allergen-induced activation of mast cells and basophils; and C) prevention of IgE-facilitated allergen presentation	27

Figure 2.12 Self-assembly of HPV-16 L1 monomers to create a HPV-based VLP (83).	28
Figure 2.13 The key properties of VLPs to induce immunogenicity; (A) the trafficking of VLPs in the lymph nodes, (B) the interactions with BCR for potent antibody response and (C) the activation of antibody response through TLR7/8/9 signaling on B cells surface by VLPs (modified from (85))	30
Figure 2.14 Overview VLPs assembly using Genetic fusion, Chemical cross-linking or SpyCatcher/SpyTag conjugation for chimeric VLPs (modified from (86))	31
Figure 2.15 Overview display VLPs assembly using SpyTag/SpyCatcher conjugation system (modified from (18))	32
Figure 3.1 Series of Synthetic gene PD1-ST fragment cloned into pUC57 vector	35
Figure 3.2 Cloning of SpyTagged-PD1 into pPIC9K vector	36
Figure 3.3 Cloning of SpyTagged-PD1 into pPICZ α A vector	37
Figure 4.1 Time-dependence of SpyTagged-PD1 expression under optimized induction conditions (cell density-OD and methanol concentration): SDS-PAGE (A) and western blot (WB, B) analysis. Red arrows correspond to the specific bands	52
Figure 4.2 Purified SpyTagged proteins; A) PD1WT-L-ST; B) PD1WT- Ext L-ST and C) PD1N52Q-Ext L-ST, Red arrow indicated the position of PD1-ST protein	53
Figure 4.3 Expression of SpyCatcher-VLP AP205; Lane 1: uninduced bacteria lysate, Lane 2: IPTG-induced bacteria lysate, Lane 3: cytoplasmic fraction and Lane 4: residual pellet after lysis. Red arrow indicated SC-VLP band	54
Figure 4.4 Purification of SpyCatcher-VLP AP205 by density gradient ultracentrifugation; A) composition of density gradient B) SDS-PAGE profile of purified SC-VLP fractions. Lanes 1-9: fractions 2- 11; and (C) Lane 10: purified SC-VLP after 300 kDa dialysis and concentrated with 10 kDa ultrafiltration	55
Figure 4.5 Conjugation of WT or N52Q PD1-ST to SC-VLP(A) SDS-PAGE analysis. Lane 1: purified PD1WT, Lane 3: conjugation of PD1WT to SC-VLP, Lane 4: purified PD1WT-L-ST, Lanes 2, 5, 8 and 11: purified SC-VLP, Lane 6: conjugation of PD1WT-L-ST to SC-	

VLP, Lane 7: purified PD1WT-Ext L-ST, Lane 9: conjugation of PD1WT-ExtL-ST to SC-VLP, Lane 10: purified PD1N52Q-Ext L-ST, Lane 12: conjugation of PD1N52Q-Ext L-ST to SC-VLP. The red boxes show degradation bands. (B) western blot analysis of PD1-Ext L-ST/SC-VLP conjugation using anti-SC-VLP antibodies	57
Figure 4.6 Detection of protease activity in preparations of purified PD1WT; PD1WT-L-ST; PD1WT-ExtL-ST and PD1N52Q-ExtL-ST in the presence or the absence of E-64 and using the chromogenic substrate Boc-QAR-pNA	59
Figure 4.7 PD1 crystallographic structure between the N- or C-terminus pointing in opposite orientation	60
Figure 4.8 Optimization of the experimental conditions for the expression of the new Spytagged-PD1 with double mutant: SDS-PAGE (A) and western blot (WB, B) analysis. Red arrow indicated the specific band after confirmed by western blot	61
Figure 4.9 Purification of PD1N purified by (A) Ion exchange (IEX); Lane 1: crude PD1N before purified, Lane 2: Flow through, Lane 3: fraction eluded at 100 mM NaCl, Lane 4: fraction eluded at 200 mM NaCl, Lane 5: fraction eluded at 300 mM NaCl, Lane 6: fraction eluded at 500 mM NaCl, Lane 7: fraction eluded at 1M NaCl, (B) gel filtration chromatographies (GF); Lane 1 to 9: purified PD1N fraction 29 to 37 and (C) the pooled purified PD1N after concentrated with 10 kDa ultrafiltration	62
Figure 4.10 New purified SpyTagged proteins at C- and/or N-terminal with double mutant amino acid. Red arrow indicated the position of PD1-ST protein	63
Figure 4.11 Pigment removal of PD1N by Blue Sepharose bead; (A) before and (B) after removed pigment.	64
Figure 4.12 Detection of protease activity in batches of double mutant purified PD1C and ST-PD1-ST using the chromogenic substrate Boc-QAR-pNA	64
Figure 4.13 Conjugation of PD1N and PD1C to SC-VLP in different pH SDS-PAGE analysis: Lane 1: purified ST-Ext L-PD1C34AN52Q, Lane 2: conjugation of ST-Ext L-PD1C34AN52Q to SC-VLP at pH 7, Lane 3: conjugation of ST-Ext L-PD1C34AN52Q to SC-VLP at pH 5, Lanes 4 and 8: SC-VLP, Lane 5: purified PD1C34AN52Q-L-ST, Lane 6:	

conjugation of PD1C34AN52Q-L-ST to SC-VLP at pH 7, Lane 7: conjugation of PD1C34AN52Q-L-ST to SC-VLP at pH 5..... 65

Figure 4.14 VLPN and VLPC optimizing molar ratio conjugation and dialysis using SDS-PAGE analysis Lane 1: purified ST-Ext L-PD1C34AN52Q, Lane 2: conjugation of ST-Ext L-D1C34AN52Q to SC-VLP, Lanes 3 and 7: purified SC-VLP; Lane 4: purified VLP-PD1N after removal of excess ST-Ext L-PD1C34AN52Q; Lane 5: purified PD1C34AN52Q-L-ST, Lane 6: conjugation of PD1C34AN52Q-L-ST to SC-VLP; Lane 8: purified VLP-PD1C after removal of excess PD1C34AN52Q-L-ST..... 66

Figure 4.15 DLS of VLP-PD1N, VLP-PD1C nanoparticles compared to SC-VLP. The average diameter as well as the polydispersity percentage (%Pd) are shown 67

Figure 4.16 Detection of RNA in purified and RNase A-treated or untreated SC-VLP, VLP-PD1N and VLP-PD1C by agarose gel electrophoresis and ViSafe Green staining .. 68

Figure 4.17 IgE binding capacity and allergenicity of VLP-PD1N and VLP-PD1C 70

Figure 4.18 Immunogenicity of VLP-PD1N and VLP-PD1C in mice (A) Immunization and bleeding schedule; (B) Post-prime (day 14) and post-boost (days 28 and 42) ProDer p 1-specific IgG1 and IgG2a antibody titers following immunizations with VLP-PD1N, VLP-PD1C, VLP + PD1N, VLP+PD1C; (C) Post-boost (day 42) Der p 1-specific IgG1 and IgG2a antibody titers; (D) IFN- γ and IL-5 levels secreted by splenocytes from immunized mice restimulated with PD1. One representative of 2 similar experiments is shown. * P<0.05 for statistically significant difference 73

Figure 4.19 Blocking capacity of IgG antibodies generated by VLP-PD1N and VLP-PD1C (A) Inhibition of human IgE binding to nDer p 1 by pooled sera from immunized mice (day 42) determined by ELISA IgE inhibition assay. The binding of specific IgE from five Der p 1-sensitized patients to coated nDer p 1 was measured in the presence or the absence of the different mouse antisera diluted 10 or 50 times. The inhibition percentage was calculated as follows: $(1 - (OD_{450_{nm} I} / OD_{450_{nm} C})) \times 100\%$. $OD_{450_{nm} I}$ and $OD_{450_{nm} C}$ represent optical density values in the presence or absence of mouse serum, respectively. *P < 0.05 for IgE inhibition by VLP-PD1-immunized sera compared with VLP + PD1-immunized sera; (B) Inhibition of nDer p 1-induced

basophil degranulation by antiserum from mice immunized with VLP-PD1. RBL-SX38 cells, primed with five HDM allergic patients and positive for Der p 1, were activated with 0.01 μ g/ml nDer p 1 in the presence or absence of different mouse antisera (day 42) diluted 100 times. The inhibition percentage was calculated as follows: $(1 - (\beta\text{-hexosaminidase actual release I} - (\beta\text{-hexosaminidase Spontaneous release S}) / (\beta\text{-hexosaminidase control release C} - (\beta\text{-hexosaminidase Spontaneous release S}))) \times 100\%$. β -hexosaminidase release I, S and C represent the percentage of degranulation in the presence or the absence of mouse serum, respectively. *P <0.05 for statistically significant difference 75

Figure 6.1 Future plan for (A) prophylactic and (B) Therapeutic vaccinations with VLP-PD1 in a Der p 1 sensitization mouse model (modified from (95)) 82

Figure 6.2 Inhibition of the IgE facilitated antigen presentation by blocking IgG antibodies (modified from (14)) 83

Figure 6.3 Principle of the FAB-assay (modified form 109); The tested allergen forms a complex with either IgE or blocking IgG antibodies. These complexes are incubated with EBV-transformed B cells expressing CD23 (Fc ϵ RII). The presence of bounded complexes to CD23 on cell surface are stained with anti-IgE-FITC and the IgE levels are detected by flow cytometry 84

LIST OF ABBREVIATIONS

HDM	House Dust Mite	TSLP	Thymic stromal lymphopoietin
Der p	<i>Dermatophagoides pteronyssinus</i>	ILC2s	type 2 innate lymphoid cells
PD1	ProDer p 1	FcεRI	Fc receptor I for IgE
T _H 2	T-Helper 2	DCs	Dendritic cells
T _H 1	T-Helper 1	FcεRII	Fc receptor II for IgE
AIT	Allergen-specific immunotherapy	CD23	Clusters of Designation 23
SLIT	sublingual immunotherapy	CD4+	cluster of differentiation 4
SCIT	subcutaneous immunotherapy	Der f	<i>Dermatophagoides farinae</i>
IgG ₄	immunoglobulin of subclass 4	Eur m	<i>Euroglyphus maynei</i>
VLPs	Virus-like particles	Blo t	<i>Blomia tropicalis</i>
TJs	Tight junction	PM _{2.5}	particulate matter 2.5
PRRs	Pathogen Recognition Receptors	WHO	World Health Organisation
TLR	Toll-like Receptor	IUIS	International Union of Immunological Societies
PAMPs	Pathogen-associated molecular patterns	ISAC	Information Sharing and Analysis Center
LPS	<i>Lipopolysaccharides</i>	AA	Amino acid
DAMPs	damage-associated molecular patterns	Cys	<i>Cysteine</i>
HMGB1	high-mobility group box 1	His	Histidine
ATP	Adenosine triphosphate	Gln	Glutamine
GM-CSF	Granulocyte-macrophage colony-stimulating factor	Asn	<i>Asparagine</i>
IL	<i>Interleukin</i>	CCL	C-C Motif Chemokine Ligand
		a1	antitrypsin

SPs	Surfactant proteins	Fc γ RIIb	Fc receptor IIB for IgG
DC-SIGN	Dendritic Cell-Specific Intercellular adhesion molecule-3-Grabbing Non-integrin	IgE-FAB	IgE-facilitated binding
PAR	protease-activated receptors	LNs	lymph nodes
CX3CL	C-X3-C Motif Chemokine Ligand	APCs	Antigen Presenting Cells
TGF- β	transforming growth factor-beta	BCR	B-Cell Receptor
Tregs	regulatory T cells	RNA	Ribonucleic acid
Bregs	regulatory B cells	Lys	Lysine
IgE	Immunoglobulin E	Asp	<i>Aspartic acid</i>
IgG	Immunoglobulin G	FbaB	fibronectin-binding protein
DNA	deoxyribonucleic acid	μ g	microgram
mRNA	messenger Ribonucleic Acid	μ l	microliter
ILIT	Intralymphatic immunotherapy	mM	millimolar
EPIT	Epicutaneous immunotherapy	ml	milliliter
OIT	Oral immunotherapy	M	Molar
LCs	Langerhans cells	$^{\circ}$ C	degree Celsius
SPT	Skin Prick Test	V	Voltage
mAbs	monoclonal antibodies	μ F	microfarad
ITIM	immunoreceptor tyrosine-based inhibition motif	Ω	ohm
		nm	nanometer

CHAPTER I

INTRODUCTION

Allergens are environmental proteins which trigger typical T_H2 -biased allergic responses in atopic patients, leading to various allergic diseases including asthma, rhinoconjunctivitis, sinusitis, food allergy, atopic dermatitis and anaphylaxis (1, 2). Certainly, allergic diseases can be considered as a major public health problem in Thailand as we can consider that, similarly to western and Asian countries, roughly 70-90% of Thai population are sensitized to allergens (3, 4).

House dust mite (HDM) represents one of the most important allergenic sources worldwide. Currently, more than 30 HDM allergen groups which can induce specific IgE in atopic patients have been identified (5). The group 1 allergen, from the HDM species *Dermatophagoides pteronyssinus* (Der p 1) is one of the most potent HDM allergen as more than 80 percent of HDM allergic populations are sensitized to Der p 1 (6). Der p 1 belongs to the papain-like cysteine protease family and expressed as an inactive zymogen named ProDer p 1 (PD1). Whereas the prosequence locks the active site of Der p 1, this sequence plays as well as the role of chaperonin for the appropriate Der p 1 folding (7). The autocatalytic maturation of Der p 1 under acidic conditions gradually degrades the prosequence to restore the proteolytic activity of the allergen (8, 9).

Natural Der p 1 can be isolated from exhausted mite culture extracts at, however, limited amounts. The alternative is the expression of recombinant Der p 1. By this method, we could expect to obtain unlimited amount of this protein (10). Although prokaryotic expression system such as *E. coli* is commonly selected as the first choice to produce recombinant proteins, the prokaryotic expression level of Der p 1 is low and the protein does not display any enzymatic activity due to improper folding (11). For that reason, yeast expression system such as *Pichia pastoris* was selected and able to produce, secrete and correctly folded recombinant ProDer p 1 (PD1) (12). The subsequent maturation of PD1 into active Der p 1 can take place in a second step.

Conventional allergen-specific immunotherapy (AIT) based on the repeated sublingual or subcutaneous administrations of the sensitizing allergen extracts, aims to shift the allergen-specific T_H2 response in allergic patients to a non-pathogenic one through the induction of allergen-specific T_H1 or T regulatory (Treg) cells (13). Effective AIT clearly improves the quality of life through the reduction of clinical symptoms and medication usage and shown to reduce seasonal increases in specific IgE. However, the clinical efficacy of AIT depends on the quality of natural allergen extracts and several issues negatively impact successful AIT as efficacy, side effect, low patient adherence and cost of the treatment due to its duration (14). New immunotherapeutic approaches based on highly purified and characterized recombinant allergen derivatives have been an alternative to improve AIT in terms of treatment duration, side effect and efficacy (15). However, as proteins are intrinsically poorly immunogenic, treatments based on recombinant allergen administration request the use of adjuvant to improve the immunogenicity. However, only few adjuvants can be used in humans and display some limitations as formulation, toxicity, and cost.

Strategies favoring the development of blocking allergen-specific IgG antibodies seem to be preferable as judged by the successful Phase 1b evaluation of neutralizing anti-Fel d 1 monoclonal IgG4 antibodies. A single passive antibody administration reduced the clinical symptoms of cat allergy with the same efficiency as a 2 year long conventional AIT with cat allergen extracts (16, 17).

In the context, Virus-like particles (VLPs) displaying multiples copy of major HDM allergens could represent an interesting approach to optimize AIT for the treatment of HDM allergy. One of the most useful VLP platform is based on the production of recombinant coat protein of bacteriophage AP205. Indeed, the expressed protein in *E.coli* self-assembles spontaneously to create a particle with 180 copies of the coat protein. In order to display HDM allergens to the VLP surface, the SpyTag/SpyCatcher technology is a convenient conjugation system which allows to maintain any antigen under a correct fold (18, 19). AP205 VLP coat protein fused with the SpyCatcher protein can maintain its capacity to self-assemble (20). Any HDM

allergen expressed with a SpyTag at the N-or C-terminus can be conjugated to SpyCatcher-VLP through an iso-peptide bond formation.

The goal of this project aims to evaluate the allergenicity and the immunogenicity of a new vaccine candidate based on bacteriophage-based virus like particle (VLP) displaying multi-copies of hypoallergenic form of Der p 1 allergen using the SpyTag/SpyCatcher technology (Fig.1.1)

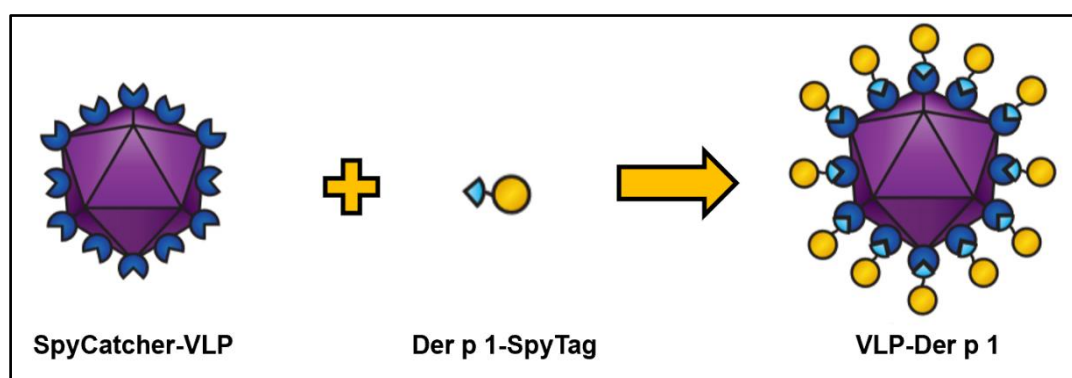


Figure 1.1 Der p 1-SpyTag conjugated with SpyCatcher-VLPs model (Modified from (18))

We hypothesize that our vaccine candidate, VLP-D1 could represent a new treatment of HDM allergy displaying several advantages over conventional AIT: hypoallergenicity, higher immunogenicity, shortening of treatment duration, cost-effectiveness. If our vaccine candidate shows promising preclinical results, this will lead to further testing of prophylactic and therapeutic efficacy in mouse models of HDM allergy followed by trials for the evaluation of clinical efficacy in cohorts of HDM-allergic patients.

CHAPTER II

LITERATURE REVIEW

2.1 Allergy

Allergy is an abnormal adaptive immune response against various non-infectious environmental factors known as allergens. The most common allergenic sources are animal dander, pollen, latex, cockroach, house dust mite (HDM) and certain type of food as milk, egg, wheat, peanut, or seafood. The allergic response is typically mediated by allergen-specific IgE and T-helper 2 (T_H2) cells which leads to various inflammatory disorders e.g., allergic rhinitis or asthma, rhinoconjunctivitis and atopic dermatitis (2). The development, the maintenance and the severity of the allergic responses relies on many factors such as, genetic predisposition (notably atopy), allergen exposure, environmental factors (pollutants, viruses, or bacteria) or microbiome (21, 22). According to estimates, 1-2% of the global population is affected by HDM allergy (23). In Asia, the percentages of HDM sensitization varied from 40-80%, the highest prevalence was found in Singapore (70-90%), Taiwan (85-90%), and South India (90%) (Fig. 2.1). Conversely, North India (7.8%), Vietnam (9-23%) and Philippines (33-47%) showed the lowest rate of HDM sensitized population. In Thailand, HDM sensitization levels ranged from 40 to 60 percent in atopic patients with an upward trend (3) and the incidence rate increased from 60% nearly to 80% in 2017 (24).

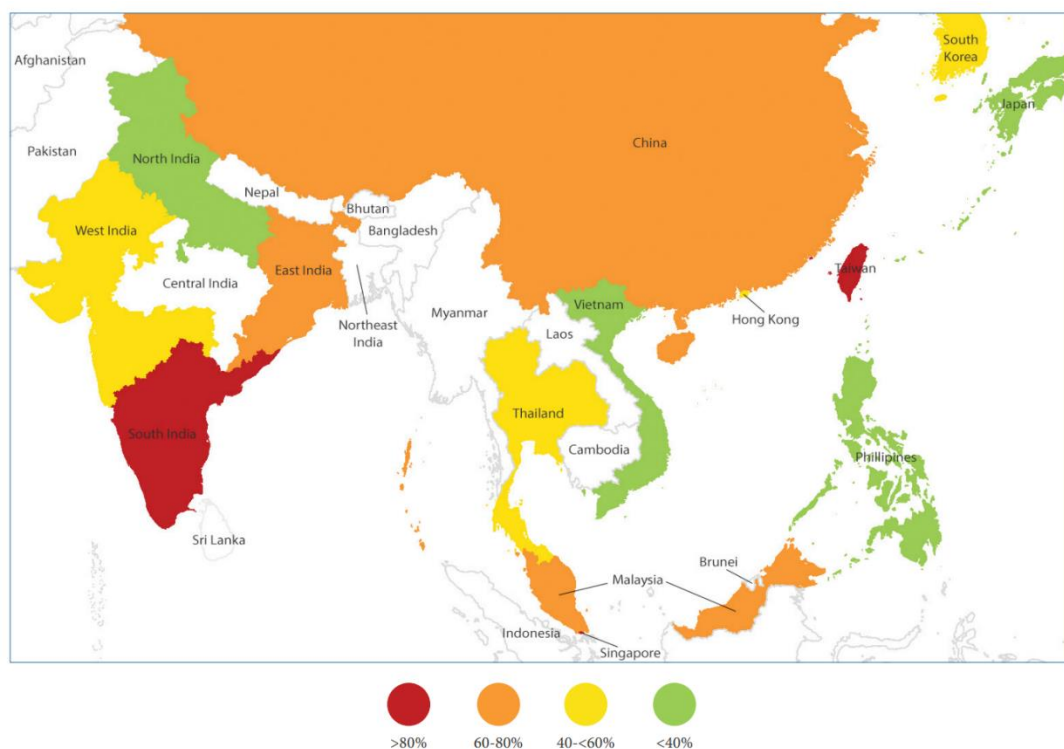


Figure 2.1 The prevalence rate of HDM sensitized patient in countries from South, South-East and Far East Asia (3)

2.2 Mechanism of the allergic response

The mechanism of the allergic response can be divided into three phases: the sensitization, early-phase reaction, and the late-phase response (25). As the project is related to HDM allergy, we will describe the allergic response triggered by airborne allergens.

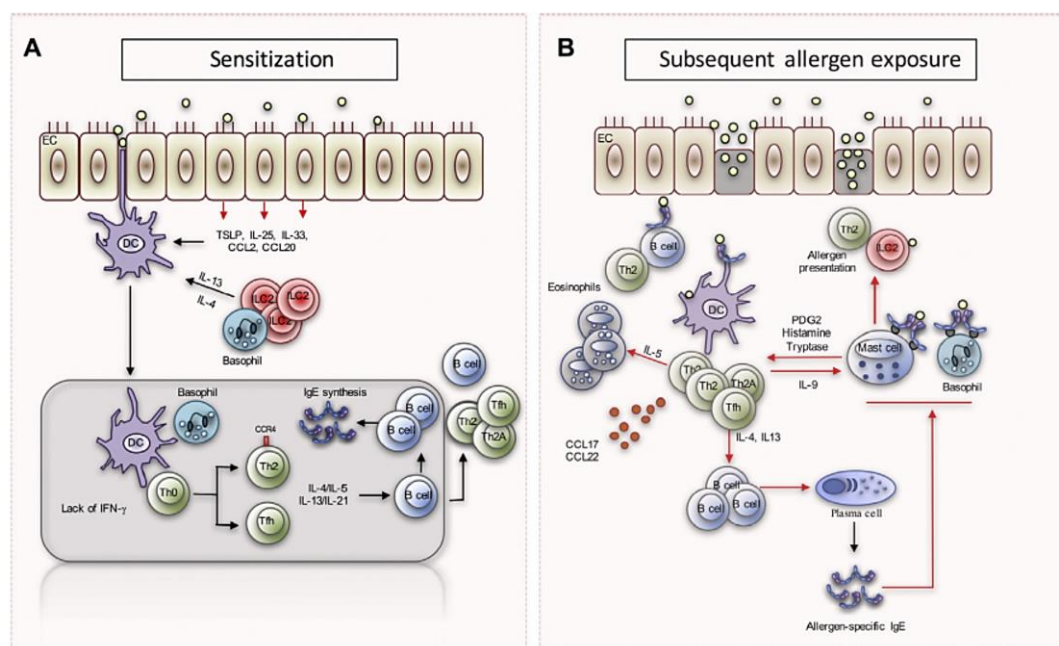


Figure 2.2A and 2.2B mechanism of the allergic response (28)

CHULALONGKORN UNIVERSITY

2.3 Sensitization phase of the allergic response

During the sensitization step (Fig. 2.2A), the inhalation of airborne allergens by atopic patients (subjects predisposed to produce specific IgE) results in the activation of the airway epithelium together with the disruption of the epithelial barrier integrity (26). Some allergens displaying proteolytic activities are directly involved in the disruption of epithelial barrier integrity through cleavage of the epithelial tight junction proteins (TJs). In addition, these airborne allergens are also associated with multiple innate immune activators such as chitin from mite's exoskeleton, endosymbiotic bacteria together with microbial/environmental (bacteria, fungi, pollutants, viruses, microparticles) compounds present in the house dust. When in

contact with airborne allergens, airway epithelium can be damaged and/or activated to trigger potent innate immune response through Pathogen Recognition Receptors (PRRs, including TLR2, TLR4, Dectin-1) interactions with microbial pathogen-associated molecular patterns (PAMPs as LPS, chitin, β -glucans) or to damage-associated molecular patterns (DAMPs as high-mobility group box 1 (HMGB1), ATP, Uric Acid) (27). Such process results in the expression of series of proinflammatory cytokines which promote the T_H2 polarization (28). Particularly, GM-CSF, IL-25, IL-33 and TSLP initiate the T_H2 polarization by the activation of type 2 innate lymphoid cells (ILC2s) and basophils, the stimulation of ILC2s by epithelial IL-25 and IL-33 leading to production of the T_H2 cytokines IL-5 and IL-13 whereas B cells can secrete IL-4 (29). These cytokines not only play important roles in the T_H2 differentiation of allergen-specific Th cells but also in isotype switching of B cells to generate allergen-specific IgE antibodies. The specific IgE can be bound to the high-affinity receptor for IgE (Fc ϵ RI) receptors present on the surface of mast cells and basophils. It must be pointed that during the sensitization phase, there is no clinical manifestation of allergy (28).

2.4 Early-phase of the allergic response

During the early-phase reaction (Fig.2.2B), the allergen re-exposure induces the binding of allergens to immobilized IgE carried by mast cells and basophils. Such interactions cause the Fc ϵ R1 crosslinking which triggers the cell degranulation and the subsequent release of histamine, lipid mediators such as prostaglandins and cysteinyl leukotrienes, chemokines, and other cytokines such as IL-4, IL-5, and IL-13. The release of such mediators contributes to the development of the allergic symptoms including vasodilation, erythema (reddening) of the skin, contraction of bronchial smooth muscle and secretion of mucus, resulting in sneezing, itching, swelling and/or wheezing. It must be pointed out that IgE could bind with inactive Fc ϵ R1 on the surface of dendritic cells (DCs) and monocytes, Fc ϵ R2 (also known as CD23), on the surface of B cells. Consequently, allergen re-exposure can trigger the allergen presentation by DCs and B cells via Fc ϵ R1/CD23-IgE complexes. The allergen uptake is followed by their intracellular processing into peptides to activate allergen specific CD4+ T cells which lead into the late phase of the allergic reaction (28).

2.5 Late phase of the allergic response

Late-phase reactions thought to be orchestrated partly by of the persistent release of inflammatory mediators by activated mast cells during early-phase reactions (IL-4, IL-5, IL-9 and IL-13) and by allergen-specific T_H2 cells (28). Indeed, the production of IL-4, IL-5, IL-9 and IL-13 by allergen-specific T_H2 cells stimulates the development and recruitment of eosinophils in the airways, the differentiation of mast cells and the inflammation of airway smooth muscles (1). After 2-6 hours from allergen exposure, late-phase reactions typically develop and peak during 6–9 hours. In lower airway of asthmatic patient, leukocytes recruited in late-phase reactions consist of T cells, granulocytes (eosinophils and smaller numbers of neutrophils and basophils) and monocytes leads to airway hyperresponsiveness which can be analyzed from bronchoalveolar lavage fluid (30).

2.6 House dust mite (HDM)

In 1964 and 1967, scientists clarified the taxonomy and determined dust mite as the source of HDM allergen (31). Dust mites are members of the phylum Arthropods, class Arachnida, subclass Acari, classified into the family *Pyroglyphidae* (Fig. 2.3) which generally can be divided into house dust mite and storage mite (32-35). *Dermatophagoides pteronyssinus* (Der p), *Dermatophagoides farinae* (Der f), and *Euroglyphus maynei* (Eur m) are considered as a major HDM allergenic species and *Blomia tropicalis* (Blo t) classified as storage mite but they are also group as the source of allergen in houses, in tropical and semitropical zone (35).

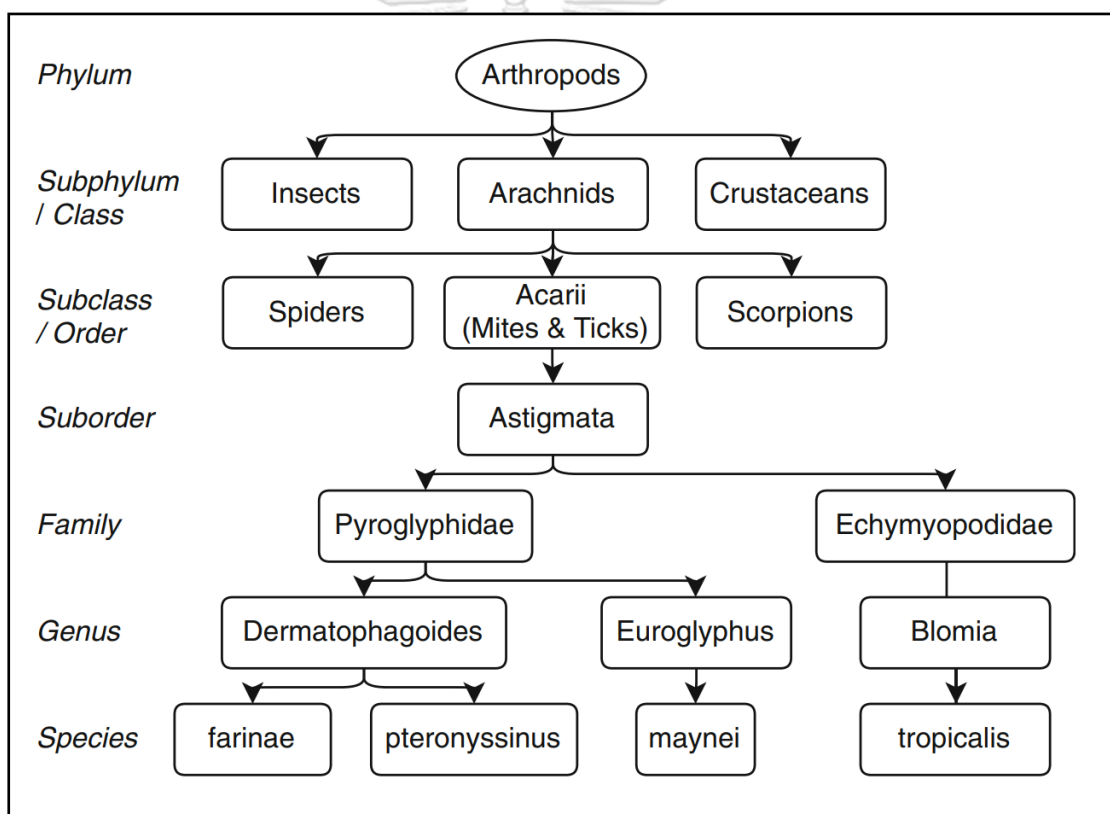


Figure 2.3 Taxonomy of HDM (35)

Under electron microscope, whole body of adult HDM has a size of around 250-350 μm in length (35). HDMs are sexual reproductive, they can live up to 48 hr with an average cycle of 60-100 days. The cycle of HDM can differ within mite families and is dependent on humidity, temperature, and food supply.

A relative humidity of 75% and a temperature of 23-30°C are essential for optimum HDM proliferation. In general, pyroglyphid have six life stages (Fig. 2.4) consisting of egg, pre-larva, larva, protonymph, tritonymph and adult (33).

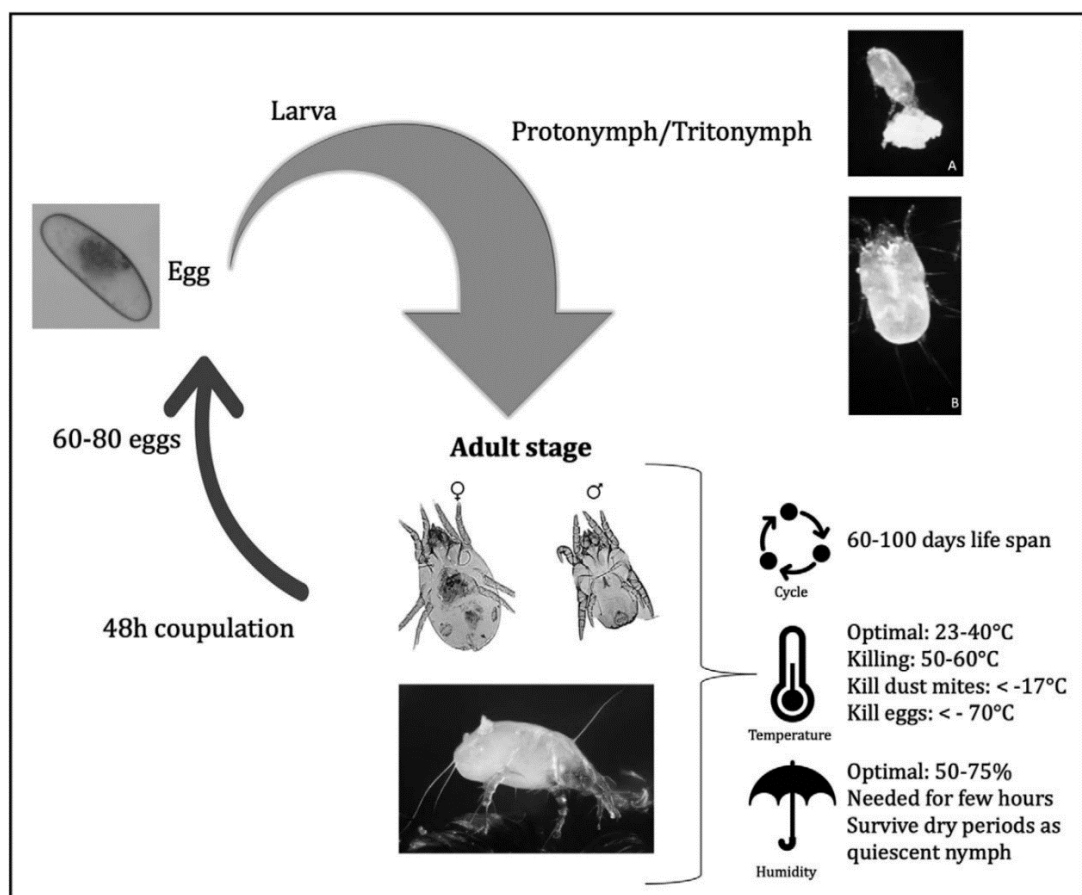


Figure 2.4 Life cycle of HDM (33)

2.7 House dust mite (HDM) allergens

In household dust, HDM allergens are present in aerosolized mite feces or fragmented bodies. Mite fecal pellets, with a 20–30 μm average diameter and surrounded by a peritrophic membrane (36), the fragment can reach the small airways which the size of particles is in between the range of 2 to 6 μm (37). As House dusts contain a large environmental factor such as bacteria, fungal spores, particulate matter ($\text{PM}_{2.5}$) (10). All these components are continuously associated with HDM mite fecal pellets and fragmented bodies.

In general, commercial, or in-house HDM allergen extracts are produced from whole mite, mite bodies or feces extracts and prepared from *in-vitro* HDM exhausted cultures. Proteomic analysis clearly identified large differences in allergenic composition and concentration between mite fecal pellets and mite bodies (38). It must be pointed out that only the most abundant HDM allergens such as Der p 1, Der p 2, Der p 3 can be directly isolated from extracts (39).

Recombinant productions of HDM allergens represent attractive alternative to HDM allergen extracts or purified natural HDM allergen in order to get access to unlimited amounts of highly purified allergens. Large-scale cost-effective productions of recombinant allergens are nowadays performed using conventional expression systems (40).

Currently, more than 39 HDM allergen groups were identified by proteomic analysis. 30 Der p derived and 36 Der f derived allergens have been officially classified by the World Health Organization (WHO) and the International Union of Immunological Societies (IUIS) Allergen Nomenclature Sub-Committee (Table. 1) (5). Whereas the biological activity of allergens from groups 1, 2, 3, 5, 6, 7, 9, 12, 13, 15 and 18 were evidenced in *in-vitro* assays (Jacquet/Robinson Allergy), the ones displayed by other mite allergens were predicted by sequential or structural homologies. Table. 1 shows that HDM allergens can be classified into 4 main groups according to their biological functions which are protease, protein displaying affinities for lipids, non-proteolytic enzyme and non-enzymatic components (41).

Table. 1 HDM Allergome from WHO-IUIS Database (5), Last accessed 14 Jul 21

Allergen group	Biological function	<i>Der p</i>	<i>Der f</i>
1	Cysteine protease		
2	MD-2-like lipid binding protein		
3	Trypsin-like serine protease		
4	Amylase		
5	Lipid binding protein		
6	Chymotrypsin-like serine protease		
7	Lipid binding protein		
8	Glutathione-S-Transferase		
9	Collagenase-like serine protease		
10	Tropomyosin		
11	Paramyosin		
12	Peritrophin		
13	Fatty acid binding protein		
14	Apolipoporphin		
15	Chitinase		
16	Gelsolin-like protein		

Allergen group	Biological function	<i>Der p</i>	<i>Der f</i>
17	Ca ²⁺ -binding protein		
18	Chitinase		
19	Anti-microbial peptide		
20	Arginine kinase		
21	Lipid binding protein		
22	Unknown		
23	Peritrophin		
24	Ubiquinol-cytochrome c reductase binding protein homologue		
25	Triosephosphate isomerase		
26	Myosin		
27	Serpin		
28	Heat shock protein 70		
29	Cyclophilin		
30	Ferritin		
31	Cofilin		
32	Pyrophosphatase		
33	α -tubulin		
34	Deaminase		
35	MD2-like lipid binding protein		
36	Unknown		
37	Chitin binding protein		
38	Bacteriolytic enzyme		
39	Troponin C		

Der p: *Dermatophagoides pteronyssinus*; *Der f*: *Dermatophagoides farinae*. Greyed out = presence

Mainly thanks to the cloning and expression of recombinant HDM allergens, a collection of studies investigated the IgE binding capacity of individual HDM allergens and classified HDM allergens as major, mid-tier and minor allergenic proteins (6). Group 1, 2 and 23 are defined as Serodominant or major allergens due to their ability to sensitize (induce the production of specific IgE) over 50% of the mite allergic subjects. Whereas Group 4, 5, 7 and 21 allergens considered as mid-tier allergen with the prevalence between 20 to 50% and the remaining allergen (Groups 3, 6, 8, 9, 10, 11, 13, 15, 16, 17, 18 and 20) showed as minor allergen with the prevalence lower than 20% in the whole study cohort (40).

In the past, the IgE reactivity has been used as important parameter for clinical treatments and commercial purposes. In fact, this terminology caused confusion among physicians in term of classification and medical treatments based on the frequency IgE-binding in the population. The concept of major and minor allergen can be used to describe the property of allergens depending on the geographical region and other factors but not necessary for clinical or commercial purposes (42). In 2021, Each of the Der p allergen groups were classified as high, moderate, or low IgE levels according to ISAC standardized IgE Units (ISU-E, 0.3-150 ISU -E range) of the frequency of IgE-binding activity in the sera of HDM allergic cohorts from Canada, Europe, South Africa and the United States of America (USA) (4) (Fig. 2.5A and 2.5B).

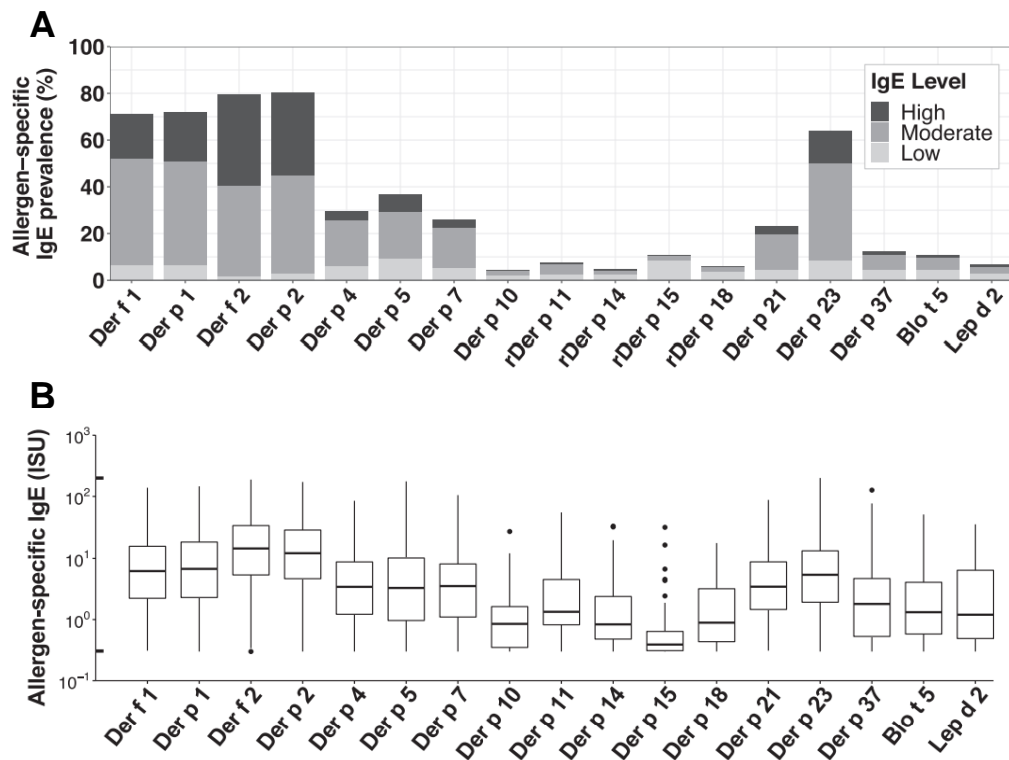


Figure 2.5 (A) IgE response to individual HDM allergen and (B) Levels of IgE specific for HDM allergens (y-axis, log₁₀ scale) in adult allergic cohorts from Canada, Europe, South Africa and the United States of America (USA) (N=685) (modified from (4))

2.8 Der p 1

Der p 1 is a cysteine protease belonging to the papain-like protease family (CA1) and are abundant especially in the fecal pellets of HDMs, suggesting that Der p 1 represents a digestive enzyme in the gut of the mite. The biological properties of Der p 1 can promote and amplify the T_H2-biased allergic response in the different cellular pathways (43). The strong protease activity of Der p 1 was shown to drastically amplify the allergenicity of Der p 1 (44) and could be explained by the protease-dependent activation of innate immune signaling pathways (45). Der p 1 was considered as the most potent HDM allergens, IgE reactivities to Der p 1 commonly reaching 80-90% in HDM allergic patients (46-48).

Der p 1 is expressed as precursor of 320 AA (PreProDer p 1) (Fig. 2.6) containing (49, 50), a leader peptide (18 AA), a prosequence (80AA) and a mature domain enzymatically active (222 AA). The Prosequence is not only a cysteine protease inhibitor which locks the Der p 1 active site but is also a chaperone which plays a critical role for the appropriate folding of the allergen (51). The catalytic site is composed on Cys34 and His170 (Der p 1 numbering) residues creating a thiolate–imidazolium ion pair interacting as well with Gln28 and Asn190 residues. Moreover, mature Der p 1 has a metal binding site, a N-glycosylation site (N52) and contains three disulfide bridges associating Cys4 and Cys117, Cys31 and Cys71, and Cys65 and Cys103 (51).

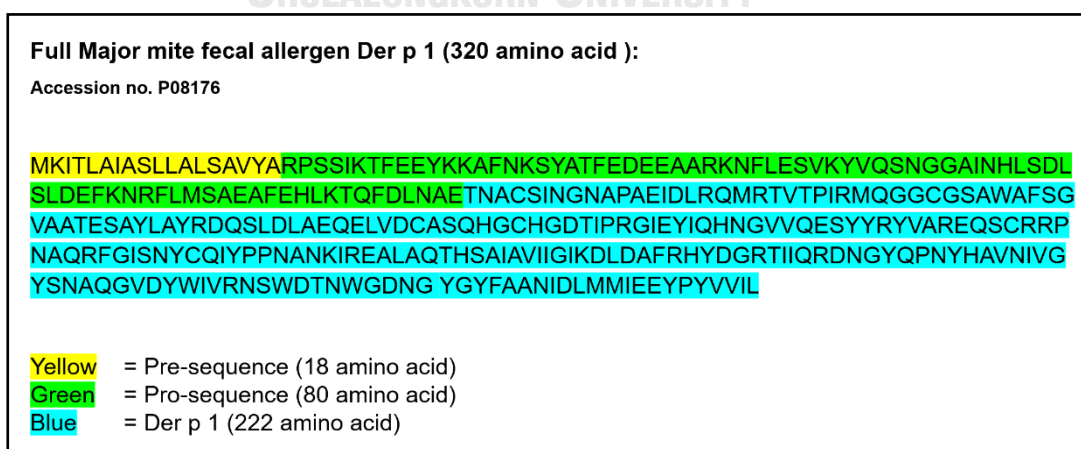


Figure 2.6 Amino-acid sequence of PreProDer p 1 (50)

The crystal structure of Derp 1 (Fig. 2.7) consists in two domains folded together in “V” configuration: a-helix domain made by three α -helices and a second one composed of five β -strands (52).

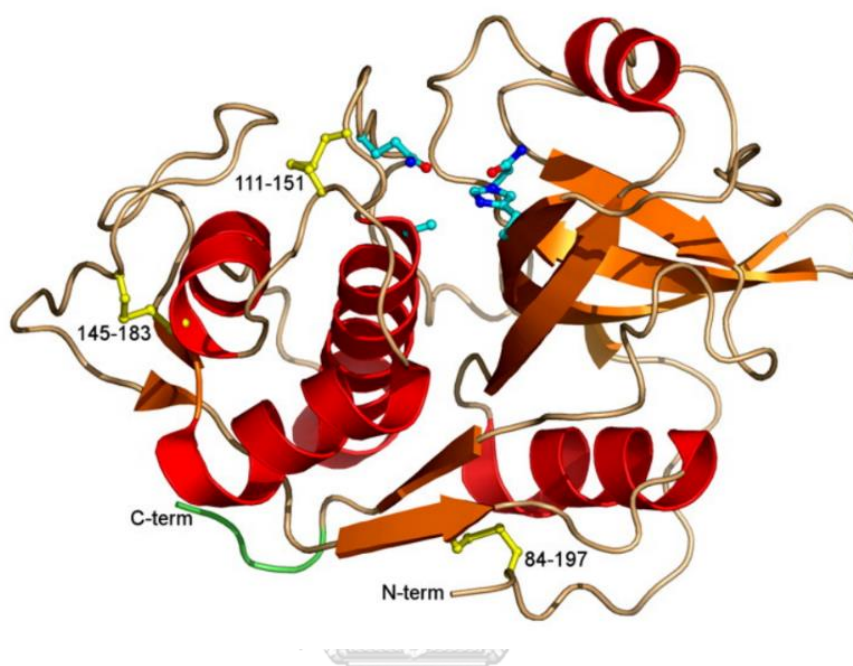


Figure 2.7 3D-Crystal structure of ProDer p 1 red color represents α -Helices, orange color represents β -strands, and yellow color represents disulfide bridges (modified from (52))

The PD1 zymogen is matured into enzymatically active Der p 1 by auto-catalytic-processing under acidic conditions, resulting in the multi-step cleavage of the Prosequence which takes place in the mite digestive tract (51, 53). The recombinant expression of correctly folded enzymatically active Der p 1 is very challenging. Previous study described that the direct expression of recombinant matured Der p 1 was unsuccessful and probably because of mature active Der p 1 could be toxic for the expressing cells and the absence of the pro-peptide (54, 55). According to the role of the Prosequence, Der p 1 needs to be expressed as a zymogen (PD1) to adopt a correct fold. The subsequent maturation of PD1 under acidic conditions could restore the cysteine protease activity of the allergen (53). The zymogen expression was successfully performed as a secreted form in eukaryotic cells (12, 56, 57). In contrast, PD1 was highly expressed in *E.coli* but as inclusion bodies (unfolded aggregates) (11).

Previous studies demonstrated that Der p 1 is the key activator of serine proteases HDM allergens Der p 3, Der p 6, and Der p 9 triggering the maturation of these allergens by the cleavage of their respective pro-peptide (8).

In mite fecal pellets, Der p 1 can cleave other unidentified target proteins (allergens, non-allergenic proteins and endosymbiotic bacteria). It is possible as well that Der p 1 is involved in the release of proteins associated to the peritrophic membrane but such biological effects remain to be investigated. When fecal pellets interact with airway mucosa, the proteolytic activity of Der p 1 could directly mediate the development of the airway inflammatory response through notably: (i) the degradation of soluble antiprotease-based lung defenses (α 1-antitrypsin, elafin and secretory leukocyte protease inhibitor) and surfactant proteins (SPs; SP-A and SP-D); (ii) the cleavage of tight junction proteins (occludin, zonula occludens-1, and cadherins) to facilitate the access of HDM allergens to immune cells (ie, type2 innate lymphoid cells [ILC2s] and dendritic cells [DCs]) in subepithelial tissue; and (iii) the production of innate proinflammatory cytokines/chemokines/alarmins (ie, IL-6, IL-8, GM-CSF, CCL2, and CCL20), (iv) the stimulation of an innate cells (ILC2 cell) and cytokines (ie IL-33 and IL-13 and IL-5) which triggered eosinophilia in the early state of airway inflammation with the absence of specific IgE production, (v) the

degradation of surface area in several cells (i.e B cells, T cells, or DCs, including CD23, CD25, CD40, dendritic cell-specific intercellular adhesion molecule 3-grabbing nonintegrin (DC-SIGN), and include DC-SIGN receptor) and downregulated T_H1 differentiation, (vi) the in-directional stimulated of PAR-1 and PAR-4 signal pathway through thrombin and (vii) the directional cleavage of membrane-bound chemokine (CX3CL1) (58).

Together with these effects, the proteolytic activity of Der p 1 could be responsible of other immunomodulations (Fig. 2.8).

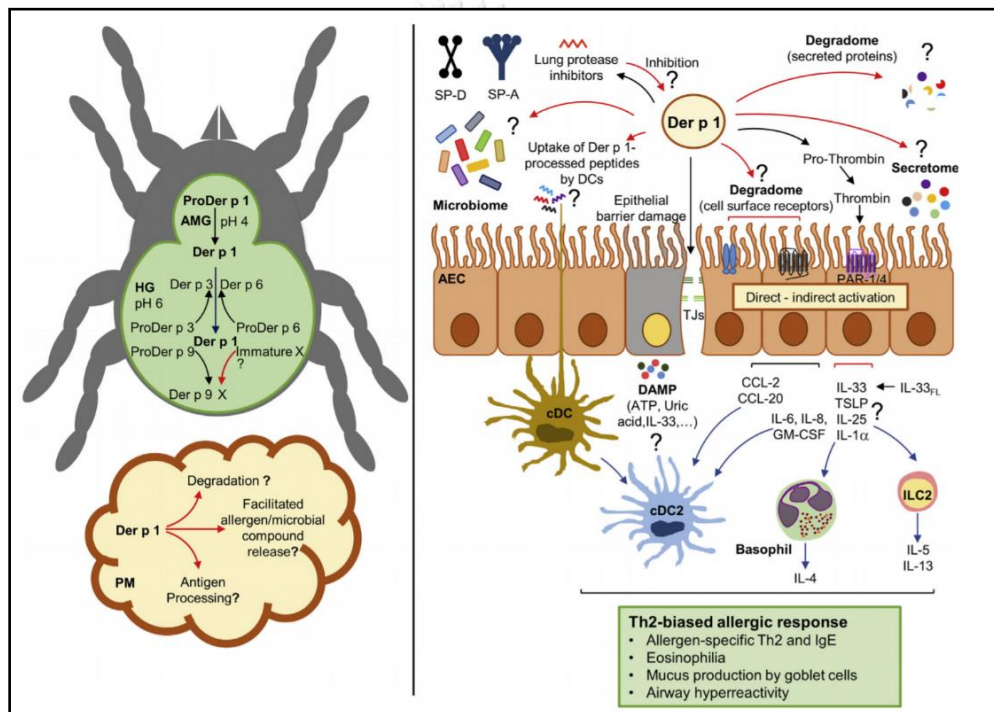


Figure 2.8 Proven and hypothetical immunomodulations mediated by the proteolytic activity of Der p 1 in the airways (58)

2.9 Allergen-specific immunotherapy

Allergen-specific immunotherapy (AIT) is a unique immune-modifying therapy which is recommended as a treatment for allergic rhinitis and asthma triggered especially by allergenic sources and notably HDM (59). Typically, conventional AIT is based on either subcutaneous (SCIT) or sublingual (SLIT) administrations of allergenic extracts (13, 60) to revert the allergic response into tolerance. These repeated allergen administrations last 2-3 years to improve the clinical symptoms, this could lead to the poor patient compliance (61, 62).

During AIT, 4 phases of events are referenced at cellular and molecular levels (Fig. 2.9). The first observed event corresponds to the desensitization characterized by reduced mast cell and basophil activation and degranulation. The process can occur within minutes to hours and lead to the reduction of systemic anaphylaxis. The second part of cellular changes includes the generation of allergen-specific regulatory T cells (Tregs), and regulatory B cells (Bregs) and suppression of allergen-specific T_H2 cells. Immunosuppressive cytokines released by Treg as interleukin 10 (IL-10), interleukin 35 (IL-35) and transforming growth factor-beta (TGF- β) together drive the suppression of the effector cells involved in allergic inflammation, such as mast cells, basophils, and eosinophils. It also prevents the proliferation of group 2 innate lymphoid cells (ILC2). The third effect of successful AIT is the induction of allergen-specific IgG4 and IgA capable to block the allergen-IgE interactions, leading to the prevention of IgE-mediated activation of mast cells and basophils. Last phase of AIT consists in long-term decrease of IgE/IgG4 ratio as well as numbers of tissue mast cells and eosinophils after several months (63, 64).

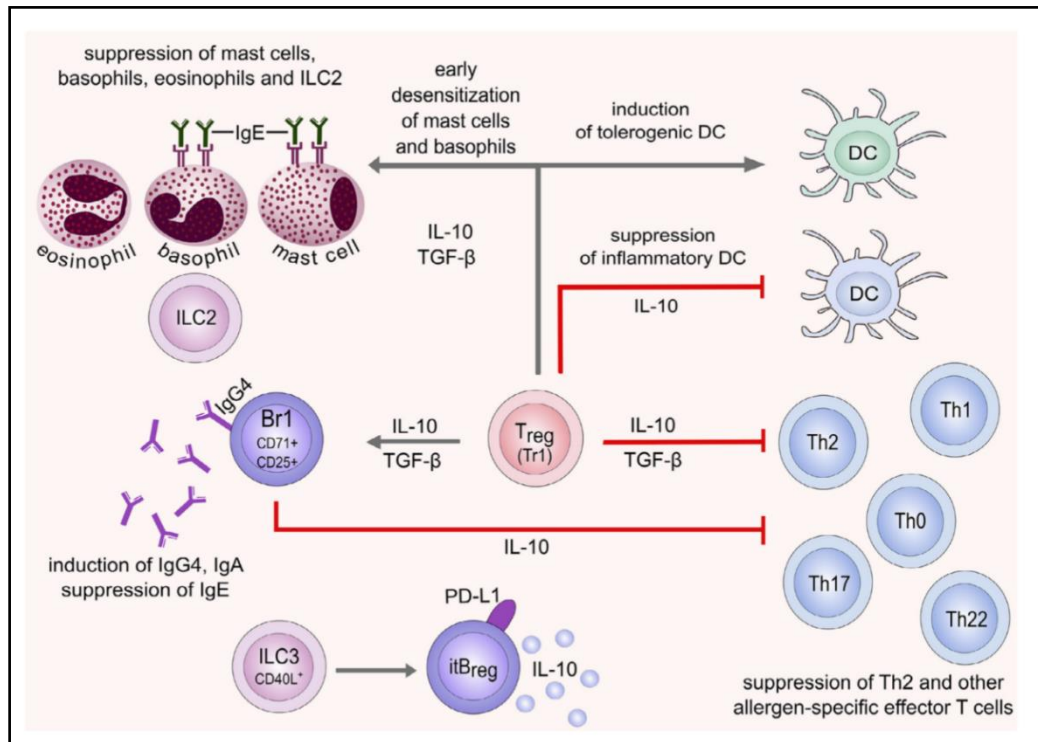


Figure 2.9 Mechanism of tolerance induction by Allergen-specific immunotherapy (63)

Together with the duration issues commonly associated with conventional AIT, anaphylactic side-effects represent important drawback as well. The incidence of AIT-induced anaphylaxis can vary from 0.1-5% in treated patients. Moreover, AIT can induce new sensitizations against allergens for which the patients were not sensitized prior to AIT (65). These two side effects result from the administration of large amounts of allergens displaying IgE reactivity along AIT protocol. It must be pointed out as well that commercial HDM allergen extracts are only standardized for Der p 1/Der p 2. The allergenic composition and concentration can not only vary from company to company but also from batch to batch (10). Aside from allergens in crude house dust mite extracts, contaminant factors such as LPS, chitin, beta-glucan also can be found and could negatively influence the success of AIT. To maximize the effectiveness of AIT, all these factors must be removed from the extracts.

Based on molecular and immunological characterization of relevant allergens, several innovative immunotherapeutic approaches (Fig.2.10) were developed and designed to replace conventional allergen extract-based AIT to improve the safety, efficacy of AIT and to reduce the duration of treatment (14, 15).

During the last decade, recombinant hypoallergenic variants were derived from multiple allergenic sources. These molecules, following the disruption of IgE binding epitopes, display very low IgE reactivity but retain their capacity to generate IgG antibody and T cell responses. However, the mapping of the IgE binding epitopes, a key prerequisite step for such development, is challenging as they are mainly conformational. Alternative method consists of chemical modification of allergen extracts to derive allergoids with reduced allergenicity (14, 15).

Synthetic peptides displaying T cell epitopes of major allergens but lacking IgE reactivity were evaluated as well. These T cell epitopes could trigger immune tolerance by different cellular mechanisms: induction of antigen-specific hyporesponsiveness (anergy), development of allergen-specific T_H1 cells, and clonal deletion of allergen-specific T_H2 cells together with the recruitment of Treg cells. Unfortunately, such vaccine candidates are poorly capable to modulate the antibody response because of the absence of B cell epitopes. Another approach consists in genetic fusion of peptides derived from the IgE binding epitopes of major allergens to a protein carrier. As IgE binding epitopes are mainly conformational, these surface-exposed peptides are hypoallergenic. Moreover, the lack of allergen-specific T cell epitopes would reduce drastically the T cell-mediated late adverse events whereas the carrier-specific T cells mediate the activation of allergen peptide-specific B cells (14, 60).

Nucleic based vaccine (DNA or mRNA-based) encoding allergens are promising AIT through the induction of allergen-specific T_H1 responses and the suppression of allergen-specific IgE. However, plasmid DNA is poorly immunogenic in primates and humans studies and conventional mRNA molecules trigger excessive levels of inflammation (15).

Another method to improve the AIT effectiveness is to optimize the administration route. Several routes were recently explored: (i) Intralymphatic immunotherapy (ILIT), This route of administration improves the antigen presentation and avoids leakage of allergens in blood vessels and tissues abundant in mast cells to minimize local and systemic side-effects, but the clinical data still showed that short-term ILIT reduced the risk of systemic adverse effects and improved clinical symptoms with the same efficiency than 3-5 years of conventional SCIT. (ii) Epicutaneous route (EPIT) could also prevents allergen absorption into the systemic circulation and maximize antigen presentation as epidermal layer of human skin which contain antigen-presenting Langerhans cells (LCs). (iii) Oral immunotherapy (OIT) is mainly found in digestion-resistant food allergens not for respiratory allergy. OIT studies indicate that beneficial effects depend on the induction of allergen-specific IgG antibodies (14, 15).

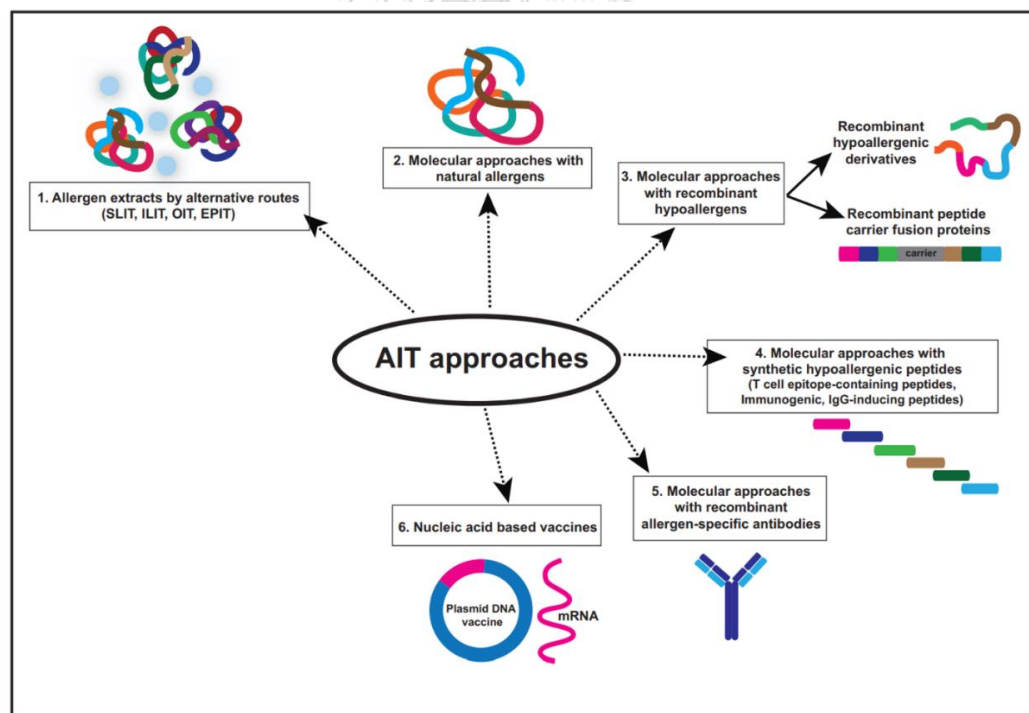


Figure 2.10 Overview of new allergen-specific immunotherapy approaches (modified from (15))

Several recombinant vaccines based on Der p 1 were evaluated in preclinical studies. Their effects on the Der p 1-specific allergic response are summarized in Table. 2.

Table. 2 Vaccine candidate development based on Der p 1 allergen (modified from (66))

Type of the vaccine/approach	Allergens	Effects	Ref.
Hypoallergenic hybrid molecules	Der p 1, 2, 7, 8	Reduced IgE reactivity, no basophil activation, IgG blocking antibodies	(67)
Hypoallergenic hybrid molecules	Der p 1, 2	No IgE reactivity, reduced SPT, T cell response, no basophil activation, IgG blocking antibodies.	(68)
Hypoallergenic hybrid molecules	Der p 1, 2	No IgE reactivity, no basophil activation, T cell response, IgG blocking antibodies	(69)
Chimeric allergens	Der p 1 and Der f 1	Reduced IgE reactivity, prophylactic evaluation with T _H 2 to T _H 1-Shift: less specific IgE/IgG1, specific IgG2a/IFN γ induction	(70)
Aggregated allergen	Der p 1 (produced in <i>E.coli</i>)	Reduced IgE reactivity, reduced basophil activation, T cell response, prophylactic efficacy and therapeutic evaluation in mouse model of HDM allergy	(11)

Type of the vaccine/approach	Allergens	Effects	Ref.
Aggregated allergen	Der p 1 (produced in CHO cells but heat denatured)	Reduced IgE reactivity, prophylactic efficacy and therapeutic evaluation in mouse model of HDM allergy	(71)
Hypoallergenic vaccines by point mutations	Der p 1, Der f 1	Reduced IgE Ab binding for immunotherapy	(72)
Hypoallergenic DNA vaccine by linear Der p 1 B cell epitope	Q β -Der p 1	Induced high specific-IgG titer within 4 weeks	(73)
T-cell epitope	Der p 1	Treg cells remained present at high frequency after 3 years Treg cells remained present at high frequency after 3 years induce Treg cell, increase IL-10 and IL-22	(74)

2.10 Importance of allergen-specific blocking IgG responses for successful AIT

The development of HDM allergen-specific blocking IgG antibodies by AIT responders represent key parameters for successful AIT (75). To our knowledge, only the blocking capacity of specific IgG1/IgG4, which compete with IgE for allergen binding, is correlated with successful AIT and, consequently, has been suggested as a biomarker to monitor the clinical efficacy of AIT (16). Safer immunotherapeutic approaches were continuously tailored to shorten the treatment protocols and to improve the efficacy of AIT (60). Strategies favoring the development of blocking allergen-specific IgG antibodies seem to be preferable as judged by the successful Phase 1b evaluation of neutralizing anti-allergen monoclonal IgG4 antibodies (15).

Recent studies reported the direct administration of allergen-specific monoclonal as a cocktail of 2 Fel d 1-specific blocking IgG antibodies (REGN1908 and REGN1909) was well-tolerated and effectively reduced the allergic response in cat allergic symptoms subjects with sustained effects up to 12 weeks in some subjects (16, 17).

Preclinical and phase 1 studies demonstrated that a single subcutaneous dose of a cocktail of 3 human IgG4 mAbs (REGN5713/14/15) bind independently and noncompetitively to Bet v 1 and provided maximal inhibition of Bet v 1 binding to human polyclonal IgE and potently blocked basophil activation *ex-vivo* and mast cell degranulation *in-vivo*. The suppression of the allergic response to other cross-reacting allergens by the novel Bet v 1 mAb cocktail may offer a therapy for the prevention and treatment of seasonal birch and related allergies with rapid onset at 1 week and sustained over 2 months (76, 77).

Several molecular mechanisms could mediate the protective effects of the allergens-specific blocking IgG (Fig. 2.11). Blocking IgG have ability to block allergen-induced IgE-dependent histamine release by basophils/mast cells. Next, inhibitory antibodies could be mediated through the co-aggregation of inhibitory (Fc γ RIIb) receptors with high-affinity Fc ϵ RI-IgE receptors. Fc γ RIIb receptors possess an immunoreceptor tyrosine-based inhibition motif (ITIM) that can be inhibit the Fc ϵ RI signaling to prevent allergen-induced activation of mast cells and basophils (78). Blocking antibodies could prevent the IgE-facilitated antigen presentation by B cells or APCs leading to reduction in T cell activation to compete with IgE for allergen binding to Fc ϵ RI/CD23 on the surface of DC/B cells. Of note, the suppression of allergen-IgE-binding to B cells (IgE-facilitated binding, IgE-FAB) correlated closely with the observed subsequent inhibition of allergen-induced T-cell proliferation (following IgE-facilitated allergen presentation (IgE-FAP) to T cells (79).

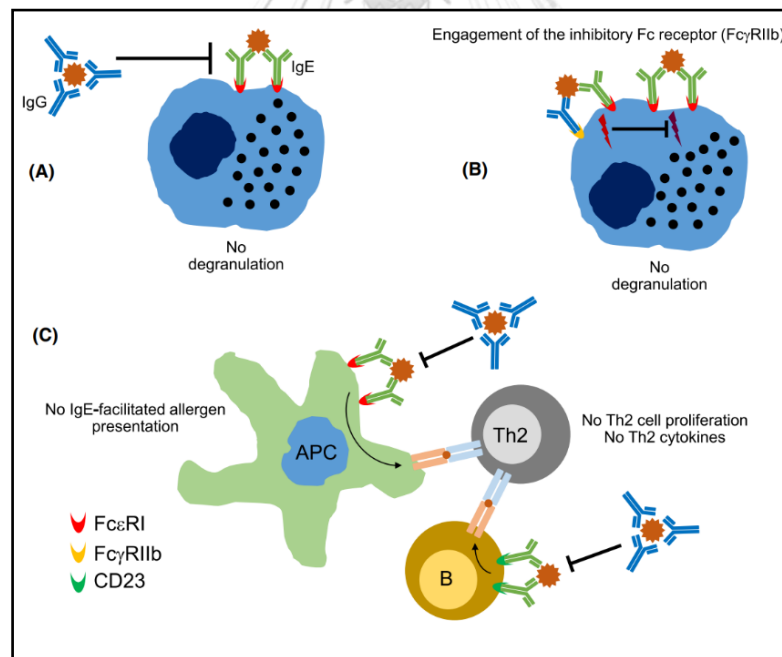


Figure 2.11 Mode of action of specific IgG blocking antibodies in successful AIT (14). (A) direct allergen neutralization, (B) prevention of the inhibitory Fc receptor (Fc γ RIIb) to allergen-induced activation of mast cells and basophils; and C) prevention of IgE-facilitated allergen presentation

2.11 Virus-like particles

Virus-like particles (VLPs) are multimeric structure made of viral capsid proteins that spontaneously self-assemble into particles (Fig.2.12). The size of VLPs ranges from 20 to 200 nanometer which is optimal of the antigen uptake by antigen-presenting cell (80-83).

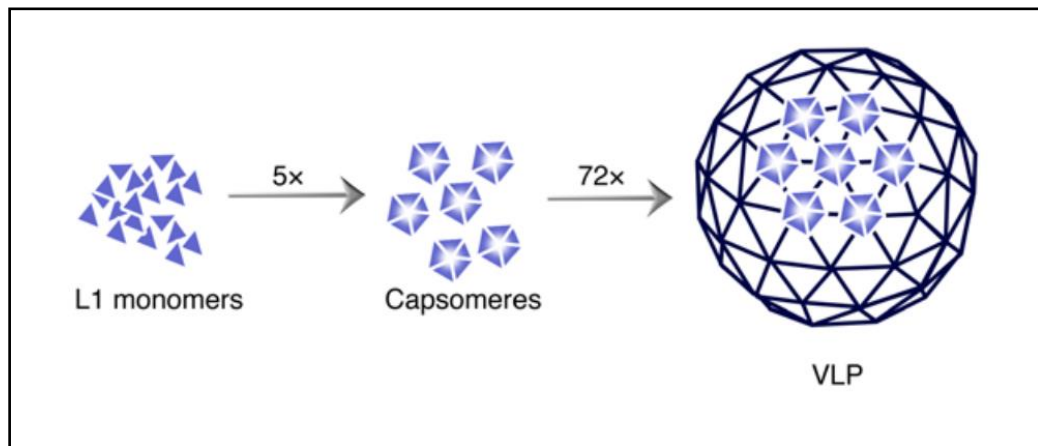


Figure 2.12 Self-assembly of HPV-16 L1 monomers to create a HPV-based VLP (83)

Subunit vaccines based on monomeric antigens are intrinsically poorly immunogenic. The immunogenicity of these vaccine candidates is drastically improved by formulation with adjuvants. In contrast VLPs, through the repetitive array of antigens at high density are highly immunogenic for the following reasons:

1) The draining of VLP to lymph nodes (LNs) is an essential property to stimulate adaptive B and T cell. Remarkably, the diameter of VLPs ranging from 10 to 200 nm are small enough to allow the direct drainage of VLPs on through 200 nm pores of the lymphatic vessel wall. Alternatively, the protein scaffold on the VLP surface can strongly interact with APCs (especially DCs and macrophage) at the injection site. These multiple interactions optimize the antigen transport/uptake mediated by APCs. Once in the B cell follicle (Fig. 2.13A), VLPs trigger the proliferation and differentiation of B cell maturation to generate the plasma cell and memory B cells (84, 85).

2) Whereas monomeric antigens weakly interact with single B cell receptor (BCR), the repeated array of VLP antigen strongly interact simultaneously with several BCRs with high affinity (Fig.2.13B). These bindings induce potent B cell activation leading to the development of high levels of antibodies with high affinity. Several parameters such as BCR affinity for the antigen, antigen valency and antigen spacing (density and steric arrangement) could influence the strength of BCR activation and consequently the antibody responses (85).

3) VLPs can retain the capacity to package nucleic acids (Fig. 2.13C). As the viral genome is not used for the heterologous expression of VLPs, the particles can package host-cell genetic materials during the assembly process. VLPs derived from ssRNA bacteriophages in bacteria typically encapsulate host-cell RNA which are Toll-like receptor (TLR) 7/8 activators. Moreover, it is possible to disassemble the ssRNA bacteriophage based VLP to replace RNA by unmethylated CpG motif rich DNA sequences (TLR9 agonist) before the reassembly inside for TLR9 activation. Intrinsic TLR7/8/9 signaling are important for B cell differentiation and up-regulation of germinal center formation leading to long-lived antibody-secreting plasma cells and memory B cells (85).

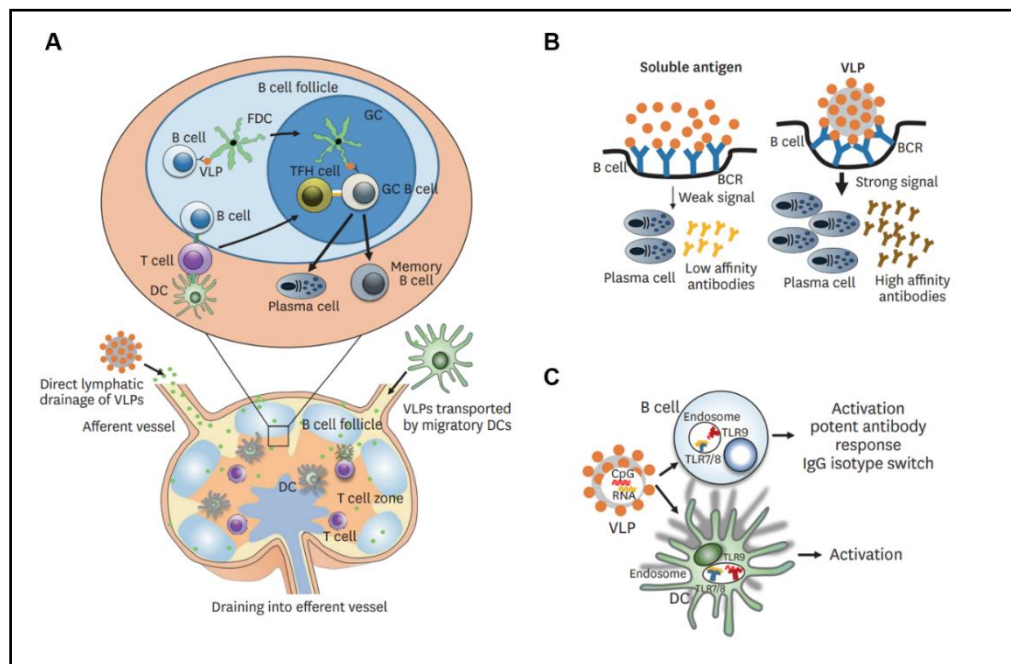


Figure 2.13 The key properties of VLPs to induce immunogenicity; (A) the trafficking of VLPs in the lymph nodes, (B) the interactions with BCR for potent antibody response and (C) the activation of antibody response through TLR7/8/9 signaling on B cells surface by VLPs (modified from (85))

The VLP protein scaffold was also used to display foreign antigens in order to amplify their immunogenicity. Two main methods (Fig.2.14) were used to create such chimeric VLPs: chemical conjugation and genetic fusion (86).

The chemical coupling normally uses reactive amino acid residue naturally displayed on VLP surface such as Cysteine. With the free sulfhydryl group, disulfide bonds can spontaneously form with other sulfhydryl-containing ligands or targeted allergen under optimal conditions (87).

For the genetic fusion, the cDNA encoding antigen is fused to gene encoding the coat protein. Once expressed, the fusion protein could reassemble to constitute VLPs. Although several chimeric VLPs were successfully designed by these two methods, conjugation heterogeneities and stability issues are commonly observed. The fusion of large antigens and steric hindrance could negatively affect the fusion protein arrays and compromise the VLP assembly (87).

Another technology is SpyTag/SpyCatcher system (Fig.2.14), this conjugation method not only greatly simplifies the conjugation between the target antigen and VLP under physiological condition but prevents steric hindrance issues and heterogenous antigen display (19, 88). This conjugation system is based on the formation of isopeptide bond between two amino acids, Lys and Asp, presents in the two split units (SpyCatcher and SpyTag) of fibronectin-binding protein (FbaB) from *Streptococcus pyogenes*. When both units present in solution, highly stable amide bond can be spontaneous forms, offer a simple way to conjugate a VLPs (20).

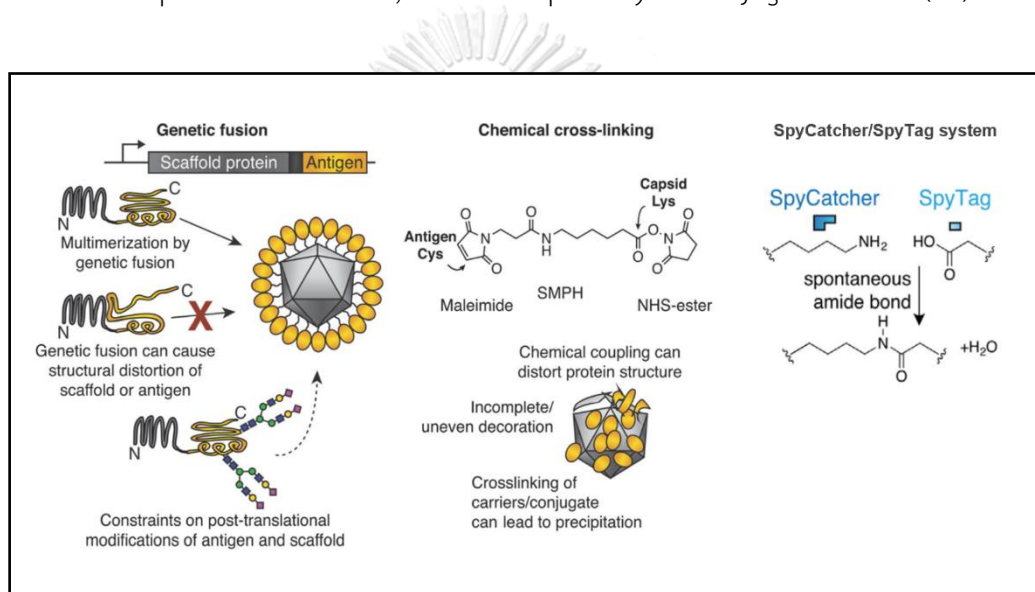


Figure 2.14 Overview VLPs assembly using Genetic fusion, Chemical cross-linking or SpyCatcher/SpyTag conjugation for chimeric VLPs (modified from (86))

From this technology, the research developed a genetically modified *Acinetobacter* phage AP205 VLPs which displays either SpyCatcher or SpyTag molecule (Figure 2.15). This VLP platform is capable to display any antigen on the particle surface without any disruption of the particles. VLP-antigens produced by this technology were shown to be highly immunogenic by notably the strong production of specific antibodies (20, 89). Other properties of AP205 VLPs showed encapsulated the host-cell RNA which could be potent to activate the TLR7/8. Moreover, TLRs

signaling mediated the isotype switching on B-cell which directly specific to IgG2a/c in mice and IgG1 in human (90, 91).

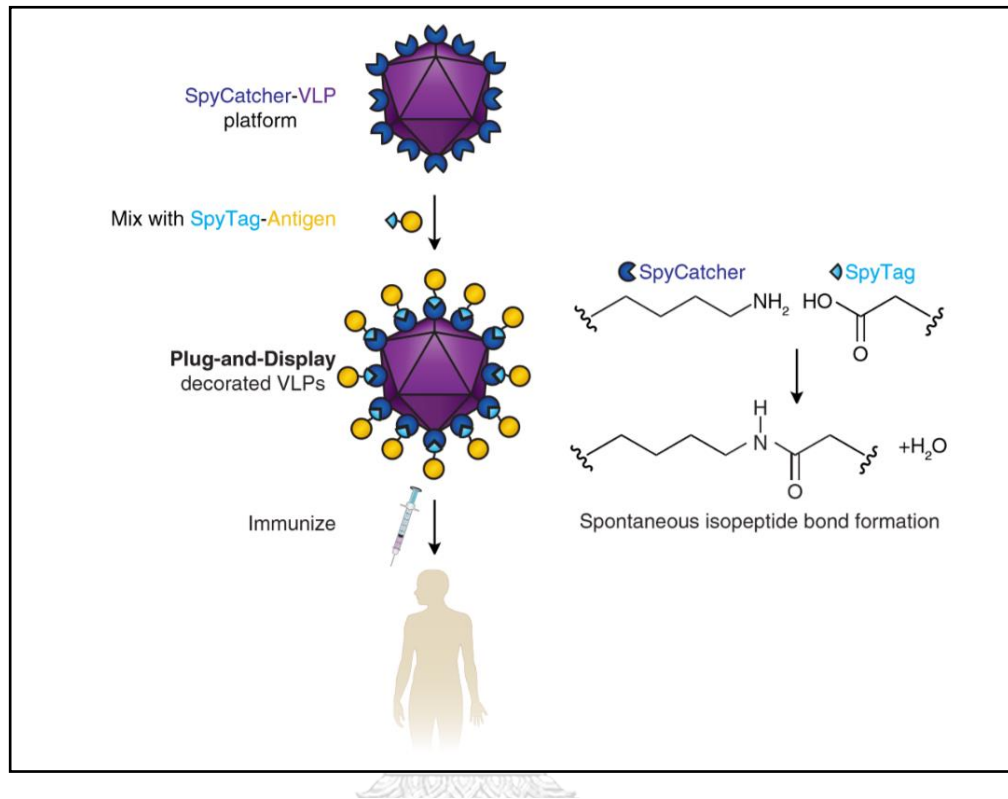


Figure 2.15 Overview display VLPs assembly using SpyTag/SpyCatcher conjugation system (modified from (18))

2.12 AIT based on VLP displaying allergens

Immunotherapeutic treatments based on VLP-allergen have been reported in both preclinical and clinical trials. A first preclinical study described the display of full-length major cat allergen Fel d 1 on the surface of bacteriophage Q β -VLPs (92). Mice immunizations showed that Q β -Fel d 1 is highly immunogenic and capable to induce potent specific antibody response following only a single immunization. The result showed vaccination with Q β -Fel d 1 can strongly reduce immediate type I allergic responses in a mouse model of mast cell degranulation, vascular leakage, anaphylaxis and eliminate IgE B cell memory responses upon antigen re-exposure (93). In clinical trial, Q β -Der p 1 (an immunodominant epitope of Der p 1, CGIYPPNANKIREALAQTHS) was evaluated in term of the safety and immunogenicity in human subjects and compared different doses and routes of immunization. The result concluded that the vaccine Q β -Der p 1 was well tolerated and has significantly higher IgG titers (73).

Another study in reported the preventive effect of virus-like nanoparticles (VNP) encapsulating the major allergen Art v 1 comparing to surface-exposed allergens in a humanized mouse model of mugwort (*Artemesia vulgaris*) allergy sensitized via intranasal administrations (94). The result showed that expressing the allergen shielded by the viral envelop was able to prevent the development of specific IgE after challenges with pollen extracts. This shielded allergen was hypoallergenic as they hardly induce degranulation of rat leukemia cells sensitized with Art v 1-specific mouse or human IgE and was able to induce T_H1/Treg cytokine response, increased Foxp3⁺ Treg numbers in lungs, and reduced lung resistance when compared to mice treated with empty particles (94).

In 2020, the study reported successfully multimerized recombinant Der p 2 (rDer p 2, D2) on the surface of VLPs (95) using the AP205 Split-protein (SpyCatcher/SpyTag) Plug and Display technology (20). Prophylactic vaccinations with hypoallergenic VLP-D2 elicited strong anti-D2 blocking IgG titers and prevented the development of HDM-induced allergic response as evidenced by the absence of specific IgE and by a marked reduction of airway eosinophilia (95).

CuMVT-VLP platform was recently reported as another platform for displaying the peanut allergen, Ara h 1 or Ara h2, to prevent peanut allergy as well in 2020. This study showed that CuMVT-rAra h 1 has hypoallergenic and develop specific IgG1 response protective against anaphylaxis. The protective effects depend on inhibitory Fc γ R1b receptor of the complex IgG with allergen in the term of anaphylaxis regulation. Moreover, in the chronic animal model showed that CuMVT-rAra h1 inhibited the remaining of eosinophil and mast cell into gastrointestinal tissue after oral challenge with peanut (96).

CHAPTER III

MATERIALS AND METHODS

3.1 Patients' sera

D. pteronyssinus ImmunoCap-positive sera from patients with HDM-associated allergic rhinitis, asthma or dermatitis were obtained from The King Chulalongkorn Memorial (n = 9), Children (n = 12), Ramathibodi (n = 2) and Phramongkutkiao (n= 1) hospitals respectively and after informed consent and approval of the local ethics committee were obtained. (IRB approval no. 023/55). Their use for the present study was approved by the Institutional Review Board of the Faculty of Medicine, Chulalongkorn University, Thailand (IRB approval no. 431/62). ELISA assays demonstrated that all the patients were sensitized to Der p 1.

3.2 Cloning of PD1-ST derivatives

To generate the SpyTagged-PD1 series, synthetic genes encoding full-length PD1 (Fig.3.1A) or a fragment of PD1 combined with a short linker (GGG) or extended linker (GSGTAGGGSGS) and SpyTag (AHIVMVDAYKPTK) were designed and cloned into pUC57 vector (GenScript Biotech, New Jersey, USA) (Fig.3.1A to 3.1E). Some genes carried single or double mutations affecting the active site cysteine residue (C34A, Der p 1 numbering) and/or the N-glycosylation site (N52Q) of mature Der p 1.

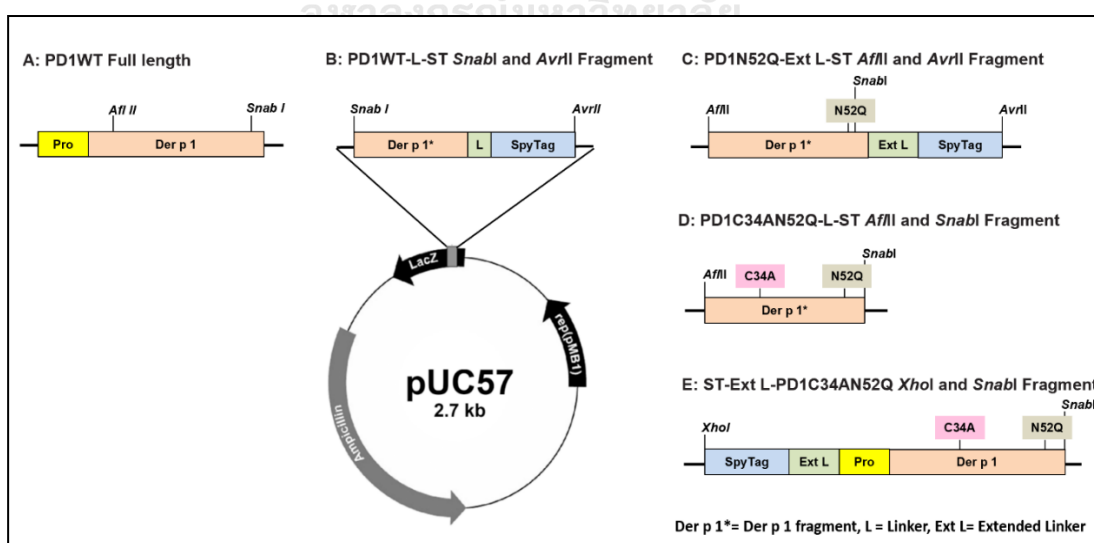


Figure 3.1 Series of Synthetic gene PD1-ST fragment cloned into pUC57 vector

The different DNA pieces encoding fragments of full-length were cloned into pNIV4846 (recombinant pPIC9K-PD1WT (12)) to replace the corresponding wild-type DNA sequence by double restrictions (New England BioLabs, United Kingdom) (Fig.3.2A to 3.2E). In that way, four expression vectors encoding PD1 fused to SpyTag at the C-terminus were generated: (i) PD1WT-L-ST, (ii) PD1WT-Ext L-ST, (iii) PD1N52Q-Ext L-ST and (iv) PD1C34AN52Q-Ext L-ST.

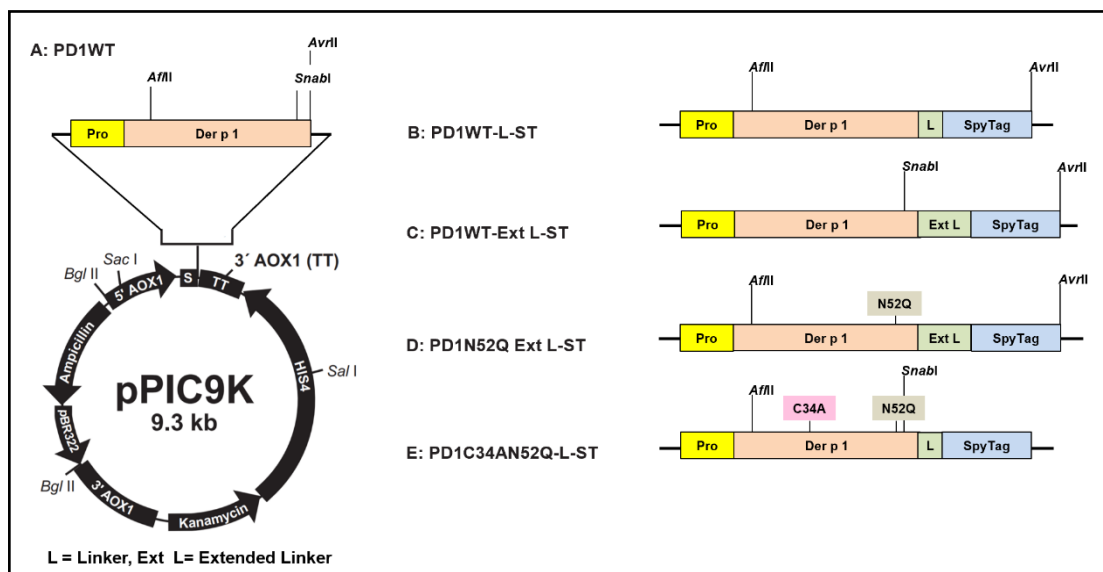


Figure 3.2 Cloning of SpyTagged-PD1 into pPIC9K vector

The synthetic genes coding for full-length ST-Ext L-PD1C34AN52Q was cloned into pPIC9K vector using the *XhoI/XbaI* restriction sites (Fig.3.3) (New England BioLabs, United Kingdom). For each construction, the enzymatic restrictions were analyzed using 1.2% agarose gel electrophoresis using TAE buffer and visualized under the UV light exposure.

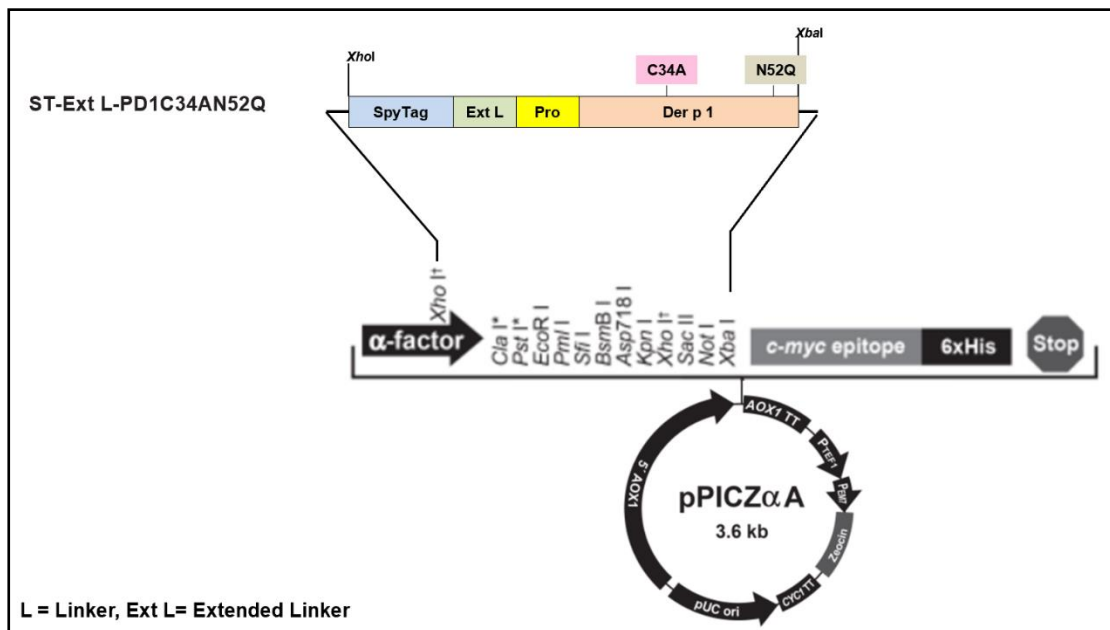


Figure 3.3 Cloning of SpyTagged-PD1 into pPICZ α A vector

3.3 In gel DNA fragment isolation

The digested expression vectors or PD1-DNA fragments used for cloning were separated by agarose gel electrophoresis and purified using QIAquick PCR & Gel Cleanup Kit (Qiagen, Düsseldorf, Germany). The agarose gel pieces containing DNA of interest were excised with sterilized sharp scalpel. The concentration of each genetic material was estimated by measuring $A_{260\text{nm}}$ using NanoDrop™ 2000 (Thermo fisher, Massachusetts, USA). The products were stored in $-20\text{ }^{\circ}\text{C}$ until use.

3.4 DNA ligation

For any ligation of DNA pieces, the insert/vector ratio was set by NEBioCalculator™ v1.10.1 (New England BioLabs, Massachusetts, USA). The insert and the vector were mixed with T4 DNA ligase buffer and 400 Units of T4 DNA Ligase (final volume of ligation mix: $20\text{ }\mu\text{l}$) for 16 hr at $16\text{ }^{\circ}\text{C}$. The ligase was subsequently inactivated at $65\text{ }^{\circ}\text{C}$ for 10 min. The products were stored in $-20\text{ }^{\circ}\text{C}$ until use.

3.5 *E. coli* competent cell preparation and Transformation

To prepare competent *E. coli* cells under aseptic conditions, *E. coli* TOP10 cells from a glycerol stock were cultured for 16 hr in normal LB (1% NaCl, 1% tryptone, 0.5% yeast extract, Bio Basic Inc., Toronto, Canada) or LB low salt broth, Lennox, Novagen (0.5% NaCl, 1% peptone, 0.5% yeast extract, Merck Millipore, Massachusetts, US) at 37 °C under shaking conditions at 200 rpm. This pre-culture was used to initiate a new culture at OD_{600nm} of 0.05 and under the same experimental conditions. Once the cell density reached OD_{600nm} of 1.0, bacteria were pelleted by centrifugation at 4,000 rpm for 5 min at 4 °C. The cells were washed with 100 mM CaCl₂ and pelleted again by centrifugation at 4000 rpm for 5 min at 4 °C. This procedure was repeated 3 times. Competent bacteria cells were finally resuspended in 500 µl of 100 mM of CaCl₂ and aliquot of 100 µl were kept on ice before transformation. For cell transformation, competent bacteria were incubated with 10 µl of each ligation mix for 12 to 15 min on ice and followed by a 42 °C heat shock for 90 sec. Cells were immediately stored on ice for 10 min. 800 µl of SOC medium (2.5 mM KCl, 10 mM MgCl₂, 20 mM Glucose and normal LB broth or LB low salt broth) was added and the cell suspensions were incubated at 37 °C for 1 hr. Cell suspensions were pelleted at 6,000 rpm for 2 min and resuspended the remaining content with 100 µl of the remaining medium. The transformed bacteria were plated on normal LB agar containing 100 µg/mL of Ampicillin for the selection of recombinant pPIC9K clones and LB low salt agar plate containing 100 µg/mL Zeocin used for the selection of recombinant pPICZαA clones. The plates were incubated at 37 °C for 16 hr to observe the growth of antibiotic resistant colonies.

3.6 Bacterial Colony PCR

Colony PCR was performed to confirm that antibiotic-resistant colonies are effectively transformed with corresponding recombinant plasmids. Five colonies from each transformation assay were picked and resuspended in 10 μl of Ultrapure™ DNase/RNase-Free Distilled Water (Invitrogen, California, USA). Then, the cells were submitted to vigorous vortexing for 15 to 20 sec and lysed at 95 °C for 5 min. For 50 μl PCR reaction, 1 μl of cell lysate was mixed with 1X GoTag® Flexi Buffer, 2 mM MgCl_2 , 0.2 mM dNTP, 0.5 μM 5'-AOX forward primer (5'-GACTGGTTCCAATTGACAAGC-3') and 0.5 μM 3'-AOX reverse primer (5'-GGATGTCAGAATGCCATTTGCC-3') and 1.25 Units of GoTag® polymerase (Promega, Wisconsin, United States). Each PCR cycle consisted in: Initial Denaturation, 95 °C, 1 min, Annealing, 55 °C, 1 min, Extension, 72 °C, 1 min using thermal cycler (Thermo fisher, Massachusetts, USA). Following 35 cycles, the different amplicons were analyzed by 1.2% Agarose Gel Electrophoresis.

3.7 Purification of recombinant plasmid for *P.pastoris* transformation

The recombinant pPIC9K or pPICZAa plasmid was isolated from bacteria using Presto™ Mini Plasmid Kit (Geneaid, New Taipei city, Taiwan). Their concentration was measured using the Nanodrop method (Thermo fisher, Massachusetts, USA). The products were stored in -20 °C until used.

3.8 *P.pastoris* transformation

To prepare yeast competent cell, *P.pastoris* SMD1168 strain was cultured in YPD medium (1% yeast extract, 2% peptone and 2% dextrose, Bio Basic Inc., Toronto, Canada) under shaking conditions using 250 rpm at 30 °C for 16 hr. This pre-culture was used to re-initiate another culture at a starting $\text{OD}_{600\text{nm}}$ of 0.3. Once the cell density reached $\text{OD}_{600\text{nm}}$ 1.3, the cells were pelleted at 4,000 rpm at 4 °C for 5 min. Yeast cells were washed with sterile Endotoxin free water, resuspended with 8 ml of competent buffer (100 mM LiAc, 10 mM DTT, 0.6 M Sorbitol, 10 mM Tris-HCl pH 7.5) and subsequently incubated on ice for 30 min. The cells were pelleted by centrifugation and washed three times with 1 M Sorbitol. Finally, the cell pellets

were subsequently resuspended in 500 μ l of 1 M Sorbitol. A series of 80 μ l aliquots was prepared and pre-chilled on ice before transformation.

Recombinant pPICZ α A or pPIC9K plasmids were linearized following *Pme*I or *Sal*I digestion (10 U of enzyme/ 20 μ g of DNA) (New England BioLabs, Massachusetts, USA) and purified by QIAquick PCR & Gel Cleanup Kit (Qiagen, Düsseldorf, Germany). Each linearized DNA was mixed with 80 μ l of *P. pastoris* competent cells for transformation by electroporation. The electroporation proceeded into 2 mm cuvettes (BioRad, California, USA) using the following settings: 5mS automatic pulse at 1,500 V, 25 μ F, 200 Ω (BioRad, California, USA). Any cell suspension transformed with recombinant pPICZ α A plasmid was directly plated on YPDS agar (1% yeast extract, 2% peptone, 2% dextrose, 1M Sorbitol and 2% agar) containing 0.1 and 0.25 mg/mL Zeocin respectively. The plates were incubated at 30°C for 3 to 4 days for clone selection. Yeast cells transformed with any pPIC9K plasmid were directly plated on RDB agar then incubated at 30°C for 3 to 4 days. RDB positive clones were subsequently selected on YPD agar plates containing 0.25 mg/mL to 2 mg/mL of Geneticin respectively. Yeast colony PCR confirmed the presence of recombinant pPIC/pPICz vectors into the selected clones.

3.9 Cloning of SpyCatcher-AP205 VLP (SC-VLP)

For the production of SC-VLP, the cDNA encoding the fusion protein was cloned into pET-15b vector. One Shot® BL21 Star™ (DE3) (Thermo fisher, Massachusetts, USA) *E.coli* cells were transformed with the recombinant construction (20). These materials were kindly provided by our collaborator, Prof. Adam Sander from the Department of Immunology and Microbiology, University of Copenhagen, Denmark).

3.10 Protein Expression

3.10.1 Recombinant SpyTagged-ProDer p 1

Single antibiotic-resistant yeast colonies were first cultured as a small scale in 10 ml for 16 hr in YPD medium (1% yeast extract, 2% peptone and 2% dextrose) at 30 °C and shaking at 250 rpm. These pre-cultures were used to inoculate BMGY medium (1% yeast extract, 2% peptone, 100 mM potassium phosphate, pH 6.0, 1.34% YNB, 4×10^{-5} % Biotin and 1% Glycerol, Invitrogen, California, USA) to initiate a second cell growth under the same culture conditions. When the cell density reached an OD_{600nm} of 6, the cells were pelleted and resuspended at a final OD_{600nm} between 1 and 3 in BMMY medium (BMGY medium but with Methanol instead of Glycerol, Invitrogen, California, USA) containing from 0.5 to 3% methanol to induce recombinant SpyTagged-PD1 expression for 72 hr. Every 24 hr, a sample of the culture was collected, and methanol was added to maintain the inducer concentration. The best expressing condition was used for the large-scale production (200 ml culture/flask) of each SpyTagged-PD1. At the day of the collection, a cocktail of protease inhibitors to (Roche, Basel, Switzerland) was immediately added culture medium containing PD1C34AN52Q-L-ST (PD1C) or ST-Ext L-PD1C34AN52Q (PD1N),

3.10.2 Recombinant SpyCatcher-AP205 VLP (SC-AP205 VLP)

An aliquot of the glycerol stock of recombinant SC-AP205 VLP *E.coli* Shuffle strain was re-streaked on LB plates containing 100 µg/mL Ampicillin. A single colony was then transferred into 2XYT Broth (2X of LB Broth, Bio Basic Inc., Toronto, Canada) for an overnight culture under agitation (200 rpm) at 37 °C. The day after, another culture in 2XYT Broth was reinitiated with a starting OD_{600nm} 0.05. Once the OD_{600nm} reached 0.8 to 1, protein expression was induced at 16 °C by addition of 0.1 mM of IPTG in the culture. After 16 hr, bacterial pellet was collected by centrifugation at 14,000 rpm for 1 min.

3.11 Protein Purification

3.11.1 Purification of recombinant SpyTagged-PD1

For the purification of recombinant Spytagged proteins were based on a combination of ion exchange and gel filtration chromatographies. After 72 hr of protein expression, large scale (200 ml) of different yeast culture supernatants containing secreted SpyTagged-PD1 were diluted ten times with Endotoxin free water and adjusted to pH 9.0 with 5 M NaOH. These samples were applied onto Q Sepharose XL beads (XR 16/20 column, Cytiva, Massachusetts, USA) equilibrated with 20 mM of Tris-HCl pH 9.0. The column was washed with the equilibrating buffer to remove unbound proteins. The column was subsequently eluted by gradually increasing the NaCl concentration in the equilibrating buffer (100 mM, 200 mM, 300 mM, 500 mM and 1 M of NaCl). The fractions at each elution step were analyzed using 12% SDS-PAGE. The proteins eluted with 100 and 200 mM NaCl were concentrated by ultrafiltration (Amicon Ultra-10K membrane, Merck Millipore, Massachusetts, US) and further purified by gel filtration using Superdex 75 (HR column 10/30, Cytiva, Massachusetts, USA), equilibrated in PBS pH 7.2 or 100 mM Acetate buffer pH 5.0. The fractions containing purified SpyTagged-PD1 were pooled and concentrated by ultrafiltration (10 kDa Vivaspin® Cytiva, Massachusetts, USA). The proteins were diluted with 100 ml of 100 mM acetate buffer pH 5 and re-concentrated by ultrafiltration. After purification step, the purified protein still contains some brownish pigment contamination. The protein will be separated into two parts (i) for conjugation purpose in the present of the pigment contaminations and (ii) for monomeric purified SpyTagged protein as a stock, these purified proteins require one extra step of pigment removal. The residual brownish pigment contamination was removed when purified proteins in pH 5 were incubated under agitation for 20 min with Blue Sepharose beads (Cytiva, Massachusetts, USA) equilibrated with 100 mM acetate buffer pH 5. Unbound pigments were washed away with acetate buffer pH 5 whereas bound SpyTagged-PD1 proteins were recovered by

elution with 20 mM Tris-HCl + 2 M NaCl pH 9. Finally, purified proteins were concentrated, buffer-exchanged into PBS pH 7.2 by ultrafiltration (10 kDa VivaSpin® Cytiva, Massachusetts, USA) and stored at -20°C.

3.11.2 Purification of of SpyCatcher-VLP AP205

Bacterial pellets from 200 ml induced cultures were resuspended in 20 ml of PBS and lysed using a cell disruptor (Pressure 2.56 kBar, model of cell disruptor, Constant System Limited, Northants, United Kingdom). The soluble materials containing SC-VLP were isolated by centrifugation at 14,000 rpm for 1 min. VLPs were purified by density gradient ultracentrifugation using Optiprep™ polymer (Sigma-Aldrich, Missouri, USA). The Optiprep™ density gradient was prepared into 12.5 ml polypropylene tube and consisted in 3 layers of Optiprep™ at 23%, 29% and 35% (3ml each). The 3 ml of bacterial lysates were then applied on the top of the gradient and ultracentrifuged at 39,000 rpm, 16 °C for 3.30 hr using SW41Ti rotor (Beckman Coulter, California, U.S.A). The arrest of ultracentrifugation proceeded without break. The polypropylene tubes were immediately removed from the buckets, pinned at the bottom to collect the density gradient into 24 fractions of 500 µl. The first ten fractions were analyzed by 15% SDS-PAGE. The fractions containing highly purified SC-VLP were pooled and dialyzed for 16 hr against PBS pH 7.2 using Biotech CE MWCO 300 kDa dialysis bag (Spectrum chemical, New Jersey, USA)

3.12 SDS-PAGE and Western blot analysis

All proteins were analyzed by SDS-PAGE using 15% polyacrylamide gels, Protein bands were detected by Coomassie blue R-250 staining (BioRad, California, USA). In another set of experiments, proteins separated by SDS-PAGE were transferred onto nitrocellulose membranes (Merck Millipore, Massachusetts, USA) by semi-dry method (25 V for 30 min). The membrane was blocked with 2.5% skimmed-milk in TBST (TBS; 8.76 g NaCl and 50 mM Tris-HCl, pH 7.5) with 0.05% Tween 20 overnight at 4°C then incubated 1 hr at room temperature with mouse anti-PD1 polyclonal antibodies (1/1,000 dilution, used for Spytagged ProDer p 1 detection) or

mouse anti-VLP-Der p 2 polyclonal antibodies (1/5,000 dilution, used for SpyCatcher-VLP detection) in TBST. These polyclonal sera were produced in our laboratory (95). The membrane was washed 5 mins for 3 times with TBST. Then, the membrane was incubated with alkaline phosphate-conjugated goat anti-mouse antibodies (1:5000 dilution) with 1% BSA in TBST, for 1 hr and washed 5 mins for 3 times with TBST. The antigen-antibody complexes were then detected using and 5-bromo, 4-chloro,3-indolyphosphate (BCIP)/ Nitroblue tetrazolium (NBT) substrates in staining buffer (100 mM Tris, 10 mM MgCl₂ and 100 mM NaCl in pH9.5).

3.13 Protein assay

The protein concentration was estimated using the microBCA protein assay kit (Thermo fisher, Massachusetts, USA) and bovine serum albumin as protein standard.

3.14 Enzymatic activity

To detect any residual protease activity in our purified SpyTagged-PD1 preparations, 1 µg purified protein (in total 200 µl) was incubated with 194 µl of buffer containing 50 mM Tris-HCl pH 8.0, 150 mM NaCl, 1 mM DTT and 1 mM EDTA at 37 °C for 15 min. The protease assay was initiated by addition of 2 µl of 40 µM Boc-QAR-pNA substrate in DMSO. OD_{415nm} was measured at every 5 mins time point for 30 mins. Positive protease assay was performed with 1 µg Trypsin (Invitrogen, California, USA).

3.15 Conjugation of SpyTagged-PD1 to SC-VLP

Purified PD1-ST and SC-VLP were mixed at a VLP/PD1 molar ratio ranging from 1:1.5 to 1:5, depending on the different tested SpyTagged-PD1. The conjugation was performed under gentle agitation at pH 5 or 7 for 16 hr at 4°C. The excess of unconjugated PD1 were removed by dialysis against PBS pH 7.2 using membrane with 300 kDa Cut-off (Spectrum chemical, New Jersey, USA). SDS-PAGE densitometric analysis was used to determine the conjugation yield. This amount was defined as this following formula: (band intensity of conjugated VLP / band intensity of unconjugated SC-VLP subunit + band intensity of conjugated VLP). The number of

PD1 copies/ particle corresponded to the conjugation yield multiplied by 180 (Each AP205-VLP contains 180 subunits (20)).

3.16 Dynamic light scattering (DLS) analysis

SC-VLP or VLP-PD1N and C were spun at 15,000 x g for 10 min and loaded into a Quartz cuvette (Anton Paar GmbH, Graz, Austria). The sample was measured 3 times at 25°C on a Particle Size Analyzers: Litesizer 500 model (Anton Paar GmbH, Graz, Austria), which is equipped with a 658 nm laser. The average hydrodynamic diameter and percentage polydispersity (PD) were estimated using Kalliope software.

3.17 Detection of RNA in VLP-PD1

To demonstrate the presence of RNA in VLPs displaying PD1 100 µg of VLP-PD1N and VLP-PD1C were used to isolate RNA by ethanol precipitation. The resuspended pellet in Ultrapure™ DNase/RNase-Free Distilled Water (Invitrogen, California, USA) was subsequently incubated for 1 hr at 37 °C. in the presence or the absence of 10 µg RNase A (Merck Millipore, Massachusetts, USA). RNA was detected by ViSafe Green Gel staining (Vivantis Technologies Sdn. Bhd., Selangor Darul Ehsan, Malaysia) following electrophoresis on 1.2% agarose gel.

3.18 IgE reactivity to VLP-PD1

ELISA plates (Thermo fisher, Massachusetts, USA) were coated with 100 ng/well of nDer p 1 (Indoor Biotechnologies, Virginia, USA) in 100 mM Bicarbonate buffer pH 9.6 at 4°C. Plates were washed with PBS-Tween 20, 0.05% (PBST) and blocked with 200 µl of 1% BSA in PBST (PBST-BSA) for 2 hr at room temperature. A pool of sera (1/10 dilution) from Der p 1-sensitized patients (N=20) were preincubated for 16 hr at 4°C in the presence or the absence of several concentrations of VLP-PD1N, VLP-PD1C, PD1N, PD1C or nDer p 1 (from 0.04 to 25 µg/ml, equimolar concentrations of Der p 1). These pre-treated sera were added to the plates for 2 hr at 37°C. Residual bound human IgE were detected through 1h-incubations with goat biotinylated anti-human IgE (KPL, 1/ 5000 dilution in PBST-BSA), Streptavidin-HRP (Beckton, Dickinson and Company, New Jersey, USA, (1/2000 dilution in blocking buffer)) and using TMB (Beckton, Dickinson and Company, New

Jersey, USA,) as substrate. The inhibition percentage induced by VLP-PD1N, VLP-PD1C, PD1N and PD1C-Der p 1 positive human sera were calculated as $(1 - (OD_{450} I / OD_{450} C)) \times 100\%$. $OD_{450} I$ and $OD_{450} C$ represent optical density values in the presence or absence of proteins respectively.

3.19 RBL-SX38 IgE binding assay

To demonstrate Rat basophil degranulation, RBL-SX38 cells were cultured in 96 well plate at a seeding density of 3×10^4 cells/well as previously described (95, 97). Cells were then pre-loaded with five human sera positive for Der p 1-specific IgE (1/13 dilution) for 24 hr at 37°C in RPMI serum free conditions. Any positive sera for Der p 1-specific IgE was previously diluted with 2 M D-Glucose (1:1 dilution) and heat inactivated at 56°C for 45 min. Cells were subsequently blocked with 200 μ l PIPES buffer (20 mM PIPES, 100 mM NaCl, 5 mM KCl, 0.4 mM $MgCl_2$, 1 mM $CaCl_2$, 5.6 mM D-Glucose and 0.1% (w/v) BSA) for 15 min. The RBL cells were activated with different concentration of nDerp 1, VLP-PD1N, VLP-PD1C and PD1N (0.0001 to 1 μ g/mL) in total of 100 μ l and incubated for 45 min at 37°C with 5% CO_2 . To evaluate the total cell release degranulation, as a control, the cells were treated with 5% (v/v) Triton X-100. For detection, 50 μ l of RBL substrate (50 mM p-Nitrophenyl-N-acetyl- β -D-glucosaminide, Sigma-Aldrich, Missouri, USA) was pre-diluted at 1/20 dilution in 0.2 M Citrate buffer pH 4.6 then transfer 50 μ l of supernatant to mix with the substrate and incubated for 3 hr at 37°C. the reaction was stopped by 50 μ l of 20 mM Tris-HCl pH 9.0 and detected at OD_{450nm} using ELISA microplate reader.

The inhibition of basophil degranulation was calculated as following formula:

$$\%Inhibition = \frac{1 - (\beta\text{-hexosaminidase release I}) - (\beta\text{-hexosaminidase release S})}{(\beta\text{-hexosaminidase release C}) - (\beta\text{-hexosaminidase release S})} \times 100$$

β -hexosaminidase release I, S and C represent the percentage of degranulation in the presence or the absence of mouse serum, respectively.

3.20 Mouse immunization

Our studies were approved by the Chulalongkorn University Animal Care and Use Committee (IRB approval no. 016/2562, CU-ACUC). Before immunizations, each antigen was treated with Triton X-114 to remove any contaminating LPS. Six weeks old female BALB/C mice (N=5) were intramuscularly immunized three times at 2 weeks interval with 5 µg of unadjuvanted VLP-PD1N or VLP-PD1C. As controls and to respect the antigen equimolarity between groups, animals were also immunized with monomeric PD1N (2.5 µg) or PD1C (3 µg) mixed with 2.5 or 2 µg untagged VLPs (VLP without SC) respectively. Blood samples were collected one day before the prime injection (pre-immune sera) as well as before each boost immunization. Two weeks post-boost #2 (day 42), the mice were sacrificed to collect serum and the spleen.

3.21 IgG1, IgG2a and IgE antibodies detection

ELISA plates were coated overnight with 500 ng /well nDer p 1 or PD1WT in 100 mM bicarbonate buffer pH 9.6 at 4°C. The plates were then washed with PBS-Tween 20, 0.05% (PBST) and blocked with 200 µl of 1% BSA in PBST (PBST-BSA) for 2 hr at room temperature. An individual or pool of mouse sera containing anti-Der p 1 IgG or IgE (1/100 dilution of IgG1, 1/100 dilution of IgG2a and 1/100 dilution of IgE) in PBST-BSA were added to the plates at 37°C for 1 hr. Allergen- IgG or IgE complexes were detected through 1h-incubations with goat biotinylated anti-human IgE (KPL, 1/5,000 dilution in PBST-BSA), followed by Streptavidin-HRP (Beckton, Dickinson and Company, New Jersey, USA, (1/2,000 dilution in blocking buffer)) and using TMB (Beckton, Dickinson and Company, New Jersey, USA,) as substrate. and stopped the reaction with 50 µl of 0.5 M H₂SO₄.

3.22 Lymphoproliferative assays

Each mouse spleen was collected in 10 ml of RPMI 1640 phenol red serum free medium (Gibco, Thermo fisher, Massachusetts, USA). The spleen was transferred onto a Petri dish containing a sterile Nylon mesh (Mesh opening width 210 μ M, Nyal Sefar® PA 6HD, Heiden, Switzerland). The organ, immobilized on the Nylon, was crushed with the 5 ml of sterile syringe plunger. The released splenocytes were transferred into a 15 ml falcon tube. The large spleen debris were decanted for 1 min and the supernatants were directly transferred into the new 15 ml falcon tube. The cells were pelleted at 1,200 rpm for 3 min. The cells were resuspended in 1 ml ACK lysis buffer to lyse red blood cells (154 mM Ammonium Chloride, 10 mM Potassium Bicarbonate, 0.01 mM EDTA, Thermo fisher, Massachusetts, USA) The reaction was neutralized by addition of 9 ml RPMI 1640 phenol red serum free medium. The cells were once again isolated by centrifugation and resuspended in 10 ml of RPMI 1640 phenol red serum-free medium. The cell density was determined with a hemacytometer in a trypan blue (Thermo fisher, Massachusetts, USA) exclusion assay. A cell sample containing 3.6×10^6 cells was transferred into a centrifuge tube. The cell pellets were resuspended with 1.2 ml 50 μ M of β -mercaptoethanol with 5% FBS in RPMI 1640 phenol red serum free medium and 100 μ l of this cell suspension were added into each well (300,000 cells/well) of a Nunc® 96-well round (U) bottom plate (Thermo fisher, Massachusetts, USA) with containing 4 μ g of PD1WT or 0.8 μ g Concanavalin A (Con A) as a positive control (Sigma-Aldrich, Missouri, USA). The plate was incubated at 37°C, 5% CO₂ for 72 hr. After 72 hr, 160 μ l of the supernatant was collected into the microcentrifuge tube and stored in -20°C until use.

3.23 Cytokine detection

The production of IFN- γ and IL-5 in lymphoproliferative assays was measured in the supernatant of restimulated cells (1/5 dilution), using mouse IL-5 or IFN- γ ELISA kit (Beckton, Dickinson and Company, New Jersey, USA) and following the recommended instructions provided in the kit.

3.24 ELISA Inhibition assay

ELISA plates were coated overnight with 100 ng/well nDer p 1 in 100 mM bicarbonate buffer pH 9.6 at 4 °C. The plates were then washed with PBS-Tween 20, 0.05% (PBST) and blocked with 200 μ l of 1% BSA in PBST (PBST-BSA) for 2 hr at 37°C. Pools of sera from each group of immunized mice (1/10 or 1/50 dilution in blocking buffer) were added to the plates for 16 hr at room temperature. Following a washing step with PBST, five human sera containing anti-Der p 1 IgE (1/10 and 1/50 dilution in PBST-BSA) were added to the plates at 37°C for 2 hr. Detection of residual IgE reactivity to nDer p 1 was measured as described above in IgE reactivity method. The inhibition percentage induced by the Der p 1-specific mouse sera was calculated as $(1 - (OD_{450nm} I / OD_{450nm} C)) \times 100\%$. $OD_{450nm} I$ and $OD_{450nm} C$ represent optical density values in the presence or absence of mouse serum, respectively.

3.25 RBL-SX38 Inhibition assay

RBL-SX38 cells were cultured and pre-loaded with five human sera positive for Der p 1-specific IgE same as previously method described above in RBL-SX38 IgE binding assay. The RBL cells were activated with 0.01 μ g/mL nDerp 1 mixed with pre-immune or post-boost #2 mouse sera (1/100 dilution in PIPES buffer) in total of 100 μ l for 45 min at 37°C with 5% CO₂. Residual basophil degranulation was determined by the detection of β -hexosaminidase activity in culture supernatants as previously mentioned in above in RBL-SX38 IgE binding assay.

3.26 Statistic

For the statistical analysis of the data, Prism software (version 6.0; GraphPad) was used. The immunogenicity experiments were repeated two times and a representative experiment is presented. For comparison between the two treatments, a Mann Whitney t test and Two-way Anova were used from which $P < 0.05$ was considered statistically significant.



CHAPTER IV

RESULTS

4.1 Cloning, expression and purification of wild-type (WT) or N52Q SpyTagged-PD1 proteins

The procurement of recombinant folded Der p 1 is fastidious and strictly dependent on the production and maturation of the Der p 1 zymogen (ProDer p 1, PD1) in eukaryotic cells (12). SpyTag (ST) was genetically fused to the C-terminus of wild-type PD1 (PD1WT) or PD1N52Q (mutation of the mature Der p 1 N-glycosylation site, Der p 1 numbering) using the following linkers: GGS (L) or GSGTAGGGSGS (Ext L) to allow flexible presentation on the surface of AP205 VLP. For that purpose, synthetic genes encoding fragments of PD1 fused to ST were designed in order to replace the corresponding wild type PD1 sequences into the original recombinant pPIC9K-PD1WT (Table. 3). The three proteins were expressed in *P.pastoris* to ensure proper folding (12, 52).

The three SpyTagged proteins were expressed under a secreted form by addition of methanol in the yeast culture medium. During these assays, we optimized the cell density (from OD 1 to 3) as well as the methanol concentration (from 0.5% to 3%) to reach the highest expression levels. Finally, the duration of methanol induction was also optimized (Fig.4.1A). The SpyTagged-PD1 expression was confirmed by western blot analysis using polyclonal anti-mouse PD1 antibodies (Fig.4.1B).

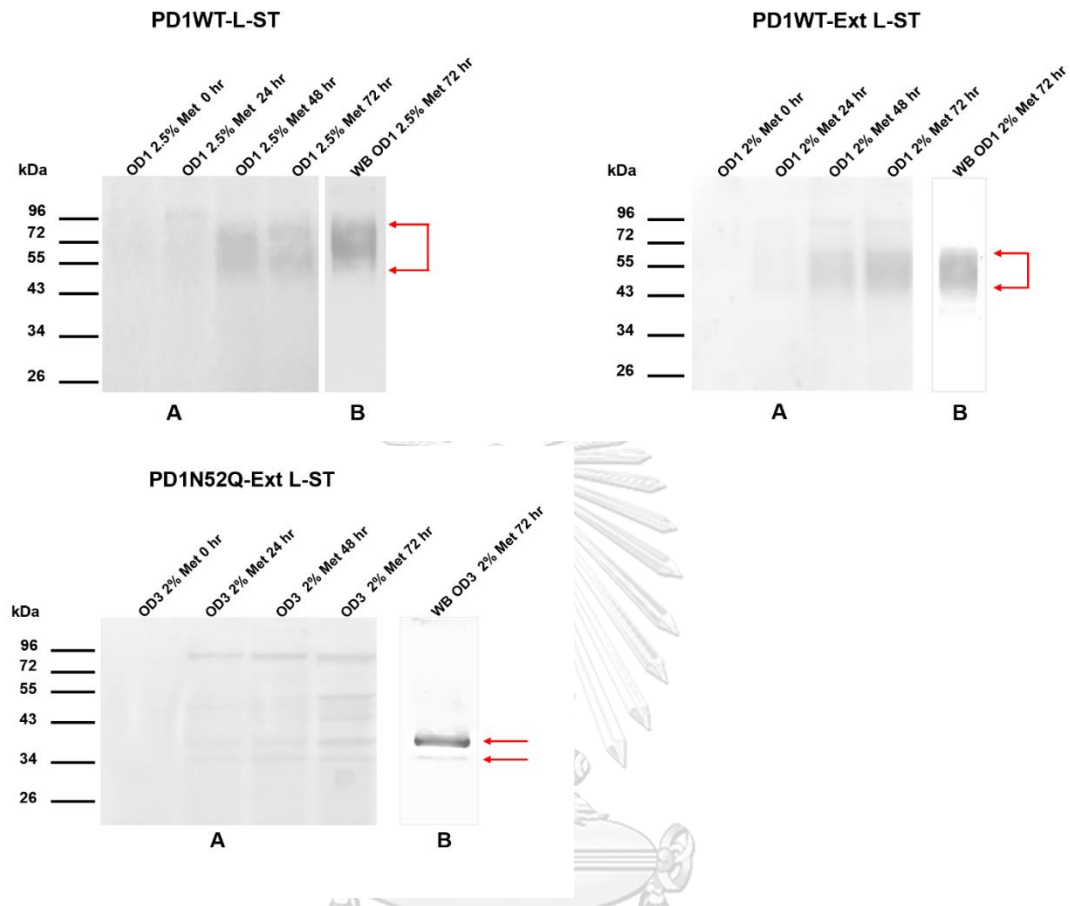


Figure 4.1 Time-dependence of SpyTagged-PD1 expression under optimized induction conditions (cell density-OD and methanol concentration): SDS-PAGE (A) and western blot (WB, B) analysis. Red arrows correspond to the specific bands

The large heterogeneity of the PD1 Mw was due to the hyper-mannosylation of the mature Der p 1 N-glycosylation site (N52, Der p 1 numbering). This hyper-glycosylation was previously observed for PD1WT expressed in *P. pastoris* (41). The three SpyTagged-PD1 were successfully purified by conventional chromatographies and ultrafiltration. SDS-PAGE showed PD1-L-ST and PD1-Ext L-ST were hyper-glycosylated and observed as smeared band around 50 kDa (Fig.4.2A and 4.2B) while PD1N52Q-Ext L-ST observed two protein bands of 34 and 36 kDa respectively (Fig. 4.2C).

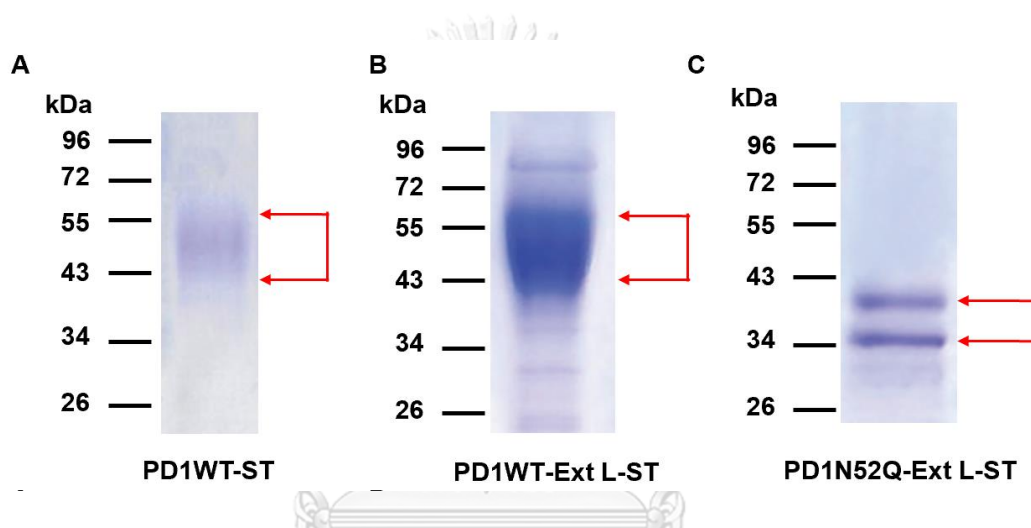


Figure 4.2 Purified SpyTagged proteins; A) PD1WT-L-ST; B) PD1WT- Ext L-ST and C) PD1N52Q-Ext L-ST, Red arrow indicated the position of PD1-ST protein

4.2 Expression and purification of SC-VLP

The expression of SC-VLP in *E.coli* BL21 strain was induced by addition of 0.1 mM IPTG in the culture medium for 16 hr at 16°C, and following protocols previously published (20). The SDS-PAGE analysis of the bacteria lysate showed clearly that SC-VLP was essentially produced in the cytoplasmic fraction (soluble) (Figure 4.3)

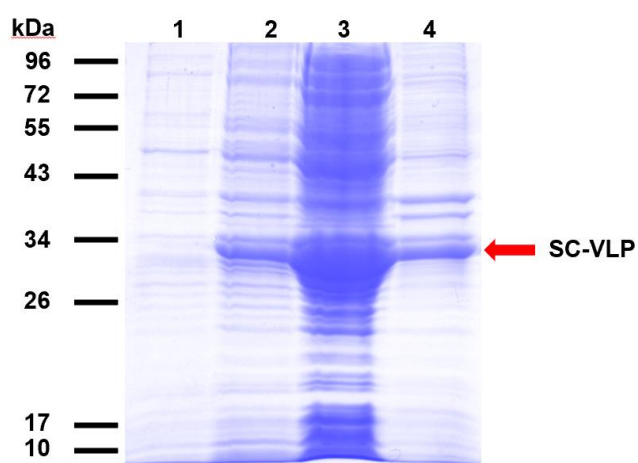


Figure 4.3 Expression of SpyCatcher-VLP AP205; Lane 1: uninduced bacteria lysate, Lane 2: IPTG-induced bacteria lysate, Lane 3: cytoplasmic fraction and Lane 4: residual pellet after lysis. Red arrow indicated SC-VLP band

SC-VLP was purified by density gradient ultracentrifugation method, using Optiprep™ gradient made by 23%, 29%, 35% layers (3ml each). Directly after the ultracentrifugation, the density gradient was fractionated into 24 fractions (12 ml /fraction) from the bottom to the top and fractions 2 to 11 were analyzed by SDS-PAGE (Figure 4.4A). The result showed that the purified SC-VLP was detected in fraction 3 to 6 (Figure 4.4B). To remove Optiprep™ reagent and residual contaminants, SC-VLPs (pooled fractions 3-6) were dialyzed against PBS pH 7.2 using a 300 kDa dialysis bag. The purity of homogenous VLP preparations was evidenced by SDS-PAGE analysis (Figure 4.4C)

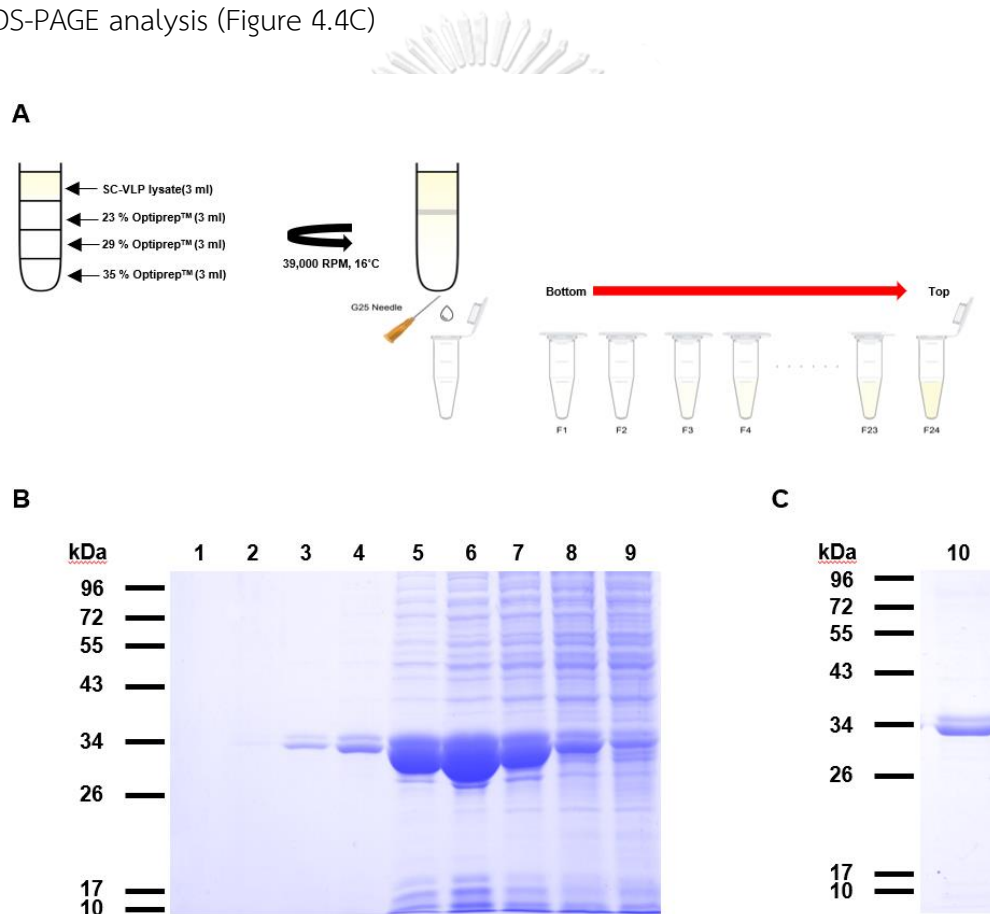


Figure 4.4 Purification of SpyCatcher-VLP AP205 by density gradient ultracentrifugation; A) composition of density gradient B) SDS-PAGE profile of purified SC-VLP fractions. Lanes 1-9: fractions 2- 11; and (C) Lane 10: purified SC-VLP after 300 kDa dialysis and concentrated with 10 kDa ultrafiltration

4.3 Conjugation and characterization of wild-type (WT) or N52Q SpyTagged-PD1 proteins to SC-VLP

The three purified PD1-ST were conjugated with SpyCatcher-VLP (SC-VLP) under standard conditions: ratio 1: 1.5, pH7, 4°C, 16 hr (95). Surprisingly, SDS-PAGE analysis indicated that neither of these three PD1-ST forms could be conjugated to SC-VLP, as evidenced by the absence of monomeric SC-AP205 coat protein band shift. Instead, lower Mw bands were generated during the incubation (Fig.4.5A in red boxes). Western blot analysis using anti-SC-VLP polyclonal antibodies indicated partial proteolytic degradation of SC-VLP (Fig.4.5B) after incubated PD1WText L-ST together with SC-VLP.



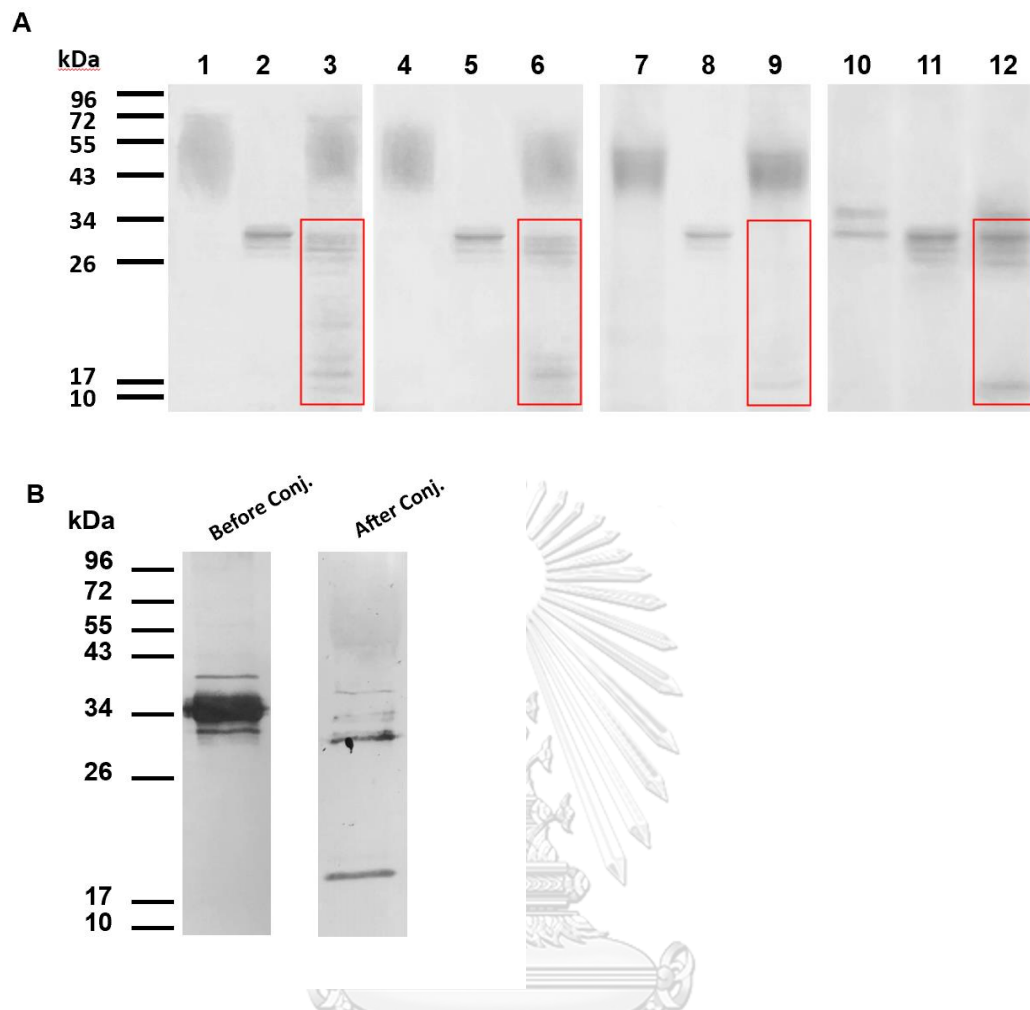


Figure 4.5 Conjugation of WT or N52Q PD1-ST to SC-VLP(A) SDS-PAGE analysis. Lane 1: purified PD1WT, Lane 3: conjugation of PD1WT to SC-VLP, Lane 4: purified PD1WT-L-ST, Lanes 2, 5, 8 and 11: purified SC-VLP, Lane 6: conjugation of PD1WT-L-ST to SC-VLP, Lane 7: purified PD1WT-Ext L-ST, Lane 9: conjugation of PD1WT-ExtL-ST to SC-VLP, Lane 10: purified PD1N52Q-Ext L-ST, Lane 12: conjugation of PD1N52Q-Ext L-ST to SC-VLP. The red boxes show degradation bands. (B) western blot analysis of PD1-Ext L-ST/SC-VLP conjugation using anti-SC-VLP antibodies

As we evidenced that the SDS-PAGE profile of purified SC-VLP did not show any change with the time (data not shown), we hypothesized that the degradation could result from residual protease activity in our PD1-ST preparation. It must be pointed out that the Der p 1 zymogen (PD1) is enzymatically inactive but some levels of cysteine protease activity were commonly detected in PD1 batches produced in *P.pastoris* (12, 98). Consequently, protease activity assays were performed with the three PD1-ST and using Boc-QAR-pNA, a synthetic substrate used to measure Der p 1 and trypsin activity (99). In our assays, trypsin was used as positive control. As shown in Fig.4.6, residual protease activities were detected in the three protein preparations. To determine the nature of protease, protease activity assays were run in the presence of AEBSF (serine protease inhibitor) and E-64 (cysteine protease inhibitor). Whereas similar levels of protease activity were measured in the presence of AEBSF, contaminating proteases were fully inhibited by E-64. Our data confirmed the presence of trace of cysteine protease in the three PD1-ST preparations. We hypothesized that SC and/or ST could be sensitive to cysteine protease activity, leading to unsuccessful conjugation.

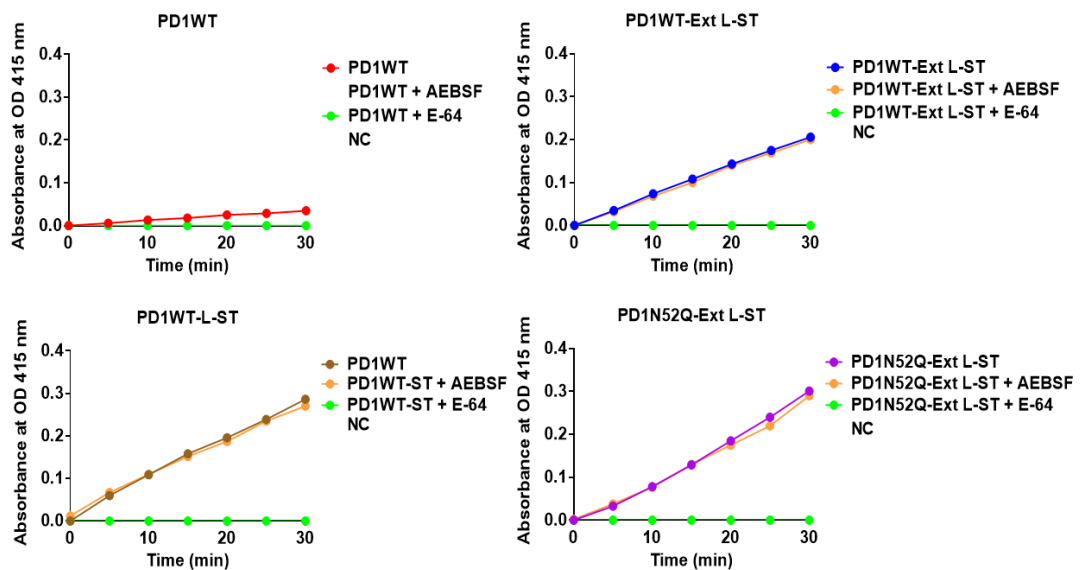


Figure 4.6 Detection of protease activity in preparations of purified PD1WT; PD1WT-L-ST; PD1WT-ExtL-ST and PD1N52Q-ExtL-ST in the presence or the absence of E-64 and using the chromogenic substrate Boc-QAR-pNA

4.4 Cloning, expression and purification of double mutant of SpyTagged-PD1 proteins

To circumvent any SC/ST degradation issues, we mutated the Der p 1 active site cysteine residue (C34A) to create a PD1-ST double mutant: PD1C34N52Q-L-ST (PD1C) (Table. 3). As the ST/SC conjugation result in unidirectional antigen display, the position of the SpyTag at the N- or C-terminus of PD1 could influence the allergen orientation on the VLP surface. Moreover, the crystallographic structure of PD1 showed that the N- and the C-terminus are far from each other, pointing in opposite orientation (Fig.4.7) (52). Consequently, to determine whether the successful conjugation is dependent on the N-/C-terminal position of SpyTag, and to evaluate the impact of PD1 orientation on the immunogenicity of chimeric VLP, ST-Ext L-PD1C34AN52Q (PD1N) was successfully produced Table. 3.

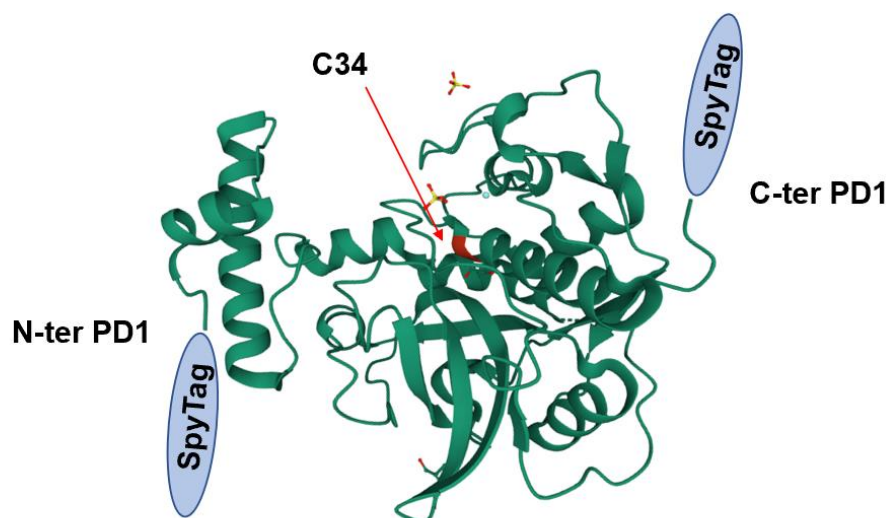


Figure 4.7 PD1 crystallographic structure between the N- or C-terminus pointing in opposite orientation

Table. 3 Description of synthetic genes designed for the production of the different SpyTagged-PD1 proteins.

SpyTagged-PD1	Synthetic gene	Length (bp)	Expression Vector
PD1-L-ST	<i>Afl</i> II-PD1(AA71-AA302)-L-ST-AvrII	762	pPICK9K
PD1-Ext L-ST	<i>Snab</i> I-PD1(AA176-AA302)-Ext L-ST-AvrII	471	
PD1N52Q-Ext L-ST	<i>Afl</i> II-PD1(AA71-AA302)-Ext L-ST-AvrII	786	
PD1C34AN52Q-L-ST (PD1C)	<i>Afl</i> II-PD1(AA71-AA302)-L-ST-AvrII	762	
ST-Ext L-PD1C34AN52Q (PD1N)	<i>Xho</i> I-ST-Ext L-PD1(AA1-AA302)- <i>Xba</i> I	1023	pPICZ α A

PD1N and PD1C were successfully expressed under standard induction conditions (OD1, 0.5% Methanol). We considered that the highest level of production was reached after 72 hr of induction (Fig.4.8A and 4.8B).

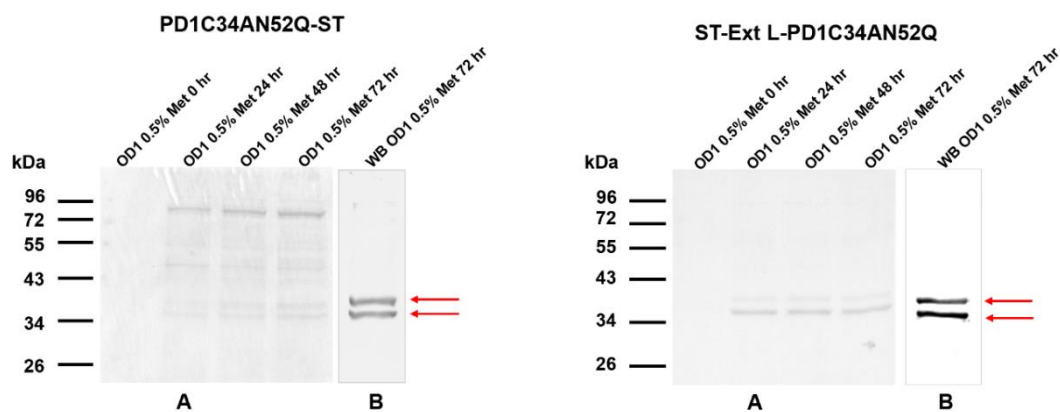


Figure 4.8 Optimization of the experimental conditions for the expression of the new Spytagged-PD1 with double mutant: SDS-PAGE (A) and western blot (WB, B) analysis. Red arrow indicated the specific band after confirmed by western blot

Both PD1N and PD1C were purified to homogeneity by a combination of IEX and gel filtration chromatographies. The purification of PD1N/PD1C using Q Sepharose beads at pH 9 could not fully remove a typical 90 kDa contaminating protein co-secreted with our target proteins (Fig. 4.9A). The pooled PD1N or PD1C positive fractions (elution 100 and 200 mM NaCl) were further purified onto a Superdex75 column correspond homogenous population as monomeric protein (Fig 4.9B and 4.9C).

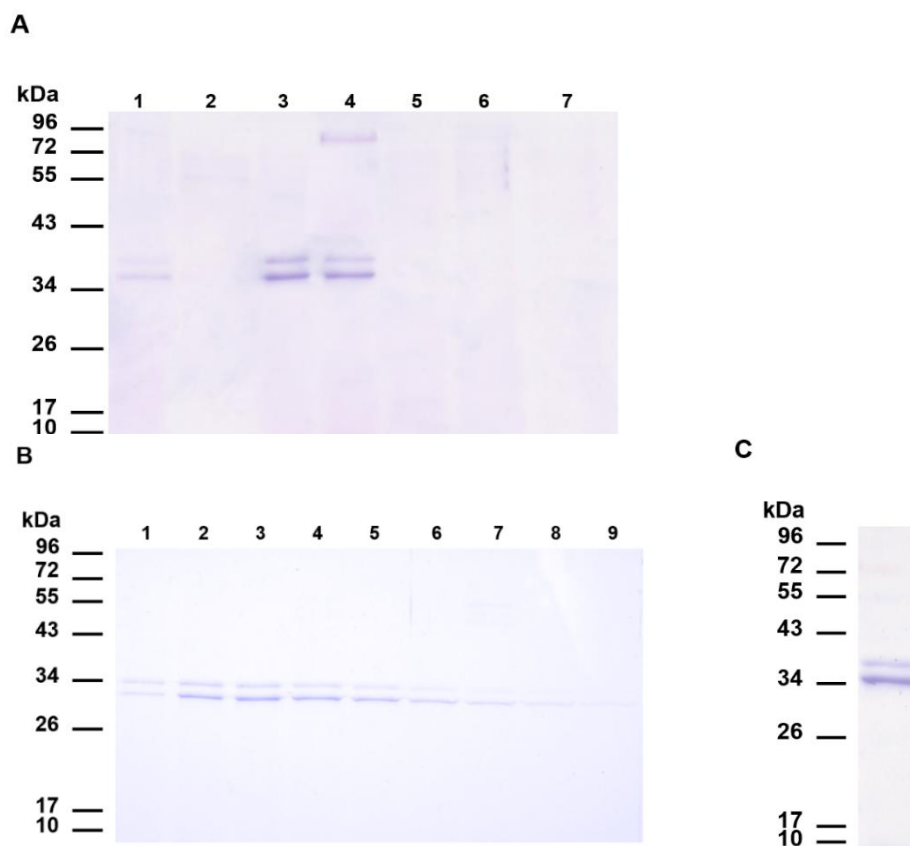


Figure 4.9 Purification of PD1N purified by (A) Ion exchange (IEX); Lane 1: crude PD1N before purified, Lane 2: Flow through, Lane 3: fraction eluded at 100 mM NaCl, Lane 4: fraction eluded at 200 mM NaCl, Lane 5: fraction eluded at 300 mM NaCl, Lane 6: fraction eluded at 500 mM NaCl, Lane 7: fraction eluded at 1M NaCl, (B) gel filtration chromatographies (GF); Lane 1 to 9: purified PD1N fraction 29 to 37 and (C) the pooled purified PD1N after concentrated with 10 kDa ultrafiltration

These PD1-ST with double mutant were successfully purified by conventional chromatographies and ultrafiltration. SDS-PAGE showed PD1C34AN52Q- L-ST (PD1C) and ST-Ext L-C34AN52Q (PD1N) observed two protein bands of 36 and 38 kDa respectively (Fig.4.10).

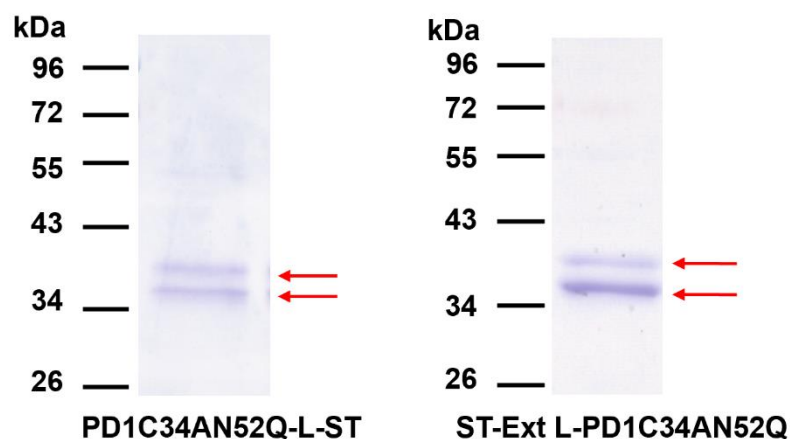


Figure 4.10 New purified SpyTagged proteins at C- and/or N-terminal with double mutant amino acid. Red arrow indicated the position of PD1-ST protein

Whereas contaminating proteins could not be evidenced in our purified PD1N and PD1C preparations (Fig.4.10), residual brownish pigments were still detected. We could successfully remove these pigments using Blue Sepharose bead whereas PD1N/PD1C bound to the beads, pigments did not interact with the matrix. SDS-PAGE profile of protein eluted with 1M NaCl at pH9 confirmed that PD1N/PD1C were pigment-free (Fig 4.11).

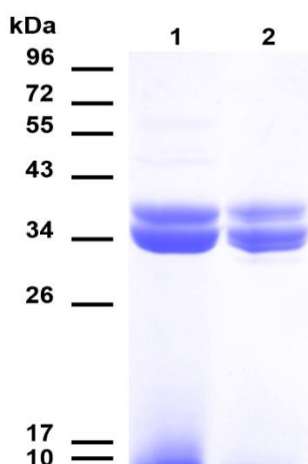


Figure 4.11 Pigment removal of PD1N by Blue Sepharose bead; (A) before and (B) after removed pigment.

As expected, PD1N and PD1C were enzymatically inactive (Fig.4.12). These results confirmed that residual cysteine protease activity detected in WT/N52Q PD1-ST batches were due to the matured Der p 1 present in tiny amounts (Fig. 4.6).

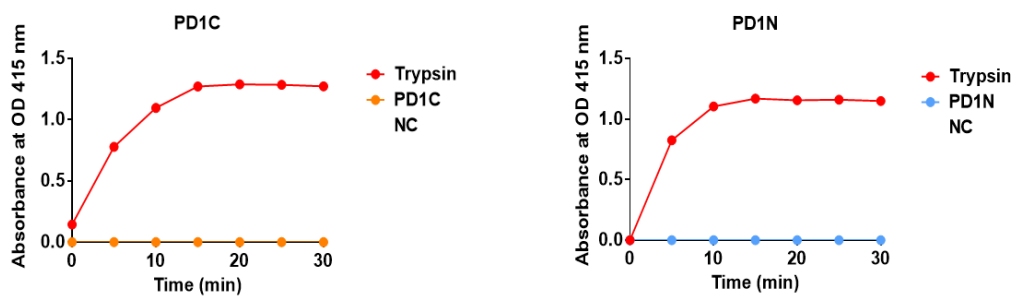


Figure 4.12 Detection of protease activity in batches of double mutant purified PD1C and ST-PD1-ST using the chromogenic substrate Boc-QAR-pNA

4.5 Conjugation of double mutant PD1-ST to SC-VLP

Although SC-VLP remained intact, the conjugation of both PD1N and PD1C to VLP showed poorly efficient at physiological pH (Fig.4.13). As the intermolecular isopeptide bond between ST and SC is slightly pH dependent (88), conjugation assays were performed at pH 5 with both double mutant PD1-ST. Under these conditions, 65 kDa protein bands, which match the theoretical size of SC-VLP subunit (27 kDa): PD1 (37 kDa) conjugates, were clearly observed by SDS-PAGE.

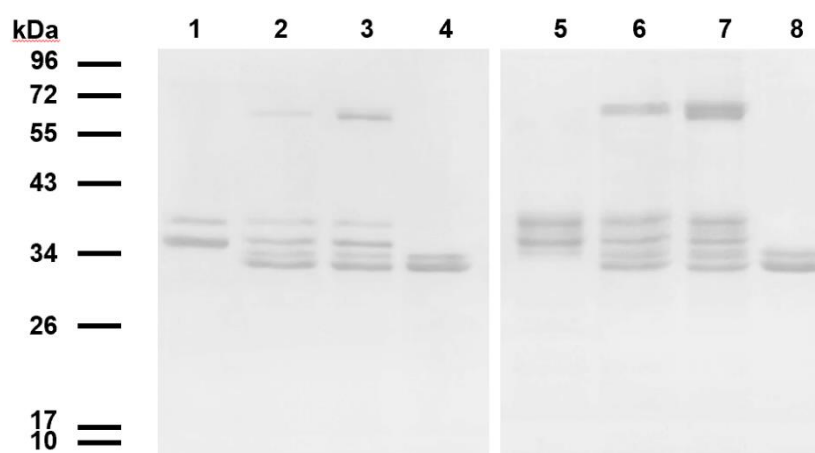


Figure 4.13 Conjugation of PD1N and PD1C to SC-VLP in different pH SDS-PAGE analysis: Lane 1: purified ST-Ext L-PD1C34AN52Q, Lane 2: conjugation of ST-Ext L-PD1C34AN52Q to SC-VLP at pH 7, Lane 3: conjugation of ST-Ext L-PD1C34AN52Q to SC-VLP at pH 5, Lanes 4 and 8: SC-VLP, Lane 5: purified PD1C34AN52Q-L-ST, Lane 6: conjugation of PD1C34AN52Q-L-ST to SC-VLP at pH 7, Lane 7: conjugation of PD1C34AN52Q-L-ST to SC-VLP at pH 5

To increase the chance in term of obtaining fully conjugated with SC-VLP, PD1N or PD1C was mixed with SC-VLP at different molar ratio at pH 5. Under our experimental conditions, we considered that 1:2 ratio of SC-VLP to PD1N and 1:1.5 ratio of SC-VLP to PD1C allowed the full conjugation (Fig.4.14, Lane 2 and 6) in large-scale. After a typical conjugation assay, excess unconjugated monomeric PD1C/PD1N was successfully removed by dialysis, using 300 kDa dialysis bag, only VLP-PD1 conjugation band was observed. Surprisingly, the residual unconjugated SC-AP205 coat protein was detected in VLP-PD1 preparation (Fig.4.14, Lane 4).

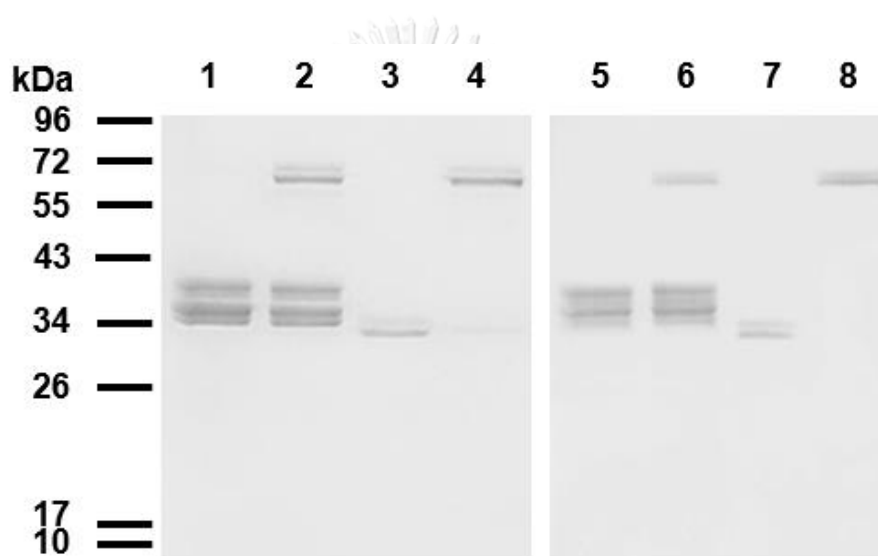


Figure 4.14 VLPN and VLPC optimizing molar ratio conjugation and dialysis using SDS-PAGE analysis Lane 1: purified ST-Ext L-PD1C34AN52Q, Lane 2: conjugation of ST-Ext L-D1C34AN52Q to SC-VLP, Lanes 3 and 7: purified SC-VLP; Lane 4: purified VLP-PD1N after removal of excess ST-Ext L-PD1C34AN52Q; Lane 5: purified PD1C34AN52Q-L-ST, Lane 6: conjugation of PD1C34AN52Q-L-ST to SC-VLP; Lane 8: purified VLP-PD1C after removal of excess PD1C34AN52Q-L-ST

4.6 Dynamic light scattering (DLS) of VLP-PD1

Densitometric analysis showed that each VLP-PD1N and VLP-PD1C particle displayed 150 and 180 PD1 copies respectively. The homogeneity of the VLP-PD1N and VLP-PD1C preparation was characterized by dynamic light scattering (DLS) (Fig.4.15). Whereas SC-VLP were considered as ~50 nm monodispersed particles (Pd%~9), VLP-PD1N and VLP-PD1C are more polydisperse (Pd%~28) with a hydrodynamic diameter of 118 and 112 nm respectively.

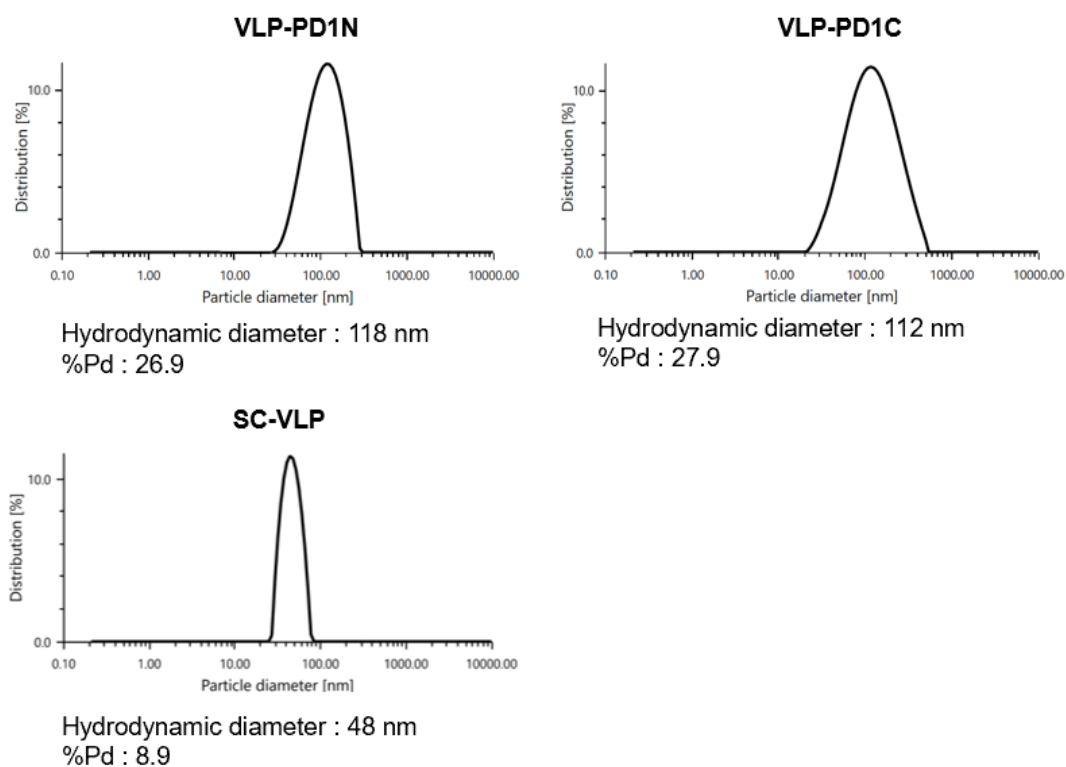


Figure 4.15 DLS of VLP-PD1N, VLP-PD1C nanoparticles compared to SC-VLP. The average diameter as well as the polydispersity percentage (%Pd) are shown

4.7 RNA detection in VLP-PD1

VLPs were further characterized for the presence of encapsulated bacterial RNA whether these RNA can trigger TLR7/8 signaling pathways (85). Agarose gel analysis showed that RNA can be detected in among three VLPs preparations as evidenced by the absence of nucleic acid detection following RNase A treatment (Fig.4.16).

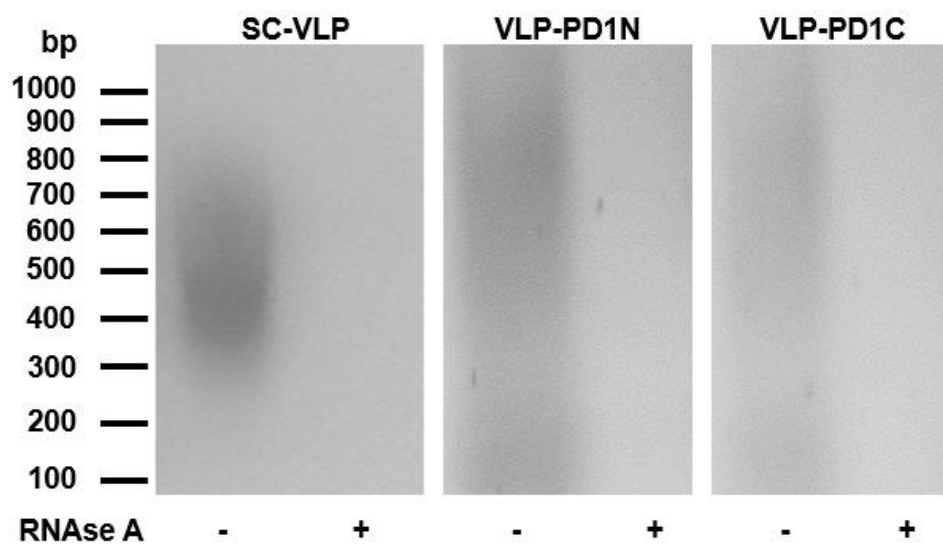


Figure 4.16 Detection of RNA in purified and RNase A-treated or untreated SC-VLP, VLP-PD1N and VLP-PD1C by agarose gel electrophoresis and ViSafe Green staining

4.8 Allergenicity of VLP-PD1

The ability of VLP-PD1N and VLP-PD1C to compete with nDer p 1 for the IgE binding was first assessed in ELISA IgE competition assay using plates coated with nDer p 1 and a pool of human sera from Der p 1-sensitized patients (N=20). Competitions with monomeric PD1N and PD1C were performed as controls and the amount of any competitor was normalized to Der p 1 content. Whereas 0.04 $\mu\text{g/ml}$ nDer p 1 inhibited more than 60% of the IgE binding to coated nDer p 1, the 50% inhibition with both VLP-PD1 was barely reached at the highest concentration tested (25 $\mu\text{g/ml}$) suggesting that VLP-PD1 particles were hypoallergenic (Fig.4.17A). The IgE binding capacity of VLP-PD1N and VLP-PD1C was even weaker than for monomeric PD1N and PD1C ($P<0.05$). As expected, nDer p 1 triggered potent allergen concentration-dependent mediator release. Under the same experimental conditions, PD1N was confirmed to be less allergenic than nDer p 1 ($P<0.05$). Remarkably, the capacity of both VLP-PD1N and VLP-PD1C to induce basophil degranulation was almost completely abolished with the exception of partial basophil activation at a 1 $\mu\text{g/ml}$ concentration ($P<0.05$) (Fig.4.17B).

Taken together, our data evidenced that monomeric SpyTagged-PD1 proteins do not display all the IgE binding epitopes of Der p 1 and that multimerization of PD1 amplifies its hypoallergenicity.

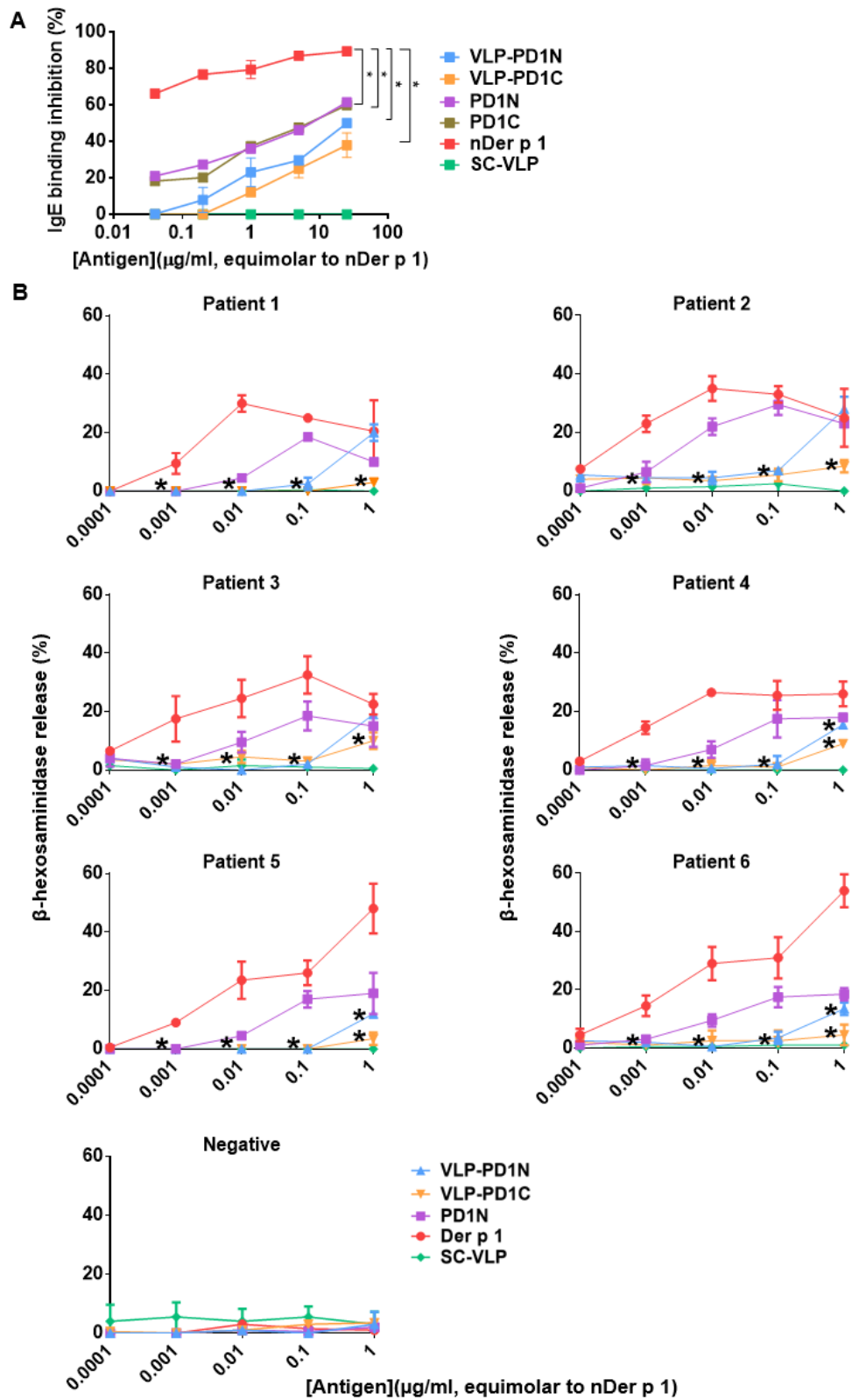


Figure 4.17 IgE binding capacity and allergenicity of VLP-PD1N and VLP-PD1C

Figure 4.17 (Continue) (A) Specific IgE cross-inhibition assay. The IgE reactivity to nDer p 1 was measured with a pool of 20 Der p 1-positive sera preincubated with increasing inhibitor allergen concentrations of nDer p 1, VLP-PD1N, VLP-PD1C, PD1C34AN52Q-L-ST, ST-Ext L-PD1C34AN52Q (equimolar concentrations of Der p 1) or saline. Results are expressed as the percentage inhibition of IgE binding to nDer p 1. * $P < 0.05$: significant differences in IgE inhibition. (B) Allergenicity of VLP-PD1N, VLP-PD1C measured in RBL-SX38 degranulation assay. RBL-SX38 cells were primed with Der p 1-positive sera from HDM-allergic patients ($N=6$) or with one serum from non-allergic subject. Basophil degranulations were triggered by addition of equimolar concentrations of nDer p 1, VLP-PD1C, VLP-PD1N, ST-Ext L-PD1C34AN52Q. As control, cells were activated with SC-VLP. The percentage of the total release of β -hexosaminidase minus the spontaneous release is shown. * $P < 0.001$ for significant difference between nDer p 1 and VLP-PD1N/VLP-PD1C.

4.9 Immunogenicity of VLP-PD1

In BALB/c mice (Fig. 4.18A), intramuscular administrations of unadjuvanted VLP-PD1N and VLP-PD1C triggered potent PD1-specific IgG responses (Fig.4.18B). Two weeks post-prime, specific IgG1/IgG2a responses elicited by VLP-PD1 were already detectable but not with equimolar amounts of monomeric PD1N or PD1C mixed with untagged VLPs ($P < 0.05$) (Fig.4.18C). The dramatic increase of PD1 immunogenicity by VLP display was confirmed by enhanced specific IgG titers following each of the two booster immunizations. The low specific IgG1/IgG2a ratio measured following VLP-PD1 immunizations suggested that both unadjuvanted particles promote T_{H1} -biased humoral responses. ELISA assays using nDer p 1 as coating antigen confirmed that specific IgG1/IgG2a generated by VLP-PD1N or VLP-PD1C are similarly capable to recognize Der p 1 ($P > 0.05$) (Fig.4.18C). These data suggest that the multimeric display of PD1 in repetitive arrays, whatever the allergen orientation, induced potent Der p 1-specific IgG responses with a T_{H1} trend. The development of such T_{H1} -biased humoral response was confirmed by our inability to detect any PD1/nDer p 1-specific IgE in sera from VLP-PD1- immunized mice (data not shown). Finally, we analyzed the IL-5 and IFN- γ production from spleen cells isolated from immunized mice and restimulated with PD1WT. Immunizations with both VLP-PD1 or monomeric PD1 equally triggered large and low amounts of IFN- γ and IL-5 respectively ($P > 0.05$) (Fig.4.18D). These results showed that VLP-PD1N or VLP-PD1C equivalently mediates typical T_{H1} -biased cellular response.

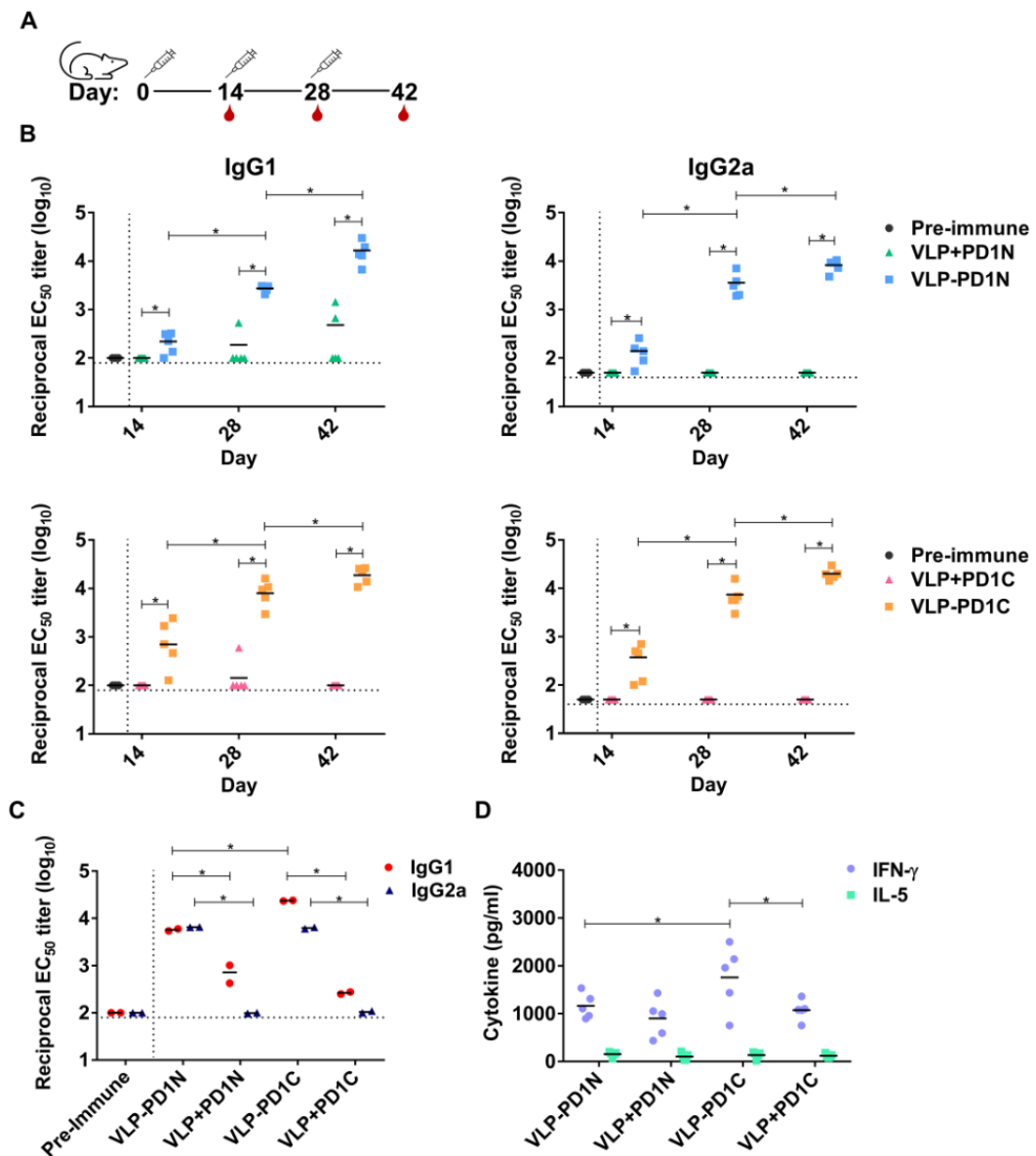


Figure 4.18 Immunogenicity of VLP-PD1N and VLP-PD1C in mice (A) Immunization and bleeding schedule; (B) Post-prime (day 14) and post-boost (days 28 and 42) ProDer p 1-specific IgG1 and IgG2a antibody titers following immunizations with VLP-PD1N, VLP-PD1C, VLP + PD1N, VLP+PD1C; (C) Post-boost (day 42) Der p 1-specific IgG1 and IgG2a antibody titers; (D) IFN- γ and IL-5 levels secreted by splenocytes from immunized mice restimulated with PD1. One representative of 2 similar experiments is shown. * $P < 0.05$ for statistically significant difference

4.10 Blocking capacity of VLP-PD1

In ELISA competition experiments with sera from five Der p 1-sensitized patients, pre-incubation of coated nDer p 1 with pooled sera from VLP-PD1N or VLP-PD1C-immunized mice at 1/10 dilution similarly inhibited the binding of human specific IgE to the allergen by around 60% ($P>0.05$) (Fig.4.19A). At a 1/50 dilution, the percentage of inhibition still reached 40% ($P>0.05$). The blocking capacity of antibodies from immunizations with monomeric PD1N or PD1C was significantly lower (around 15%, $P<0.05$). In RBL-SX38 assays, nDer p 1-stimulated β -hexosaminidase release was inhibited by 80% and 65% when the allergen was preincubated in a 1/100 dilution of mouse sera from VLP-PD1N or VLP-PD1C immunized mice, respectively ($P<0.05$) (Fig.4.19B). Concomitantly, basophil degranulation capacity of nDer p 1 remained unchanged in the presence of pre-immune sera or antibodies specific to the monomeric PD1-ST. Taken together, our results suggested that the PD1 array displayed by VLPs can elicit potent nDer p 1-specific IgG blocking antibody responses.

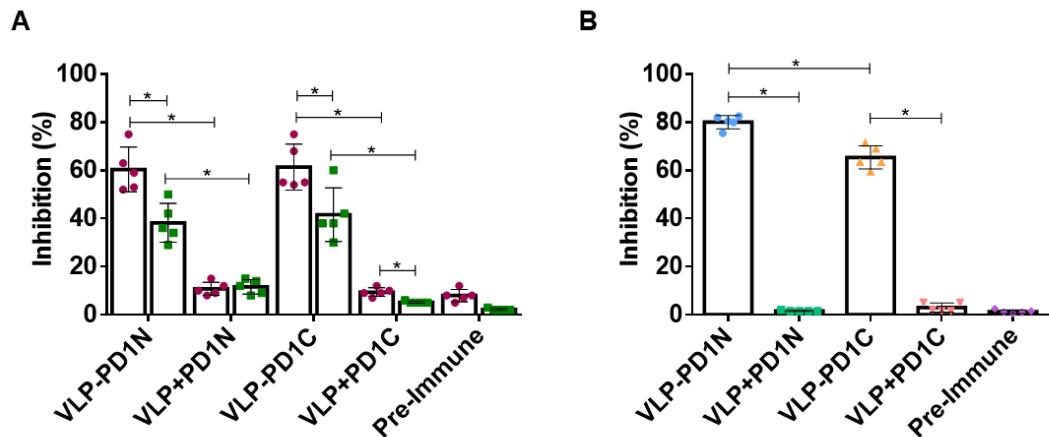


Figure 4.19 Blocking capacity of IgG antibodies generated by VLP-PD1N and VLP-PD1C (A) Inhibition of human IgE binding to nDer p 1 by pooled sera from immunized mice (day 42) determined by ELISA IgE inhibition assay. The binding of specific IgE from five Der p 1-sensitized patients to coated nDer p 1 was measured in the presence or the absence of the different mouse antisera diluted 10 or 50 times. The inhibition percentage was calculated as follows: $(1 - (OD_{450nm I} / OD_{450nm C})) \times 100\%$. $OD_{450nm I}$ and $OD_{450nm C}$ represent optical density values in the presence or absence of mouse serum, respectively. * $P < 0.05$ for IgE inhibition by VLP-PD1-immunized sera compared with VLP + PD1-immunized sera; (B) Inhibition of nDer p 1-induced basophil degranulation by antiserum from mice immunized with VLP-PD1. RBL-SX38 cells, primed with five HDM allergic patients and positive for Der p 1, were activated with $0.01\mu\text{g/ml}$ nDer p 1 in the presence or absence of different mouse antisera (day 42) diluted 100 times. The inhibition percentage was calculated as follows: $(1 - ((\beta\text{-hexosaminidase actual release I}) - (\beta\text{-hexosaminidase Spontaneous release S}) / (\beta\text{-hexosaminidase control release C}) - (\beta\text{-hexosaminidase Spontaneous release S}))) \times 100\%$. $\beta\text{-hexosaminidase release I}$, S and C represent the percentage of degranulation in the presence or the absence of mouse serum, respectively. * $P < 0.05$ for statistically significant difference

CHAPTER V

DISCUSSION

Since the molecular cloning of Der p 1 (49) and the demonstration that more than 80% of the HDM allergic populations developed Der p 1-specific sensitizations, several molecular approaches were explored to design recombinant Der p 1-based vaccines which are hypoallergenic and highly immunogenic (T-cell epitope-containing peptides, DNA vaccines, hypoallergens, (73, 74). Although tremendous progress in the structural and immunological characterization of Der p 1, development of hypoallergenic variants of this allergen remains very challenging for several reasons: 1) the mapping of Der p 1-specific IgE binding epitopes is cumbersome due to their conformational dependence and has only partially been elucidated based on crystal structures of Der p 1-antibody complexes (72); 2) the polyclonal nature of IgE responses to Der p 1 implies that only mutants with multiple residue substitutions could reach appreciable hypoallergenicity; 3) such site-directed mutagenesis could alter the development of IgG blocking antibody responses given the overlap between the IgE and IgG binding sites in Der p 1 (72); 4) the procurement of recombinant folded Der p 1 is fastidious and strictly dependent on the production and maturation of PD1 in eukaryotic cells (12); 5) simultaneous disruptions of several Der p 1 IgE binding sites could drastically down-regulate the expression and/or secretion levels of PD1 together with its solubility.

The above cited vaccine platforms were not dedicated to optimizing Der p 1-specific B cell responses. Moreover, to our knowledge, the capacity of these vaccines to develop Der p 1-specific IgG blocking antibodies were not investigated and although the development of HDM allergen-specific blocking IgG antibodies by AIT responders was shown to be key parameters for successful AIT (75). Of note, only the blocking capacity of specific IgG1/IgG4, which compete with IgE for allergen binding, is correlated with successful AIT and, consequently, has been suggested as a biomarker to monitor the clinical efficacy of AIT (100).

For all those reasons, we decided to select a molecular strategy favoring the development of blocking Der p 1-specific IgG antibodies: chimeric VLPs decorated with Der p 1. Indeed, Non-infectious VLPs, made by a repetitive array of viral coat/envelop proteins, are highly immunogenic and promote potent neutralizing antibody responses through the simultaneous engagement of multiple B cell receptor (BCR) on the B cell surface (101).

Remarkably, the decoration of VLP surfaces with wild-type allergens was recently shown to be a more convenient and straightforward strategy for developing hypoallergenic vaccines VLPs, displaying folded peanut (Ara h 1, Ara h 2) or cat (Fel d 1) allergen elicited much stronger blocking IgG responses than their monomeric counterparts (92, 95, 96).

Here, we developed a new Der p 1-based molecular AIT consisting of VLPs displaying multi-copies of PD1. Engineered VLP-PD1 triggered potent Der p 1-specific blocking IgG antibodies and mediated a T_H1 -biased T cell response. To our knowledge, it is the first time that VLPs were successfully decorated with a full-length recombinant form of Der p 1. Contrary to the previously reported heterogenous display of a single Der p 1-B cell epitope to VLPs by chemical conjugation (73), the split-protein (ST/SC) AP205 VLP display system mediated unidirectional display of PD1 at very high density. The main limitation of our vaccine design is the presence of the prosequence, which potentially could mask some IgG binding epitopes from the mature Der p 1 B cell epitope repertoire and consequently reduce the blocking capacity of the induced IgG response. However, the binding of three mature-Der p 1-specific immunodominant monoclonal antibodies (capable of competing with IgE binding) was not altered by the presence of the pro-peptide (72) which covers around 13% of the solvent accessible surface area of mature Der p 1 (52).

To our knowledge, correctly folded and enzymatically active recombinant Der p 1 has only be obtained following the expression of the Der p 1 zymogen (PD1) in yeast and its subsequent maturation under acidic conditions (12, 52, 102). Under different experimental conditions (time, antigen concentration, temperature, pH), we were unable to mature any PD1- ST protein conserving C34 residue (data not shown). In comparison with PD1WT, PD1-L-ST, PD1-ExtL-ST or PD1N52Q-ExtL-ST exhibited higher residual protease activity (Fig. 4.6). We hypothesized that ST fusion to PD1 C-terminus could lead to structural distortion of the prosequence, rendering the Der p 1 active site more accessible. The failure to conjugate any PD1-ST with C34 to SC-VLP resulted from partial SC cleavage, as evidenced by the detection of degradation bands in conjugation assays (Fig.4.5). To our knowledge, the cysteine protease sensitivity of the SC/ST conjugation system has not been reported so far. The mutation of the Der p 1 active site cysteine residue (C34A) allowed the successful conjugation of folded PD1N and PD1C to SC-VLP. Our results clearly evidenced that VLP-PD1N and VLP-PD1C are similarly hypoallergenic and share the same capacity to trigger potent blocking IgG response, indicating that the immunological properties of these vaccines are independent on the orientation of PD1 on the VLP surface.

As similarly observed with wild-type PD1 (11, 12), monomeric PD1N or PD1C displayed lower allergenicity than nDer p 1 in IgE competition and RBL assays. These results confirmed that the prosequence shields some Der p 1-specific IgE binding epitopes. The multimerization of PD1 onto VLP further decreased its allergenicity, leading to a speculation of possible inaccessibility of Der p 1-specific IgE to their cognate epitopes by the unidirectional, repetitive array of PD1. Remarkably, VLP-PD1N and VLP-PD1C were hardly able to activate the degranulation of RBL cells preloaded with Der p 1-specific human IgE. The inability of VLP displaying correctly folded allergen to elicit basophil/mast cell activation were previously evidenced with particles decorated with Fel d 1, Ara h 1, Ara h 2 or Der p 2 respectively (92, 95, 96). Surface plasmon resonance experiments highlighted that the IgE binding capacity of Fel d 1 displayed on VLPs was very poor and this residual binding was unable to trigger basophil activation (93). We hypothesized that these mechanisms remain valid to explain the absence of basophil activation by both VLP-PD1. Moreover, the high

density of PD1 attached to VLPs could lead to supra-optimal PD1 concentrations, a condition which inhibits the downstream signal transduction responsible for basophil degranulation (103). As previously reported for VLP-D2 (95), both VLP-PD1 were shown to be highly immunogenic, even in the absence of adjuvants. The potent specific IgG responses elicited by the chimeric particles result from an optimal B cell activation, which is promoted by dual engagement of BCR and activation of TLR7 in a T-cell independent manner. Indeed, repetitive arrays of antigens commonly stimulate stronger BCR signaling than monomeric counterparts (31). Moreover, the TLR7 signaling driving VLP-specific B cell response (91, 104) is mediated by bacterial RNA encapsulated in AP205-based VLP-PD1 particles (Fig.4.16). Of note, the presence of TLR7 ligand within recombinant VLPs was shown to favor the differentiation of primary into secondary plasma cells capable to generate higher antibody titers with stronger affinity (105). Remarkably, the humoral and cellular response triggered by VLP-PD1 was T_H1 - biased as evidenced by low specific IgG1/IgG2a ratio, the absence of allergen-specific IgE and high levels IFN- γ . Similar activation of specific T_H1 cells following administrations of unconjugated VLP with monomeric PD1N or PD1C confirmed previous observations on the pro- T_H1 adjuvant capacity of bacterial RNA packaged in RNA bacteriophage-based VLPs (106). The increased levels in serum allergen-specific antibodies, commonly observed during AIT protocols (IgG and specifically of IgG4 isotype for SCIT, IgA for SLIT) (107), correlated poorly with clinical outcome (100). In contrast, successful AIT was significantly associated with the functional capacity of these antibodies to block the allergen-IgE interactions. Effective reduction of the allergic symptoms in cat-allergic patients by administrations of Fel d 1-specific neutralizing IgG monoclonal antibodies could suggest that generation of blocking antibody responses could be sufficient to treat IgE-mediated allergy (17). Remarkably, these blocking antibodies suppressed Fc ϵ RII/Fc ϵ RII-mediated allergic responses but were capable as well to down-regulate the T_H2 cytokine (IL-4, IL-5 and IL-13) (16). The IgG response elicited by immunizations with VLP-PD1N or VLP-PD1C was shown to efficiently inhibit the binding of IgE to coat Der p 1 and to prevent the Der p 1-induced basophil degranulation. The higher blocking

capacity of the VLP-PD1-induced IgG measured in the RBL assay could be explained by a preincubation of nDer p 1 with mice sera in solution. Under these conditions, all the conformational B cell epitopes of nDer p 1 are freely accessible to specific IgG antibodies. In IgE ELISA assay, we assume the coating of Der p 1 to solid phase induced structural changes in the allergen, affecting some conformational IgG as well as IgE binding epitopes. Of note, nDer p 1 and PD1WT produced in *P.pastoris* shared the same IgE reactivity when coated in ELISA plates whereas in solution, the IgE binding to Der p 1 is higher than the one measured with PD1 (12, 98). Taken together, we demonstrated for the first time that the unidirectional display of full-length PD1 at very high density on VLP surfaces is a straightforward strategy to develop Der p 1-based hypoallergenic vaccines in the aim to trigger potent Der p 1-specific blocking IgG antibodies and Th1 cells.



CHAPTER VI

CONCLUSION AND PERSPECTIVE

To our knowledge, it is the first time that VLPs were successfully decorated with a full-length recombinant form of Der p 1. We consider that VLP-PD1C and VLP-PD1N could pave the way for next-generation of AIT against HDM allergy by their robust capacity to promote high levels of IgG blocking antibodies and the development of T_H1 -biased cellular response. As single VLP-allergen approaches were shown to be effective for the treatment of peanut/cat allergy (Ara h 1, Ara h 2, Fel d 1 (92, 96), the Der p 1-specific blocking antibodies triggered by VLP-PD1 could be sufficient to down-regulate the allergic responses mediated by the HDM allergen cocktail.

Our promising preclinical data should encourage investigations on the prophylactic (Fig.6.1A), as well as the therapeutic (Fig.6.1B) capacity of these VLP-PD1 in mouse models of HDM allergy. The induction of Der p 1 allergic response can be done by a 2 steps protocol: 1) sensitization with enzymatically active Der p 1 formulated with alum; 2) airway challenges with HDM allergen extracts to trigger eosinophilia in the lungs. It would be too expensive to challenge with natural Der p 1. It must be pointed out that Der p 1 is the most abundant HDM allergen in allergen extracts.

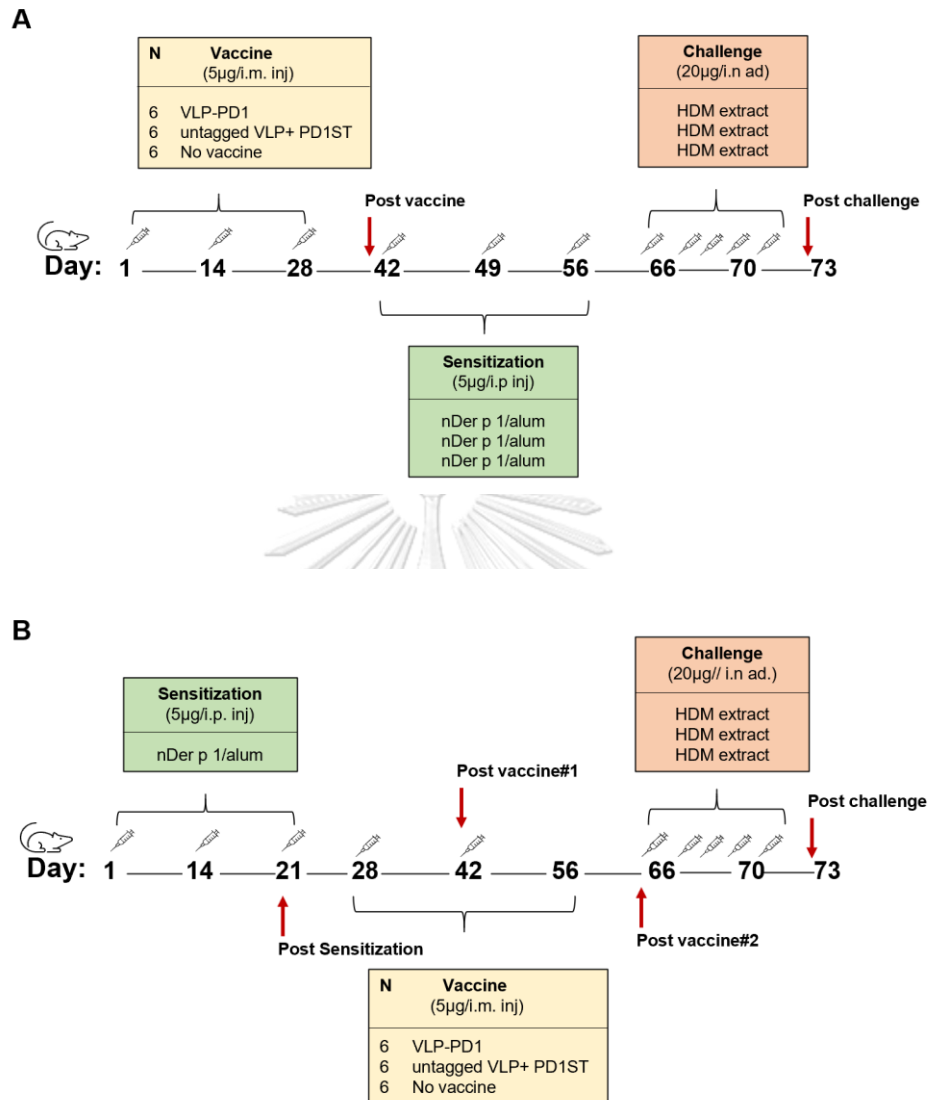


Figure 6.1 Future plan for (A) prophylactic and (B) Therapeutic vaccinations with VLP-PD1 in a Der p 1 sensitization mouse model (modified from (95))

Whereas our present work showed that high levels of Der p 1-specific blocking IgG antibodies can be obtained with unadjuvanted VLP-PD1, it is highly probable that the blocking IgG response could be further increased by formulation with extrinsic adjuvants as shown for AP205-VLPs combined with squalene-in-water emulsion or monophosphoryl lipid A (108). Such VLP-adjuvant formulations could be tested as well in mice models.

Whereas our competitive assays evidenced that specific IgG antibodies elicited by both VLP-PD1 can directly neutralize Der p 1, future experiments are needed to determine whether these antibodies are capable to engage the inhibitory Fc receptor (Fc γ RIIb) (14). For that purpose, we could test our vaccines in Fc γ RIIb-deficient mouse models of HDM allergy or use Fc γ RIIb-specific monoclonal antibody to block the receptor before animal testing. It would be interesting as well to know whether the Der p 1-specific blocking antibodies are capable as well to inhibit the IgE facilitated antigen presentation at the level of B cells (Fig. 6.2, (14)). For that purpose, we could use the IgE-Facilitated Allergen Binding (IgE-FAB) *in-vitro* assay (Fig. 6.3,(109)).

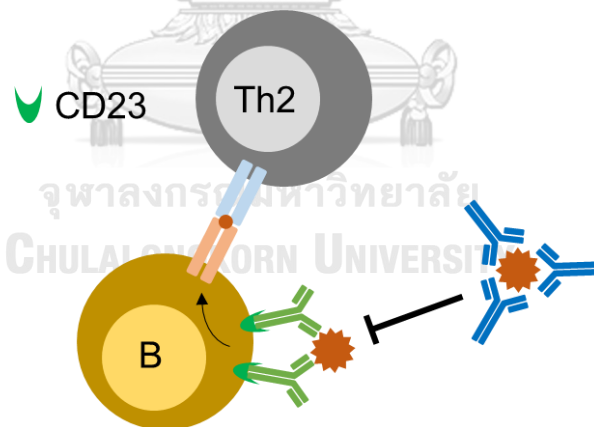


Figure 6.2 Inhibition of the IgE facilitated antigen presentation by blocking IgG antibodies (modified from (14))

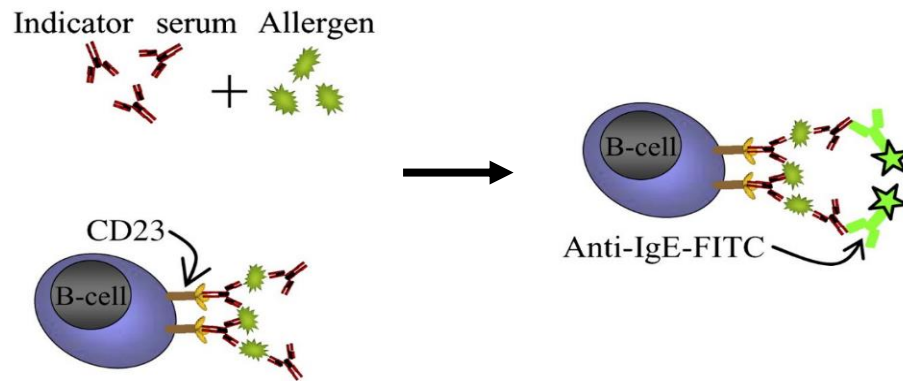


Figure 6.3 Principle of the FAB-assay (modified form 109); The tested allergen forms a complex with either IgE or blocking IgG antibodies. These complexes are incubated with EBV-transformed B cells expressing CD23 (Fc γ RII). The presence of bounded complexes to CD23 on cell surface are stained with anti-IgE-FITC and the IgE levels are detected by flow cytometry

If the efficacy data of VLP-PD1 in immunoprophylaxis and/or immunotherapy are not good enough, it would be possible to test a combination of VLP-PD1 and VLP-Der p 2. Indeed, we successfully produced and characterized VLP decorated with full length Der p 2 using the same conjugation technology (95). Finally, future experiments will be planned for the physico-chemical characterization of VLP-PD1. Notably, the chimeric particles will be analyzed by transmission electron microscopy (TEM). Such characterization was made impossible during the present study because of the Covid-19 pandemic (no access to TEM platform). The stability of VLP-PD1 under different storage conditions (-80, -20, +4) will be examined. Finally, the binding of VLP-PD1 to immobilize Der p 1-specific IgE could be further examined by surface plasma resonance technology in order to confirm the poor affinity of PD1 array for immobilized IgE.

REFERENCES

1. Galli SJ, Tsai M, Piliponsky AM. The development of allergic inflammation. *Nature*. 2008;454(7203):445-54.
2. Salazar F, Ghaemmaghami AM. Allergen recognition by innate immune cells: critical role of dendritic and epithelial cells. *Front Immunol*. 2013;4:356.
3. Tham EH, Lee AJ, Bever HV. Aeroallergen sensitization and allergic disease phenotypes in Asia. *Asian Pac J Allergy Immunol*. 2016;34(3):181-9.
4. Muddaluru V, Valenta R, Vrtala S, Schleder T, Hindley J, Hickey P, et al. Comparison of house dust mite sensitization profiles in allergic adults from Canada, Europe, South Africa and USA. *Allergy*. 2021;76(7):2177-88.
5. WHO/IUIS. ALLERGEN NOMENCLATURE 2021 [Available from: <http://www.allergen.org/search.php?allergenname=Der+&allergensource=&TaxSource=&TaxOrder=&foodallerg=all&bioname=>].
6. Thomas WR. Hierarchy and molecular properties of house dust mite allergens. *Allergol Int*. 2015;64(4):304-11.
7. Reithofer M, Jahn-Schmid B. Allergens with Protease Activity from House Dust Mites. *Int J Mol Sci*. 2017;18(7).
8. Herman J, Thelen N, Smargiasso N, Mailleux AC, Luxen A, Cloes M, et al. Der p 1 is the primary activator of Der p 3, Der p 6 and Der p 9 the proteolytic allergens produced by the house dust mite *Dermatophagoides pteronyssinus*. *Biochim Biophys Acta*. 2014;1840(3):1117-24.
9. Chruszcz M, Pomes A, Glesner J, Vailes LD, Osinski T, Porebski PJ, et al. Molecular determinants for antibody binding on group 1 house dust mite allergens. *J Biol Chem*. 2012;287(10):7388-98.
10. Jacquet A. Characterization of Innate Immune Responses to House Dust Mite Allergens: Pitfalls and Limitations. *Frontiers in Allergy*. 2021;2(7).
11. Walgraffe D, Matteotti C, El Bakkoury M, Garcia L, Marchand C, Bullens D, et al. A hypoallergenic variant of Der p 1 as a candidate for mite allergy vaccines. *J Allergy Clin Immunol*. 2009;123(5):1150-6.

12. Jacquet A, Magi M, Petry H, Bollen A. High-level expression of recombinant house dust mite allergen Der p 1 in *Pichia pastoris*. *Clin Exp Allergy*. 2002;32(7):1048-53.
13. Kucuksezer UC, Ozdemir C, Cevhertas L, Ogulur I, Akdis M, Akdis CA. Mechanisms of allergen-specific immunotherapy and allergen tolerance. *Allergol Int*. 2020;69(4):549-60.
14. Pechsrichuang P, Jacquet A. Molecular approaches to allergen-specific immunotherapy: Are we so far from clinical implementation? *Clin Exp Allergy*. 2020;50(5):543-57.
15. Akinfenwa O, Rodriguez-Dominguez A, Vrtala S, Valenta R, Campana R. Novel vaccines for allergen-specific immunotherapy. *Curr Opin Allergy Clin Immunol*. 2021;21(1):86-99.
16. Shamji MH, Singh I, Layhadi JA, Ito C, Karamani A, Kouser L, et al. Passive Prophylactic Administration with a Single Dose of Anti-Fel d 1 Monoclonal Antibodies REGN1908-1909 in Cat Allergen-induced Allergic Rhinitis: A Randomized, Double-Blind, Placebo-controlled Clinical Trial. *Am J Respir Crit Care Med*. 2021;204(1):23-33.
17. Orengo JM, Radin AR, Kamat V, Badithe A, Ben LH, Bennett BL, et al. Treating cat allergy with monoclonal IgG antibodies that bind allergen and prevent IgE engagement. *Nat Commun*. 2018;9(1):1421.
18. Brune KD, Leneghan DB, Brian IJ, Ishizuka AS, Bachmann MF, Draper SJ, et al. Plug-and-Display: decoration of Virus-Like Particles via isopeptide bonds for modular immunization. *Sci Rep*. 2016;6:19234.
19. Aves KL, Goksoyr L, Sander AF. Advantages and Prospects of Tag/Catcher Mediated Antigen Display on Capsid-Like Particle-Based Vaccines. *Viruses*. 2020;12(2).
20. Thrane S, Janitzek CM, Matondo S, Resende M, Gustavsson T, de Jongh WA, et al. Bacterial superglue enables easy development of efficient virus-like particle based vaccines. *J Nanobiotechnology*. 2016;14:30.
21. Woodfolk JA, Commins SP, Schuyler AJ, Erwin EA, Platts-Mills TA. Allergens, sources, particles, and molecules: Why do we make IgE responses? *Allergol Int*. 2015;64(4):295-303.
22. Hellings PW, Steelant B. Epithelial barriers in allergy and asthma. *J Allergy Clin Immunol*. 2020;145(6):1499-509.

23. Biddulph P, Colloff, M.J.: Dust Mites. *Experimental and Applied Acarology*. 2010;52(4):449-50.
24. Tantilipikorn P, Pinkaew B, Talek K, Assanasen P, Triphoon Suwanwech TS, Bunnag C. Pattern of allergic sensitization in chronic rhinitis: A 19-year retrospective study. *Asian Pac J Allergy Immunol*. 2020.
25. Holgate ST. Innate and adaptive immune responses in asthma. *Nat Med*. 2012;18(5):673-83.
26. Lambrecht BN, Hammad H. Allergens and the airway epithelium response: gateway to allergic sensitization. *J Allergy Clin Immunol*. 2014;134(3):499-507.
27. Hammad H, Lambrecht BN. Barrier Epithelial Cells and the Control of Type 2 Immunity. *Immunity*. 2015;43(1):29-40.
28. Shamji MH, Durham SR. Mechanisms of allergen immunotherapy for inhaled allergens and predictive biomarkers. *J Allergy Clin Immunol*. 2017;140(6):1485-98.
29. Artis D, Spits H. The biology of innate lymphoid cells. *Nature*. 2015;517(7534):293-301.
30. Eifan AO, Durham SR. Pathogenesis of rhinitis. *Clin Exp Allergy*. 2016;46(9):1139-51.
31. Spieksma FT, Dieges PH. The history of the finding of the house dust mite. *J Allergy Clin Immunol*. 2004;113(3):573-6.
32. Sanchez-Borges M, Fernandez-Caldas E, Thomas WR, Chapman MD, Lee BW, Caraballo L, et al. International consensus (ICON) on: clinical consequences of mite hypersensitivity, a global problem. *World Allergy Organ J*. 2017;10(1):14.
33. Vitiello G, Biagioni B, Parronchi P. The multiple roles of mite allergens in allergic diseases. *Curr Opin Allergy Clin Immunol*. 2019;19(6):623-31.
34. Colloff MJ. Taxonomy and identification of dust mites. *Allergy*. 1998;53(48 Suppl):7-12.
35. Miller JD. The Role of Dust Mites in Allergy. *Clin Rev Allergy Immunol*. 2019;57(3):312-29.
36. Tovey ER, Chapman MD, Platts-Mills TA. Mite faeces are a major source of house dust allergens. *Nature*. 1981;289(5798):592-3.
37. Darquenne C. Aerosol deposition in health and disease. *J Aerosol Med Pulm*

Drug Deliv. 2012;25(3):140-7.

38. Waldron R, McGowan J, Gordon N, McCarthy C, Mitchell EB, Fitzpatrick DA. Proteome and allergenome of the European house dust mite *Dermatophagoides pteronyssinus*. PLoS One. 2019;14(5):e0216171.

39. Batard T, Hrabina A, Bi XZ, Chabre H, Lemoine P, Couret MN, et al. Production and proteomic characterization of pharmaceutical-grade *Dermatophagoides pteronyssinus* and *Dermatophagoides farinae* extracts for allergy vaccines. Int Arch Allergy Immunol. 2006;140(4):295-305.

40. Vrtala S, Huber H, Thomas WR. Recombinant house dust mite allergens. Methods. 2014;66(1):67-74.

41. Thomas WR, Smith WA, Hales BJ, Mills KL, O'Brien RM. Characterization and immunobiology of house dust mite allergens. Int Arch Allergy Immunol. 2002;129(1):1-18.

42. Caraballo L, Valenta R, Acevedo N, Zakzuk J. Are the Terms Major and Minor Allergens Useful for Precision Allergology? Front Immunol. 2021;12:651500.

43. Jacquet A, Robinson C. Proteolytic, lipidergic and polysaccharide molecular recognition shape innate responses to house dust mite allergens. Allergy. 2020;75(1):33-53.

44. Kikuchi Y, Takai T, Kuhara T, Ota M, Kato T, Hatanaka H, et al. Crucial commitment of proteolytic activity of a purified recombinant major house dust mite allergen Der p1 to sensitization toward IgE and IgG responses. J Immunol. 2006;177(3):1609-17.

45. Zhang J, Chen J, Robinson C. Cellular and Molecular Events in the Airway Epithelium Defining the Interaction Between House Dust Mite Group 1 Allergens and Innate Defences. Int J Mol Sci. 2018;19(11).

46. Moingeon P. Progress in the development of specific immunotherapies for house dust mite allergies. Expert Rev Vaccines. 2014;13(12):1463-73.

47. Bronnert M, Mancini J, Birnbaum J, Agabriel C, Liabeuf V, Porri F, et al. Component-resolved diagnosis with commercially available *D. pteronyssinus* Der p 1, Der p 2 and Der p 10: relevant markers for house dust mite allergy. Clin Exp Allergy. 2012;42(9):1406-15).

48. Weghofer M, Thomas WR, Krongvist M, Mari A, Purohit A, Pauli G, et al. Variability of IgE reactivity profiles among European mite allergic patients. *Eur J Clin Invest.* 2008;38(12):959-65.
49. Chua KY, Kehal PK, Thomas WR. Sequence polymorphisms of cDNA clones encoding the mite allergen Der p I. *Int Arch Allergy Immunol.* 1993;101(4):364-8.
50. Chua KY, Kehal,P.K. and Thomas,W.R. RecName: Full=Peptidase 1; AltName: Full=Allergen Der p I; AltName: Full=Major mite fecal allergen Der p 1; AltName: Allergen=Der p 1; Flags: Precursor (Peptidase 1).
51. Chevigne A, Campizi V, Szpakowska M, Bourry D, Dumez ME, Martins JC, et al. The Lys-Asp-Tyr Triad within the Mite Allergen Der p 1 Propeptide Is a Critical Structural Element for the pH-Dependent Initiation of the Protease Maturation. *Int J Mol Sci.* 2017;18(5).
52. Meno K, Thorsted PB, Ipsen H, Kristensen O, Larsen JN, Spangfort MD, et al. The crystal structure of recombinant proDer p 1, a major house dust mite proteolytic allergen. *J Immunol.* 2005;175(6):3835-45.
53. Dumez ME, Herman J, Campizi V, Galleni M, Jacquet A, Chevigne A. Orchestration of an uncommon maturation cascade of the house dust mite protease allergen quartet. *Front Immunol.* 2014;5:138.
54. Scobie G, Ravindran V, Deam SM, Thomas M, Sreedharan SK, Brocklehurst K, et al. Expression cloning of a dust mite cysteine proteinase, Der p1, a major allergen associated with asthma and hypersensitivity reactions. *Biochem Soc Trans.* 1994;22(4):448S.
55. Chua KY, Kehal PK, Thomas WR, Vaughan PR, Macreadie IG. High-frequency binding of IgE to the Der p allergen expressed in yeast. *J Allergy Clin Immunol.* 1992;89(1 Pt 1):95-102.
56. Massaer M, Mazzu P, Haumont M, Magi M, Daminet V, Bollen A, et al. High-level expression in mammalian cells of recombinant house dust mite allergen ProDer p 1 with optimized codon usage. *Int Arch Allergy Immunol.* 2001;125(1):32-43.
57. Jacquet A, Haumont M, Massaer M, Daminet V, Garcia L, Mazzu P, et al. Biochemical and immunological characterization of a recombinant precursor form of the house dust mite allergen Der p 1 produced by *Drosophila* cells. *Clin Exp Allergy.*

2000;30(5):677-84.

58. Chevigne A, Jacquet A. Emerging roles of the protease allergen Der p 1 in house dust mite-induced airway inflammation. *J Allergy Clin Immunol.* 2018;142(2):398-400.
59. Casale TB, Stokes JR. Immunotherapy: what lies beyond. *J Allergy Clin Immunol.* 2014;133(3):612-9: quiz 20.
60. Dorofeeva Y, Shilovskiy I, Tulaeva I, Focke-Tejkl M, Flicker S, Kudlay D, et al. Past, present, and future of allergen immunotherapy vaccines. *Allergy.* 2021;76(1):131-49.
61. Gellrich D, Eder K, Hogerle C, Becker S, Canis M, Groger M. De novo sensitization during subcutaneous allergen specific immunotherapy - an analysis of 51 cases of SCIT and 33 symptomatically treated controls. *Sci Rep.* 2020;10(1):6048.
62. Nelson HS, Calderon MA, Bernstein DI, Casale TB, Durham SR, Andersen JS, et al. Allergen Immunotherapy Clinical Trial Outcomes and Design: Working Toward Harmonization of Methods and Principles. *Curr Allergy Asthma Rep.* 2017;17(3):18.
63. Globinska A, Boonpiyathad T, Satitsuksanoa P, Kleuskens M, van de Veen W, Sokolowska M, et al. Mechanisms of allergen-specific immunotherapy: Diverse mechanisms of immune tolerance to allergens. *Ann Allergy Asthma Immunol.* 2018;121(3):306-12.
64. van de Veen W, Wirz OF, Globinska A, Akdis M. Novel mechanisms in immune tolerance to allergens during natural allergen exposure and allergen-specific immunotherapy. *Curr Opin Immunol.* 2017;48:74-81.
65. Valenta R, Linhart B, Swoboda I, Niederberger V. Recombinant allergens for allergen-specific immunotherapy: 10 years anniversary of immunotherapy with recombinant allergens. *Allergy.* 2011;66(6):775-83.
66. Akdis M. New treatments for allergen immunotherapy. *World Allergy Organ J.* 2014;7(1):23.
67. Martinez D, Cantillo JF, Herazo H, Wortmann J, Keller W, Caraballo L, et al. Characterization of a hybrid protein designed with segments of allergens from *Blomia tropicalis* and *Dermatophagoides pteronyssinus*. *Immunol Lett.* 2018;196:103-12.
68. Chen KW, Blatt K, Thomas WR, Swoboda I, Valent P, Valenta R, et al. Hypoallergenic Der p 1/Der p 2 combination vaccines for immunotherapy of house dust

mite allergy. *J Allergy Clin Immunol*. 2012;130(2):435-43 e4.

69. Asturias JA, Ibarrola I, Arilla MC, Vidal C, Ferrer A, Gamboa PM, et al. Engineering of major house dust mite allergens Der p 1 and Der p 2 for allergen-specific immunotherapy. *Clin Exp Allergy*. 2009;39(7):1088-98.

70. Zhao BB, Diao JD, Liu ZM, Li CP, Jiang YX. Generation of a chimeric dust mite hypoallergen using DNA shuffling for application in allergen-specific immunotherapy. *Int J Clin Exp Pathol*. 2014;7(7):3608-19.

71. Magi M, Garcia L, Vandenbranden M, Palmantier R, Jacquet A. Heat denaturation affects the ProDer p 1 IgE reactivity and downregulates the development of the specific allergic response. *J Allergy Clin Immunol*. 2004;114(3):545-52.

72. Glesner J, Vailes LD, Schlachter C, Mank N, Minor W, Osinski T, et al. Antigenic Determinants of Der p 1: Specificity and Cross-Reactivity Associated with IgE Antibody Recognition. *J Immunol*. 2017;198(3):1334-44.

73. Kundig TM, Senti G, Schnetzler G, Wolf C, Prinz Vavricka BM, Fulurija A, et al. Der p 1 peptide on virus-like particles is safe and highly immunogenic in healthy adults. *J Allergy Clin Immunol*. 2006;117(6):1470-6.

74. Larche M, Hickey P, Hebert J, Hafner R. Safety and Tolerability of Escalating Doses of House Dust Mite- Peptide Antigen Desensitization (HDM-PAD). *Journal of Allergy and Clinical Immunology*. 2013;131(2):AB37.

75. Komlosi ZI, Kovacs N, Sokolowska M, van de Veen W, Akdis M, Akdis CA. Mechanisms of Subcutaneous and Sublingual Aeroallergen Immunotherapy: What Is New? *Immunol Allergy Clin North Am*. 2020;40(1):1-14.

76. Gevaert P, De Craemer J, De Ruyck N, Rottey S, de Hoon J, Hellings PW, et al. Novel antibody cocktail targeting Bet v 1 rapidly and sustainably treats birch allergy symptoms in a phase 1 study. *J Allergy Clin Immunol*. 2021.

77. Atanasio A, Franklin MC, Kamat V, Hernandez AR, Badithe A, Ben LH, et al. Targeting immunodominant Bet v 1 epitopes with monoclonal antibodies prevents the birch allergic response. *J Allergy Clin Immunol*. 2021.

78. Gomez G. Current Strategies to Inhibit High Affinity FcεRI-Mediated Signaling for the Treatment of Allergic Disease. *Front Immunol*. 2019;10:175.

79. Matsuoka T, Shamji MH, Durham SR. Allergen immunotherapy and tolerance.

Allergol Int. 2013;62(4):403-13.

80. Bachmann MF, Jennings GT. Vaccine delivery: a matter of size, geometry, kinetics and molecular patterns. *Nat Rev Immunol*. 2010;10(11):787-96.

81. Bachmann MF, Rohrer UH, Kundig TM, Burki K, Hengartner H, Zinkernagel RM. The influence of antigen organization on B cell responsiveness. *Science*. 1993;262(5138):1448-51.

82. Hua Z, Hou B. TLR signaling in B-cell development and activation. *Cell Mol Immunol*. 2013;10(2):103-6.

83. Lowy DR. HPV vaccination to prevent cervical cancer and other HPV-associated disease: from basic science to effective interventions. *J Clin Invest*. 2016;126(1):5-11.

84. Cyster JG, Allen CDC. B Cell Responses: Cell Interaction Dynamics and Decisions. *Cell*. 2019;177(3):524-40.

85. Pechsrichuang P, Namwongnao S, Jacquet A. Bioengineering of Virus-like Particles for the Prevention or Treatment of Allergic Diseases. *Allergy Asthma Immunol Res*. 2021;13(1):23-41.

86. Brune KD, Howarth M. New Routes and Opportunities for Modular Construction of Particulate Vaccines: Stick, Click, and Glue. *Front Immunol*. 2018;9:1432.

87. Charlton Hume HK, Vidigal J, Carrondo MJT, Middelberg APJ, Roldao A, Lua LHL. Synthetic biology for bioengineering virus-like particle vaccines. *Biotechnol Bioeng*. 2019;116(4):919-35.

88. Zakeri B, Fierer JO, Celik E, Chittock EC, Schwarz-Linek U, Moy VT, et al. Peptide tag forming a rapid covalent bond to a protein, through engineering a bacterial adhesin. *Proc Natl Acad Sci U S A*. 2012;109(12):E690-7.

89. Domingo-Espin J, Unzueta U, Saccardo P, Rodriguez-Carmona E, Corchero JL, Vazquez E, et al. Engineered biological entities for drug delivery and gene therapy protein nanoparticles. *Prog Mol Biol Transl Sci*. 2011;104:247-98.

90. Carroll-Portillo A, Lin HC. Bacteriophage and the Innate Immune System: Access and Signaling. *Microorganisms*. 2019;7(12).

91. A CG, Roesti ES, El-Turabi A, Bachmann MF. Type of RNA Packed in VLPs Impacts IgG Class Switching-Implications for an Influenza Vaccine Design. *Vaccines (Basel)*. 2019;7(2).

92. Schmitz N, Dietmeier K, Bauer M, Maudrich M, Utzinger S, Muntwiler S, et al. Displaying Fel d1 on virus-like particles prevents reactogenicity despite greatly enhanced immunogenicity: a novel therapy for cat allergy. *J Exp Med*. 2009;206(9):1941-55.
93. Engeroff P, Caviezel F, Storni F, Thoms F, Vogel M, Bachmann MF. Allergens displayed on virus-like particles are highly immunogenic but fail to activate human mast cells. *Allergy*. 2018;73(2):341-9.
94. Kratzer B, Kohler C, Hofer S, Smole U, Trapin D, Iturri J, et al. Prevention of allergy by virus-like nanoparticles (VNP) delivering shielded versions of major allergens in a humanized murine allergy model. *Allergy*. 2019;74(2):246-60.
95. Soongrung T, Mongkorntanyatip K, Peepim T, Jitthamstaporn S, Pitakpolrat P, Kaewamatawong T, et al. Virus-like particles displaying major house dust mite allergen Der p 2 for prophylactic allergen immunotherapy. *Allergy*. 2020;75(5):1232-6.
96. Storni F, Zeltins A, Balke I, Heath MD, Kramer MF, Skinner MA, et al. Vaccine against peanut allergy based on engineered virus-like particles displaying single major peanut allergens. *J Allergy Clin Immunol*. 2020;145(4):1240-53 e3.
97. Satitsuksanoa P, Kennedy M, Gilis D, Le Mignon M, Suratannon N, Soh WT, et al. The minor house dust mite allergen Der p 13 is a fatty acid-binding protein and an activator of a TLR2-mediated innate immune response. *Allergy*. 2016;71(10):1425-34.
98. Lazaro-Gorines R, Lopez-Rodriguez JC, Benede S, Gonzalez M, Mayorga C, Vogel L, et al. Der p 1-based immunotoxin as potential tool for the treatment of dust mite respiratory allergy. *Sci Rep*. 2020;10(1):12255.
99. Dumez ME, Teller N, Mercier F, Tanaka T, Vandenberghe I, Vandenbranden M, et al. Activation mechanism of recombinant Der p 3 allergen zymogen: contribution of cysteine protease Der p 1 and effect of propeptide glycosylation. *J Biol Chem*. 2008;283(45):30606-17.
100. Shamji MH, Layhadi JA, Sharif H, Penagos M, Durham SR. Immunological Responses and Biomarkers for Allergen-Specific Immunotherapy Against Inhaled Allergens. *J Allergy Clin Immunol Pract*. 2021;9(5):1769-78.
101. Donaldson B, Lateef Z, Walker GF, Young SL, Ward VK. Virus-like particle vaccines: immunology and formulation for clinical translation. *Expert Rev Vaccines*.

2018;17(9):833-49.

102. Chevigne A, Barumandzadeh R, Gros Lambert S, Cloes B, Dehareng D, Filee P, et al. Relationship between propeptide pH unfolding and inhibitory ability during ProDer p 1 activation mechanism. *J Mol Biol.* 2007;374(1):170-85.

103. Huber M. Activation/Inhibition of mast cells by supra-optimal antigen concentrations. *Cell Commun Signal.* 2013;11(1):7.

104. Clingan JM, Matloubian M. B Cell-intrinsic TLR7 signaling is required for optimal B cell responses during chronic viral infection. *J Immunol.* 2013;191(2):810-8.

105. Krueger CC, Thoms F, Keller E, Leoratti FMS, Vogel M, Bachmann MF. RNA and Toll-Like Receptor 7 License the Generation of Superior Secondary Plasma Cells at Multiple Levels in a B Cell Intrinsic Fashion. *Front Immunol.* 2019;10:736.

106. Gomes AC, Mohsen MO, Mueller JE, Leoratti FMS, Cabral-Miranda G, Bachmann MF. Early Transcriptional Signature in Dendritic Cells and the Induction of Protective T Cell Responses Upon Immunization With VLPs Containing TLR Ligands-A Role for CCL2. *Front Immunol.* 2019;10:1679.

107. Shamji MH, Larson D, Eifan A, Scadding GW, Qin T, Lawson K, et al. Differential induction of allergen-specific IgA responses following timothy grass subcutaneous and sublingual immunotherapy. *J Allergy Clin Immunol.* 2021.

108. Janitzek CM, Carlsen PHR, Thrane S, Khanna VM, Jakob V, Barnier-Quer C, et al. The Immunogenicity of Capsid-Like Particle Vaccines in Combination with Different Adjuvants Using Different Routes of Administration. *Vaccines (Basel).* 2021;9(2).

109. Principle of the FAB-assay [Available from: <http://gbsleiden.com/fab-assay/>].



จุฬาลงกรณ์มหาวิทยาลัย
CHULALONGKORN UNIVERSITY

VITA

NAME Ms. Sirikarn Jitthamstaporn

DATE OF BIRTH 10 October 1992

PLACE OF BIRTH Bangkok, Thailand

INSTITUTIONS ATTENDED Chulalongkorn University

HOME ADDRESS 20 Ramkamheang 118 yeak 41
Ramkamheang road, Saphansoog district
Bangkok, Thailand 10240

PUBLICATION

- 1) Virus-like particles displaying major HDM allergen Der p 2 for prophylactic allergen immunotherapy
- 2) Prophylactic effects of virus like particles displaying the major HDM allergen Der p 2 in a mouse model of HDM allergy